UNIVERSITAT DE BARCELONA

Role of ZEB1 in macrophages during homeostasis, inflammation and cáncer

Marlies Cortés Hinojosa

Universitat de Barcelona

IDIBAPS
Institut
D'Investigacions
Biomèdiques
August Pi i Sunyer

Villarroel 170
08036 Barcelona
Tels 227 57 07
451 62 86
Fax 451 52 72
idibaps@medicina.ub.es

Memoria presentada por Marlies Cortés Hinojosa para optar al grado de Doctor en Biomedicina por la Universitat de Barcelona

"Role of ZEB1 in macrophages during homeostasis, inflammation and cancer"

Esta Tesis Doctoral se ha desarrollado en el Institut d'investigacions Biomèdiques August Pi i Sunyer (IDIBAPS) en la Facultad de Medicina de la Universitat de Barcelona, bajo la dirección de Antonio Postigo y del Dr. Carles Enrich como tutor

Programa de Doctorado en Biomedicina 2017

Dr. Antonio Postigo	**Dr. Carles Enrich**	**Marlies Cortés Hinojosa**
Director	Tutor	Doctoranda

“Cuando creíamos que teníamos todas
las respuestas, de pronto, cambiaron
todas las preguntas.”

— Mario Benedetti

“It seemed when stress and madness were
eliminated from my daily life there wasn’t much
left you could depend on.”

— Charles Bukowski

Agradecimientos

Una de las partes más difíciles de este proceso, quizás sean los agradecimientos, porque tengo tanto que agradecer y a tantos grandes personajes de aquí y allá, de hoy y de ayer. Pero primero debo mencionarte a ti Antonio Postigo, que aunque seguro no te guste la idea, eres el primero a quien quiero agradecer, porque nada de esto hubiese sido posible sin ti. Porque me has enseñado muchísimo todos estos años, porque he aprendido contigo, he crecido y también he llorado, pero por sobretodo he reido y he podido hacer lo que venía a hacer, lograr que el camino de la ciencia sea una aventura que se vaya disfrutando, innovando, abriendo caminos y que deje esas ganas de más a cada paso. Gracias por todo.

A mi familia, que ha sido mi pedestal, cuando tantas veces me vi sobrepasada, jamás imaginé que el apoyo y amor de la familia es capaz de levantar todo, por muy abajo y perdido que parezca. Papá, has sido un ejemplo siempre, sin ti jamás podría haber tenido la entereza de terminar, ni el sentido de la responsabilidad que tanto nos inculcaste. Hermanito de mi alma y corazón, eres mi tesoro más preciado, mi ejemplo y lo más grande que tengo. Gracias Simo por ser tan bella mujer en todo sentido y por darme esos sobrinitos maravillosos que son la luz de mi vida. Y tu mamá, mujer maravillosa, única, enorme, inabarcable, no puedo si no dedicarte todo mi trabajo y mi vida a ti, porque todo lo que soy te lo debo a ti, a tu luz y a tu maestría en la vida, eres lo máximo y todo yo soy un agradecimiento a tu persona.

A veces estar sola en un sitio tan lejano y distinto a todo lo que conoces es complejo, pero la vida es sabia y me puso en el mejor sitio, con las mejores personas que podía estar. Uri, si no fuera por ti seguro no estaría escribiendo esto ahora ni quizás nunca, has sido un apoyo tremendo, como he disfrutado reir contigo, aprender de ti, a admirarte como investigador, pero por sobretodo como persona, eres excelente y te agradezco infinito todo. Ester, eres una persona tan especial, siempre dispuesta a enseñar, a apoyar, sin duda las mejores críticas que

he escuchado siempre vienen de ti, esa capacidad de análisis y entrega por lo que haces, sin dejar de lado ser una persona dulce y comprometida con el resto, mil gracias por todo. A Yeny, tanto que agradecerte también, mi super mentora, super amiga, super en todo, te agradezco y agradezco a la vida el haberte conocido. A Laura y Chiara, sus risas, nuestro acroyoga, nuestro Ragnar y todo lo que son, gracias miles. A Pablo y tantas risas junto a ti. A M. Carmen que ha sido un agrado trabajar con ella, frustrarnos juntas y compartir el tiempo con ella, gracias. A Lidia y Nuria que son un encanto de personas, siempre dispuestas a ayudar, tan jóvenes y talentosas, gracias. A Ingrid que siempre es un personaje fundamental en el Laboratorio, gracias guapa. Y así a Lucía que es una mujer espectacular, Carlos que tan gran apoyo fue, Angelita y sus risas, la Xufrecita y la Sara y nuestros agradables sortings, gracias a todos! Y por último, siguiendo en el ámbito científico, mi más especial agradecimiento a mi guapa Annemie, eres tan grande amiga, a tu lado he vivdo cada momento de este proceso desde que llegué y es gracias a ti que ahora ya veo la luz y después de ver la luz tenemos que ir al Ascot y seguir quejándonos y riéndonos de la vida por siempre … o en Valparaíso o una isla paradisiaca con unos cocos o donde sea, te adoro!

Estando acá ya en casa, en la soledad de los días, siempre ha habido seres que iluminan mis días, como tu Melita, todo mi agradeciemiento a ti y a todo lo que has sido para mi estos años acá, eres enorme y te quiero con el alma, y al Lolo también. A mi amiga del alma, que apareció de la nada y nunca más se despegaron nuestros caminos, Peggy, gracias por todo, tu sabes cuanto significas en mi vida. A mi Paty preciosa, que aunque nos vemos poquito, yo se que nuestro cariño sobrepasa tiepo y espacio. A mi Pelaito irresistible y la Pascalita que son lo mejor del mundo para cuando uno quiere abstraerse de los días duros, gracias totales! A la Adri y la Su, que son mis chicas especiales. A mi Pelu adorada, eres mi hermanita y en esta tesis como en todas la obras de mi vida siempre eres un pilar fundamental, tengo tanto tanto que agradecerte y tanto tanto que seguir viviendo a tu lado, te amo!

A mis kiltras ricas que las adoro, Maquita y Pauchi, son las mejores y espero la celebración pronto pronto. Al Harem, que siempre está ahí haciéndome reir, Canales, ya sabes que mi tesis va dedicada al Caifán, eres un gran amigo y te quiero a morir. Pame, Miche, Vale, una vida entera de agradecimiento por todo lo que han sido en mi vida. Mi Grupo querido, aunque ya poco nos vemos siempre estuvieron presentes, Dani, primita de mi corazón te amo, Pauly, lo mismo, Nori, Pancha, Sil, Gerardo, Cota, Foxy, gracias.

Al Leo Saenz, que fuiste mi gran mentor en la ciencia, gracias miles por enseñarme este lindo camino, lo mismo para Myriam Lorca, la mejor jefa y mujer de ciencia que he conocido, mil gracias por todo. A M. Inés, que eres una personita maravillosa, a David, que ha sido una gran aparición en esta etapa de mi vida … Y a ti Cosmo, que hiciste que todo esto fuera realidad y que me permitiste seguir mis sueños hasta hacerlos realidad, Gracias!

"Nothing lasts forever, so live it up, drink it down, laugh it off, avoid the drama, take chances and never have regrets because at one point everything you did was exactly what you wanted."

TABLE OF CONTENTS

ABBREVIATIONS

BMDM	Bone marrow derived macrophage
BMTC	Bone marrow total cell
CCR2	C–C chemokine receptor type 2
CD163	Cluster of differentiation 163
CD204	Scavenger Receptor A
CD206/MRC1	Mannose receptor
CFSE	Carboxyl-fluorescein diacetate succinimidyl ester
ChIP	Chromatin immunoprecipitation
CM	Conditioned medium
CSC	Cancer stem cell
CSF1	Colony stimulate factor 1
CSF2	Colony stimulate factor 2
DMEM	Dulbecco's modified Eagle Medium
EMP	Erythromyeloid progenitors
EMT	Epithelial-to-mesenchymal transition
EOC	Epithelial ovarian cancer
FACS	Flow cytometry analysis and sorting
GATA6	GATA-binding protein 6
HGSOC	High grade serous ovarian carcinoma
HIF	Hypoxia-inducible factor
HSC	Hematopoietic stem cell
IL10	Interleukin 10
IL12	Interleukin 12
IL13	Interleukin 13
IL1β	Interleukin 1 beta
IL4	Interleukin 4
JAK2	Janus Kinase 2
LPM	Large peritoneal macrophages
LPS	Lipopolysaccharide
LXRA	Liver X receptor alpha
MAPK	Mitogen-activated protein kinases
MCP1/CCL2	Monocyte chemoattractant protein 1

MEF2c	Myocyte-specific enhancer factor 2C
MHCII	Major histocompatibility complex class II
MMP9	Matrix metalloproteinase
MOSE	Mouse ovarian surface epithelial
MPS	Mononuclear phagocyte system
NK	Natural Killer
PBS	Phosphate buffered saline
PI3K	Phosphatidylinositide 3-kinases
PKC	Protein kinase C
PPARγ	Proliferator-activated receptor-γ
RFU	Relative fluorescence units
SOCS	Suppressor of cytokine signaling
SPM	Small peritoneal macrophages
STAT	Signal transducer and activator of transcription
TAM	Tumor-associated macrophage
TG	Thioglycolate
TGFβ	Tumor growth factor beta
TLR4	Toll like receptor four
TME	Tumor microenvironment
TNFα	Tumor necrosis factor alpha
VEGFα	Vascular endothelial growth factor- A
ZEB1	Zinc-finger enhancer-binding protein

INTRODUCTION

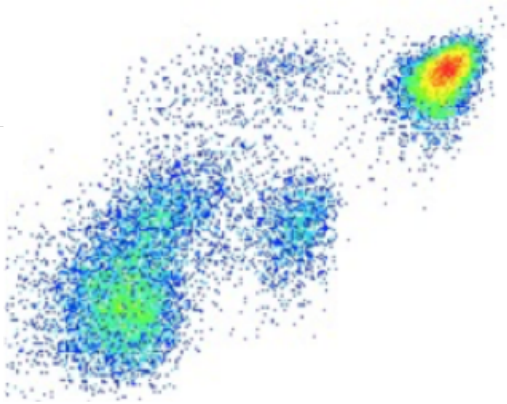

Chapter I : Myeloid cells differentiation and activation

The mononuclear phagocyte system

The immune system comprises a variety of cell types and structures, which form a complex network where each component performs a specific function with the final goal of protecting the organism against pathogens and transformed cells. Classically, the immune system has been divided into innate and adaptive elements. The innate immune system is the first-line of defense that responds to pathogenic challenge and provides a robust and rapid response, within minutes of pathogen exposure, to generate a protective inflammatory response. Moreover, innate immunity plays a central role in activating the subsequent adaptive immune response. In turn, adaptive immunity refers to a group of specialized cells that have the capability to generate a memory immune response against pathogens once innate immune cells have presented them with specific antigens. The recognition of danger signals by immune cells triggers an inflammatory response that includes the secretion of cytokines and chemokines and the recruitment of phagocytic cells. The hematopoietic cells that integrate the adaptive immunity system include B and T lymphocytes while innate immune responses are mediated by macrophages, dendritic cells, mast cells, neutrophils, eosinophils, natural killer (NK) cells, and NK T cells. Most cell populations in the innate immune system arise from hematopoietic progenitors cells in the bone marrow that constitute the so-called *mononuclear phagocyte system* (MPS).

Innate immune cells within the MPS are responsible for the maintenance of homeostatic surveillance, reaction to infection and injury as well as for the regenerative response after

the injury. Van Furth and colleagues initially proposed the concept of MPS in the 1970's with a basic and linear model (Van Furth and Cohn, 1968, Yona et al., 2013; Cassado et al., 2015). The MPS has been now expanded to include subpopulations regulated by specific growth and transcription factors as well as epigenetic modifications that result in subset-specific gene expression signatures, and distinct ontogenies, that include myeloid cells, however, some of these cells have an origin that is other than bone marrow hematopoietic stem cells (HSCs) (Davies and Taylor, 2015, Alvarez-Errico et al., 2015).

Macrophages are myeloid cells that play central roles in tissue homeostasis and pathophysiological responses like host defense against infections, tissue repair, and inflammation, through various scavenger, pattern recognition, and phagocytic receptors. These functions enable macrophages to initiate appropriate inflammatory programs upon perturbation of homeostasis. Conversely, deregulated macrophage activation could occur during inflammation and in a number of diseases, including cancer (Wynn et al., 2013; Franklin and Li, 2016).

The central paradigm established by the MPS concept were twofold: first, that tissue-resident macrophages in homeostasis are maintained through the continuous recruitment of blood monocytes produced by bone marrow HSCs and, second, that macrophages are fully differentiated cells that have lost their proliferative potential. This model occurs as a linear process wherein progenitor cells in the bone marrow generate circulating blood monocytes that upon arrival into tissues can differentiate into macrophages. It was based on the observation that blood leukocytes recruited into the inflamed peritoneum can differentiate into mature macrophages (Chow et al., 2011).

However, macrophage populations do not necessarily share the same origin, arising either from embryonic progenitors, such as yolk sac macrophages and fetal monocytes or from adult blood monocytes. Yolk sac erythromyeloid progenitors (EMPs) have both erythroid and myeloid potential. EMP-derived hematopoiesis gives rise to erythrocytes, macrophages, monocytes, granulocytes and mast cells. Macrophages are found in the mouse yolk sac before the initiation of HSCs-derived hematopoiesis as early as

embryonic day 9 (E9), before the establishment of the circulatory system (Ginhoux and Jung, 2014). Two highly coordinated waves of hematopoiesis have been identified, referred to as "primitive" and "definitive."

The first early “primitive” wave is c-Myb- and Notch1-independent and generates primitive macrophages without monocytic intermediates in the yolk sac. The second "definitive" wave begins when HSCs appear in the aorta gonadal mesonephros region at approximately day 10.5 of embryonic development (E10.5). This second wave is c-Myb- and Notch1-dependent, and these precursors are capable of maintaining blood circulating cells lifelong. EMPs embryonic precursors of yolk sac macrophages and fetal monocytes can be distinguished according to the anatomical site (extra-embryonic yolk sac versus intra-embryonic region), their differentiation potential and their dependence on transcription factors. Thus, tissue resident macrophages are thought to arise independently of blood monocytes, and also can originate by *in situ* self-renewal (Hashimoto et al., 2013).

EMP-derived macrophages from these first non-hematopoietic precursors colonize all tissues during fetal development, where they specialize in their tissue of residence after birth and appear to persist throughout adult life by local proliferation through a process of self-renewal (Varol et al., 2015; Bertrand et al., 2010). Examples of these macrophages include microglia of the central nervous system and some Langerhans cells in the epidermis (Figure 1). These results have been obtained through parabiosis of congenic mice that confirmed that the homeostatic maintenance of these macrophages populations is largely independent of blood monocytes expressing the C-C chemokine receptor type 2 (CCR2). CCR2 is highly expressed in monocytes, which is the basis of hematopoiesis derived from HSC (Hashimoto et al., 2013; Yona et al., 2013).

However, in some tissues, resident macrophages derive from circulating monocytes like intestinal macrophages of the colonic mucosa that are continually replenished from circulating monocytes. In other tissues like heart, epidermis, and peritoneal cavity, a smaller subset of monocyte-derived macrophages can be found in homeostatic

conditions, derived from the physiological recruitment of monocyte population. Nevertheless, in the context of inflammation, upon radiation or in ischemic tissues, the recruitment and differentiation of blood monocytes may be involved in the maintenance of tissue-resident macrophages population. Likewise, during aging, tissue-resident macrophages in the heart and lung are replenished from monocytes (Lavin et al., 2015; Hoeffel et al., 2015; Miró-Mur et al., 2016). Interestingly, other studies found that tissue macrophages were replaced by adult bone marrow–derived cells, not necessarily by monocytes. This indicates that adult bone marrow–derived cells can acquire phenotypic and functional features and exhibit a gene expression profile similar to the original tissue macrophage population, with the tissue environments ultimately dictating macrophages' phenotype (Gosselin et al., 2014; Lavin et al., 2014).

In mouse, expression levels of the cell surface F4/80 antigen define different macrophage subsets. Ontogenically, mouse macrophages can be classified into two broad groups based on their levels of expression of this cell surface marker F4/80, with F4/80^{low} (originating from circulating monocytes during adult hematopoiesis) and F4/80^{high} (from embryonic precursors) (Schultz et al., 2012; Pérez-de Puig et al., 2013). In the case of peritoneal macrophages, these two subpopulations are referred as *large peritoneal macrophages* (LPM, F4/80^{high}), which are the higher fraction under basal conditions and are replaced by *small peritoneal macrophages* (SPM, F4/80^{high}) upon antigenic stimulation (Ghosn et al., 2010; Okabe and Medzhitov, 2014; Rei et al., 2014). SPM are short-lived cells that can replace LPMs under inflammatory conditions, although LPMs do not seem to contribute to the SPM subpopulation (Cassado et al., 2015).

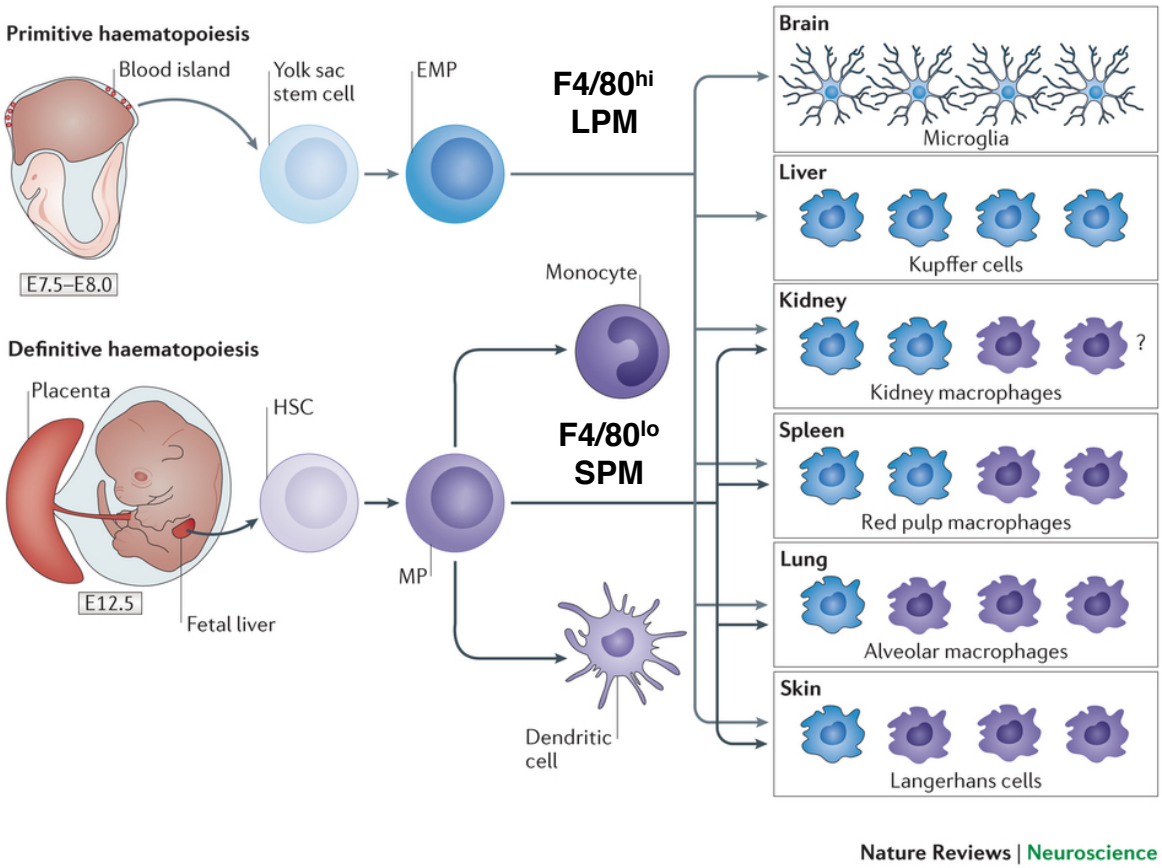

Figure 1. **Origin and differentiation of myeloid cells**. The figure displays the origin of different macrophage populations. Taken with permission from Marco Prinz & Josef Priller, Nat Rev Neurosc 15, 300–312 (2014).

The differential phenotype of macrophages across mouse tissues depends on a tissue-specific transcriptional and epigenetic regulation of their genes, supporting once again the idea that microenvironmental signals dictate the programming, activation, phenotype and cellular function of macrophages (Álvarez-Errico et al., 2015).

There are many transcription factors that regulate the functions of tissue-resident macrophages. For instance, the MAF transcription factor is more expressed in tissue macrophages than in monocytes, and both MAF and MAFB are essential for macrophage terminal differentiation (Lavin et al., 2015). Same applies to the peroxisome proliferator-activated receptor-γ (PPARγ) in alveolar macrophages, GATA-binding protein 6 (GATA6) in peritoneal cavity macrophages, Myocyte-specific enhancer factor 2C (MEF2c) in microglia, and Liver X receptor alpha (LXRA) in Kupffer cells and splenic

macrophages (Lavin et al., 2014, Rosas et al., 2014). Along PU.1, these transcription factors define phenotype and function of the macrophages in physiological or pathophysiological tissue-dependent contexts (Lawrence and Natoli, 2011).

Peritoneal macrophages are an illustration of how tissue-derived signals can shape tissue-resident macrophages functional identity. These macrophages can retain some levels of plasticity and adapt to new environmental cues, here peritoneal cavity macrophages, adoptively transferred into the lung microenvironment, downregulated *Gata6* and upregulated *Pparγ* expression, although some transcripts remained fixed and retained the signature of the tissue of origin (Lavin et al., 2014; Okabe and Medzhitov, 2014).

Macrophage Polarization

Extravasation of circulating monocytes into inflamed tissues and the tumor microenvironment promote their differentiation into macrophages and their subsequent activation along a continuum of functional phenotypes. At the extremes, these phenotypes are classically referred to as M1 and M2 polarization although intermediate phenotypes are more common *in vivo* (Lawrence and Natali, 2011; Murray et al., 2014; Xue et al., 2014 and Figure 2). Although this binary model represents a simple representation of macrophage activation, evidence in human and mouse macrophages indicates that macrophages display a broad functional spectrum of phenotypes in response to complex and ever changing signals in their specific microenvironments. Macrophage polarization is not a static state rather is an active process coordinated by genetic and molecular pathways (Martinez and Gordon, 2014; Williams et al., 2016).

Activation of macrophages towards M1 occurs in response to Th1 cytokines and results in the production of pro-inflammatory cytokines (e.g., IL1β, IL12, TNFα, SOCS3). In turn, Th2 cytokines IL4 and IL13 trigger an M2-type phenotype with upregulation of

anti-inflammatory cytokines (e.g., IL10) and scavenger receptors (e.g., CD163, CD204, CD206/MRC1) (Sica and Mantovani, 2012; Arango Duque and Descoteaux, 2014).

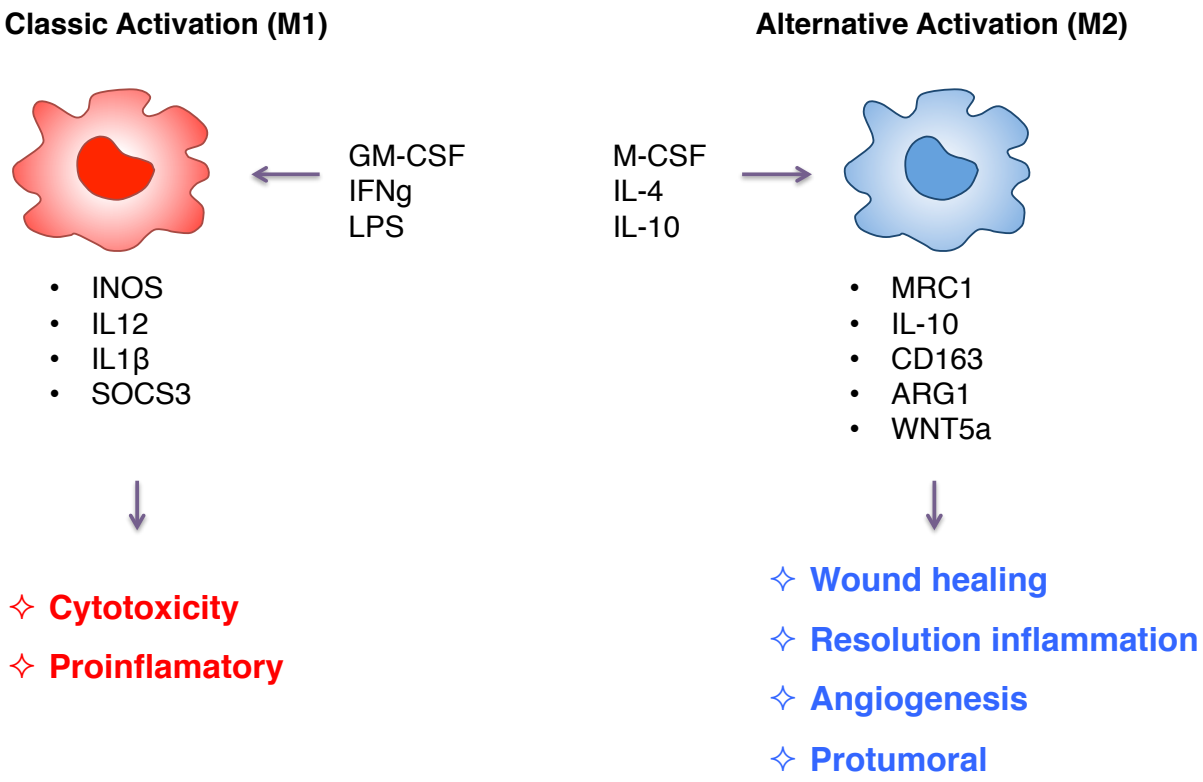

Figure 2. **Classical binary model of macrophage polarization.** The figure displays the archetypical macrophage activation that is seen *in vitro*.

SOCS proteins

Among the molecules that regulate macrophage polarization the eight members of the "*suppressor of cytokine signaling*" (SOCS) family proteins play an essential role in driving the inflammatory process. They are upregulated by cytokines or TLR ligands that cause anti- or pro-inflammatory activation. Thus, SOCS proteins regulate inflammation through several signaling cascades such as JAK-STAT, ERK, Notch,

phosphatidylinositol-3 kinase (PI3K), mitogen-activated protein kinases (MAPK), and NF-κβ pathways (Wilson, 2014; Wang et al, 2014). SOCS2 has a role in anti-inflammatory macrophages limiting pro-inflammatory activation. Accordingly, IL4 increases SOCS2 expression and macrophages deficient in SOCS2 are more inflammatory (Wilson et al., 2014).

SOCS3 is rapidly induced in macrophages and has distinct roles in shaping macrophage activation and controlling immune and inflammatory responses. Since pro-inflammatory macrophages upregulate SOCS3, it is considered an M1-associated marker. In turn, human monocyte-derived macrophages where SOCS3 has been silenced showed elevated expression of M2 markers and decrease of M1 ones (Arnold et al., 2014). Likewise, murine macrophages with ablation of *Socs3* display a decreased inflammatory response upon LPS stimulation and mice lacking *Socs3* in myeloid cells are resistant to endotoxic shock and have a reduced production of pro-inflammatory cytokines (Kubo et al., 2003; Wilson, 2014). SOCS3 has also a role in phagocytosis and its knockdown enhances the phagocytic capacity of macrophages through PI3K signaling pathway and this increase in PI3K-AKT activity would influence M1-polarization, since PI3K negatively regulates pro-inflammatory cytokine production, enhances IL10 and suppresses response in myeloid cells exposed to LPS (Arnold et al., 2014). Of note, the regulation of pro-inflammatory cytokines for SOCS3 occurs in a gene-specific manner.

Chapter II : Macrophage function

As part of the innate immune response, several functions of myeloid cells, including phagocytosis, wound healing and remodeling tissues, have a role in mediating the inflammatory process. Here, I will briefly review below three of the main macrophage functions, namely, phagocytic activity, migration to reparation/infection foci and inflammation modulation.

It is not clear if all these macrophage functions, could be complemented by non-resident monocyte-derived macrophages or whether specialized macrophage functions are specific to resident macrophage lineages. Peritoneal macrophages represent a widely used model for the study of macrophage functions since the peritoneal cavity serves as a readily accessible source of both monocyte-derived and resident macrophages offering the possibility to study phagocytosis, migration, and inflammation both *in vitro* and *in vivo.*

Phagocytosis and migration

Phagocytosis is an essential process in homeostasis and in immune defense and it consists in the recognition and engulfment of cell fragments, senescent cells or apoptotic cells. Moreover, it is a mechanism utilized by the immune system to eliminate pathogens or foreign particles and the phagocytic process is critical event in the active resolution of inflammation. Dysregulation of phagocytosis can lead to impaired host immune responses to pathogens and may even evolve to chronic inflammation and autoimmune response (Underhill and Goodridge, 2012). A number of cells in the organism have

phagocytic capabilities, however, macrophages are the most important phagocytic cells playing functions on apoptotic cell clearance and pathogen defense (Wynn et al., 2013).

Macrophage polarization modulates their phagocytic capacity. Thus, M1 macrophages produce pro-inflammatory cytokines and promote the killing of bacterial pathogens by increasing bactericidal activity. On the other hand, the M2 phenotype is critical in defense of parasitic infections and tissue remodeling. M1-actived macrophages showed better phagocytic index of nanoparticles than M2 macrophages (Qie et al., 2016). The microenvironment also regulates the phagocytic activity of macrophages; thus, IL10 derived from B cells or other cells in the peritoneum can impair phagocytosis, as well as age-related impair phagocytosis is an IL10-dependent phenomena (Martinez and Gordon, 2014). There are also molecules specific to macrophages that affect their phagocytic activity. For instance, in mice lacking *Pd-1*, macrophages display improved bacterial clearance and mice presented decreased septic mortality (Huang et al., 2009). Moreover, macrophages from *Vim* (-/-) mice, an archetypal mesenchymal gene, had an improved phagocytic function (Mor-Vaknin et al., 2013).

Migration is the fundamental locomotory mechanism for almost all cell types, but it is particularly important for immune cells as they maintain the homeostasis and defense of organism. Macrophages migrate more slowly that other immune cells, however, they respond rapidly *in vivo* and can travel considerable distances to inflammatory foci and they are therefore considered professional motile cells (Pixley, 2012).

When monocytes and macrophages migrate in response to chemotactic stimuli the process is known as chemotaxis. Chemokines are secreted proteins, which act as sentinels at mucosal barriers and for the recruitment of the first line of innate immune effector cells to infection and inflammation foci. Chemokines bind to their respective receptors expressed on the cell surface of leukocytes, and that can be either constitutively expressed or induced in inflammatory conditions, in some cases the microenvironment is regulating their expression levels. Monocytes respond to local stimuli such as cytokines and chemokines that direct migration toward inflammatory sites. Experiments using

mice with targeted deletion of chemokines, demonstrate that hematopoietic circulating cells cannot maintain homeostasis or respond to pathologic conditions (Zamilpa et al., 2011; Le Blanc and Mougiakakos, 2012).

The chemokine CCL2 (also known as monocyte chemoattractant protein 1, MCP-1) is a small secretory protein that plays an important role in the chemotaxis of macrophages towards inflammatory foci and the tumor microenvironment. Its high affinity receptor, CCR2, can modulate HSC exit from the bone marrow and their release into the circulation. Upon extravasation, monocytes differentiate into a subset of monocytes that express CCR2 and are associated with immune defense against infection and the pathogenesis of inflammatory disorders. CCR2 signaling promotes pro-inflammatory monocyte migration into peripheral tissues in response to CCL2 (Italiani and Boraschi, 2014; Deshmane et al., 2009). Binding of CCL2 to CCR2 leads to the internalization of CCL2 and triggers a number of signaling pathways such as PI3K, MAPK, Smad3, PKC and phospholipase C-γ. Stat3 and PI3K participate in endothelial activation associated with diapedesis of leukocytes during inflammation (Fang et al., 2012; Lim et al., 2014). Several signaling pathways that induces vascular permeability and extravasation, act downstream of CCR2; for instance, JAK2, Stat5, and p38MAPK. Thus, both CCL2 and its receptor CCR2 are involved in inflammation and in various diseases (Wolf et al, 2012). In fact, blockade of CCL2-CCR2 signaling is an important therapeutic strategy in both inflammatory disorders and cancer therapy.

Another chemokine that regulates the migration of monocytes and macrophages in homeostasis and pathologic process is the Colony-stimulating factor-1 (CSF1). CSF1 stimulates actin polymerization and subsequent migration. Moreover, the recruitment of macrophages to the proximity of tumors is mediated by CSF1 and CCL2 secreted by tumor cell. Furthermore, these factors are implicated in macrophage migration in several diseases, like arthritis, atherosclerosis, tumor growth, and metastasis (Pixley, 2012) and they, therefore, provide a promising therapeutic target.

In sum, although migration is critical in immune response and homeostasis maintenance, it could also have a negative role in some diseases. In that line, many studies revealed

that reduction in macrophage motility is associated with a reduction in their capacity to enhance tumor cell invasion or inflammatory disorders.

Role of macrophages in inflammation

Once at tissues, macrophages can acquire different functions and phenotypes, which are modulated by signals from the environment. Inflammation occurs in several physiolopathological conditions and diseases. Its development as well as its resolution is closely related to macrophage function.

Septic shock is a systemic inflammation that triggers a multiple organ dysfunction and is produced by bacterial infections or microbial toxins. Lipopolysaccharide (LPS) is the major cell wall component of Gram-negative bacteria that produce this inflammatory disorder. LPS stimulates immune cells through TLR4 interactions to produce several inflammatory cytokines whose overproduction can leads to death (Roger et al., 2009).

Endotoxin tolerance is the phenomenon in which immune cells, primarily monocytes and macrophages, transiently become hyporesponsive or tolerant upon repeated or prolonged exposure to LPS (Rajaiah et al., 2013). During disseminated endotoxin shock and acute sepsis, LPS induces a strong inflammatory response, but macrophages pre-exposed to LPS are hyporesponsive to a second LPS challenge and do not mount a full-fledged pro-inflammatory reaction. Both inflammation and tolerance modulate macrophage functions and cannot be separated from the process of resolving inflammation, to avoid a non-resolving inflammation such as cancer, inflammatory autoimmune diseases, or chronic inflammation that drives ongoing recruitment of monocytes to the inflammatory site (Biswas and Lopez-Collazo, 2009; Pena et al., 2011).

LPS tolerance models indicate that the macrophages have a rudimentary memory that makes them capable of recognizing the structural nature of foreign molecular patterns and discern the history and concentration of foreign stimulants, this can explain the paradigm of endotoxin priming and tolerance (Seeley and Ghosh, 2016).

In a pivotal study, Freudenberg and Galanos (1998) demonstrate that macrophages have an essential role of in LPS-tolerance induction through a mice model defective for the LPS signaling receptor. When these mice received adoptive transfer of LPS-sensitive macrophages from a wild-type mouse, they became susceptible to lethal challenges of LPS. However, when transplanted mice were first challenged with non-lethal doses of LPS and then subjected to a lethal dose of LPS, all mice survived, thereby showing that macrophages are the primary mediators of endotoxin tolerance (Freudenberg and Galanos, 1988, Biswas et al., 2007; Deng et al., 2013).

Subsequent *in vitro* studies have shown the induction of endotoxin tolerance in human monocytes and macrophages with reduced TNF expression. Likewise, compared to monocytes from healthy donors, those from sepsis patients showed an increase in the expression of anti-inflammatory cytokines like IL10 and TGFβ (Adib-Conquy et al., 2006). Consequently, endotoxin tolerance is considered to be a physiological negative feedback response that protects the host against uncontrolled inflammation.

There are two classes of genes involved in tolerance, "tolerizable genes" that are abrogated in tolerance including *TNFα*, and "non-tolerizable genes" that are upregulated in tolerance and include anti-inflammatory and wound repair genes, such as *IL10* and *matrix metalloproteinase 9* (*MMP9)* (Shalova et al., 2015; Alvarez-Errico et al., 2015)**.**

Chapter III : The tumor microenvironment

Within both healthy tissues and solid tumors it is possible to distinguish the functional section or parenchyma from the supporting stroma, being both separated by the basal lamina. The stroma includes a wide array of cell types including endothelial cells, perivascular cells, adipocytes, fibroblasts, and immune cells, especially macrophages. In tumors, the stroma is often referred as the tumor microenvironment (TME) and becomes invaded by tumor cells once the basal lamina is disrupted. Stromal cells in the TME interact closely with tumor cells and mutually affect each other. For instance, factors released by the TME can either promote or inhibit tumor cell survival, invasiveness, and metastatic dissemination, as well as access and therapeutic responsiveness (Turley et al, 2015).

In turn, malignant cells activate macrophages and fibroblast in the TME that changes constantly during tumor progression according to the oncogenic signals it receives from the tumor (Kim eta al., 2007). Different stimuli like hypoxic conditions, growth factors, and immunosuppressive cytokines supplied by the TME, endow tumor-associated macrophages (TAMs) with pro-tumor characteristics that facilitate tumor development. The capacity of carcinomas to recruit and activate TAMs largely depends on malignant cells having acquired an undifferentiated phenotype with loss of epithelial markers and expression of mesenchymal markers as part of the so-called epithelial-to-mesenchymal transition (EMT). In turn, tumor cells, particularly those than have undergone an EMT secrete factors that modulate and activate cells in the TME (Su et al., 2014).

In epithelial tissues that have dedifferentiated and undergone EMT, cells at the invasive tumor edge secrete cytokines, chemokines, growth factors and proteases that promote angiogenesis, remodel the extracellular matrix and can activate stromal cells (Rosen and Jordan, 2009).

Tumor-associated macrophages

TAMs are the largest component of the TME and despite being a highly heterogeneous population, they share some characteristics with M2 macrophages, such as wound healing and angiogenic proprieties. Nevertheless, the transcritpome of M2 macrophages and TAMs is not completely overlapping (Xue et al., 2014). It is possible to find different TAMs populations within the same tumor with a combination of both pro-inflammatory and anti-inflammatory gene expression. Moreover, macrophages involved in cancer-initiating inflammatory process may begin acting as anti-tumoral cells, however, once tumors are established, macrophages are educated to become pro-tumoral (Franklin et al., 2014; Noy and Pollard, 2014).

The mechanisms by which macrophages switch from a tumor suppressing phenotype to tumor promoting one are not fully understood. It has been suggested that environmental signals such as secreted tumor factors or hypoxia may mediate this transition. TAMs accumulate in regions of hypoxia within growing tumors, and their recruitment is mediated by an upregulation of macrophage chemoattractants (Wen et al., 2015). CCL2 is secreted in response to a variety of inflammatory stimuli; however, the primary source of CCL2 is unclear. It is possible that locally produced CCL2 derived from tumor or stromal cells enters the systemic circulation. In most tumor cells, CCL2 expression is positively correlated with monocyte infiltration. These monocytes can be polarized to an anti-inflammatory/pro-angiogenic phenotype becoming in TAMs that can promote immunosuppression in the tumor niche. Furthermore, CCL2 blocks apoptosis and enhanced migration in mammary carcinoma cells. Clinical evidence shows that elevated levels of CCL2 associate to poor prognosis in most of cancers (Ostuni et al., 2015).

TAM accumulation in the TME also correlates with angiogenesis and the subsequent acquisition of an invasive phenotype (Figure 3). At the same time, angiogenesis is facilitated by TAM-derived proteases (e.g. matrix metalloproteinases, plasmin, urokinase-type plasminogen activator/uPA and urokinase-type plasminogen activator receptor/uPAR) that are released in tumor sites, as extracellular proteolysis, which is a

requirement for blood vessel formation. For example, TAM-derived MMP9 induces the release of vascular endothelial growth factor-α (VEGFα) that is crucial for the angiogenic switch.

These enzymes also facilitate tumor invasion reorganizing the extracellular matrix and degrading the basement membrane. Moreover, inhibition of the MMP9 in macrophages blocked the release of VEGF and thereby inhibited angiogenesis and tumor growth in a cervical cancer mouse model (Ebrahem et al., 2010; Guiraudo et al., 2004). Likewise, expression of hypoxia-inducible factor (HIF1α) in cells in response to hypoxia promotes the expression of VEGF, matrix metalloproteinase 7 (MMP7), and MMP9 in TAMs (Hagerling et al., 2015; Condeelis and Pollard, 2006). Other example is Wnt Family Member 5A (WNT5A) that participate in Wnt/β-catenin-independent pathway, in macrophages induce a tolerogenic phenotype and is associated to transition from tumoricidal to tumor-promoting TAM profile (Pukrop et al., 2006; Bergenfelz et al., 2012).

ZEB1 and EMT

EMT plays an important role during embryonic development, and it also contributes in tumor initiation and progression. Tumor cells undergoing EMT acquire a pro-invasive and stem-like phenotype and exhibit enhanced self-renewal properties, increased tumorigenic potential and increased chemotherapy resistance. Expression of EMT markers in tumors correlates with poorer prognosis (Tsai and Yang, 2013).

EMT is driven by transcription factors of the TWIST, SNAIL, and ZEB families (Nieto et al., 2016). Of all EMT factors, the two members of the ZEB family, ZEB1 and ZEB2, present the best inverse correlation with epithelial markers and often function as

downstream effectors of Snail and Twist factors (Taube et al., 2010). ZEB1 (also known as δEF1), which is expressed by malignant cells at the invasive front of carcinomas is a key inducer of EMT in cancer cells. ZEB1 inhibits the terminal differentiation of a number of cell types (e.g., epithelial cells, myoblasts, chondroblasts, osteoblasts), and its levels need to be downregulated for differentiation to occur (Brabletz and Brabletz, 2010; Siles et al., 2013).

Despite ZEB1 has never been studied in myeloid cells, other EMT transcription factors have shown modulate myeloid differentiation or activation. Since, Snail and Twist have a role in anti-inflammatory macrophages (Zhang et al., 2014; Zheng et al., 2015), and ZEB2 regulates dendritic cells development (Scott et al., 2016) it was expected that ZEB1 would be playing a role in myeloid cells. Therefore, I decided to inquire whether ZEB1 is expressed and has a role in macrophage activation and function. ZEB1 contains multiple independent domains to interact with other transcriptional regulators and thus ZEB1 directly activates or represses gene expression by binding to the regulatory regions of its target genes (Postigo and Dean, 1999; Postigo et al., 2003)

Macrophages are localized primarily at the periphery of the TME and around blood vessels but decrease in number toward the center (Lewis and Pollard, 2006; Quail and Joyce, 2013). These observations suggest that TAMs modulate the phenotype of tumor cells located in the neighboring microenvironment and the occurrence of EMT in tumors may, therefore, be transient and highly dependent on the local microenvironment.

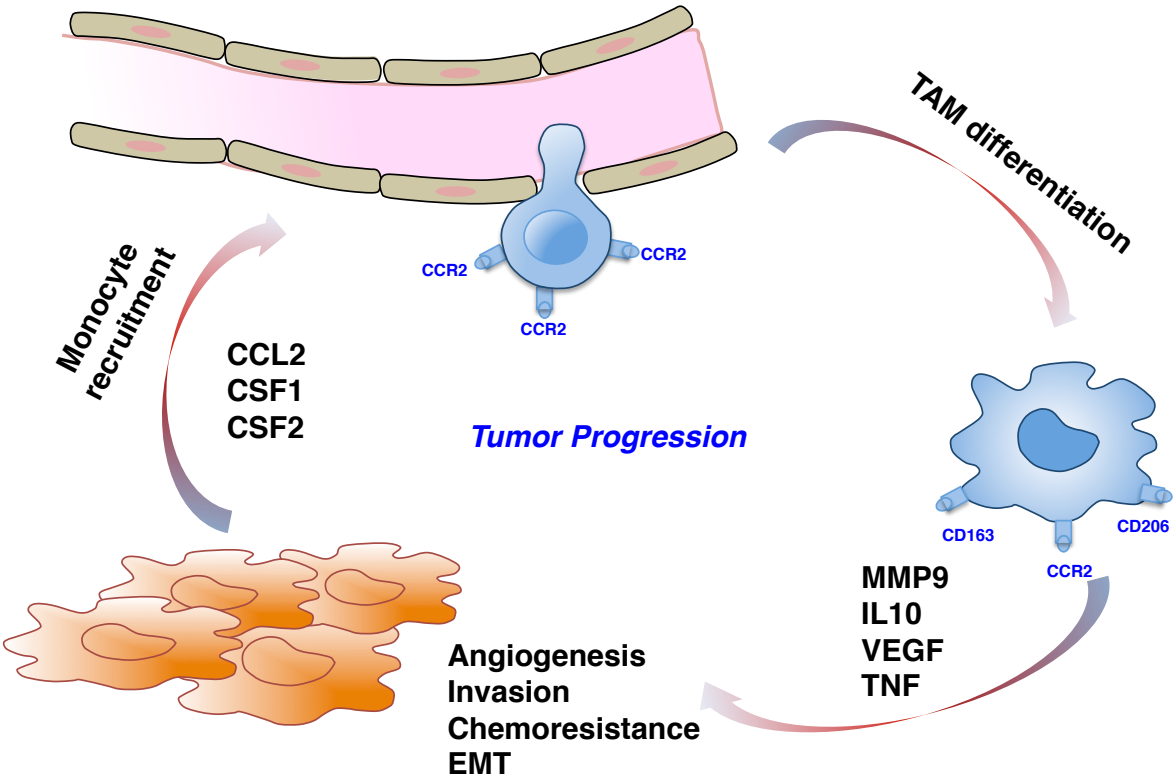

***Figure 3*. Crosstalk between cancer cells and myeloid cells in the TME.** The TME is essential for tumor growth and invasion through chemokine signaling from tumor cells that recruit immature monocyte that later mature into TAMs to promote tumor aggressiveness.

This relation between EMT and immune cells infiltration is the hallmark of many cancer types, including *inter alia* ovarian, pancreatic and prostate carcinoma.

Ovarian Cancer

Epithelial ovarian cancer (EOC) is the seventh most frequent cancer diagnosed in women accounting approximately 140,000 deaths and 200,000 patients being diagnosed annually worldwide (Brown and Palmer, 2009). EOC has a poor prognosis largely because of the presence of local and distant metastases in the majority of patients at diagnosis. Treatment options for late-stage disease are limited since despite a positive response to

platinum-based therapies, eventually, patients become resistant to chemotherapy (Lengyel, 2010; Liu and Matulonis, 2014).

Ovarian carcinomas are classified in different histological subtypes, with the high-grade serous ovarian carcinoma (HGSC) as the predominant OC (80-85%), followed by endometrioid tumors (10% of cases), while clear cell and mucinous carcinomas are rarer. These histological subtypes correspond to different epidemiological and, mutational characteristics, sites of origin and response to chemotherapy (Hasan et al., 2015). HGSC has a poorly differentiated phenotype and is highly proliferative; and given the lack of early symptoms, if is most often diagnosed advanced clinical stages (III and IV), and has therefore poor prognosis and survival rates (Chen, et al., 2014). HGSCs lines are widely used in ovarian cancer research, and of late it has been demonstrated the association among ZEB factors and *in vivo* tumor growth using a panel of these HGSCs lines (Medrano et al., 2017).

Advanced OCs develop peritoneal ascites, which contributes to the dissemination and spread of tumor cells throughout the peritoneal cavity. Ascitic fluid is also implicated in resistance to chemotherapy (Kipps et al., 2013). Chronic inflammation during the development of ovarian cancer is a key factor in tumor progression as it prevents the maturation of myeloid cells and promotes their immunosuppressive polarization. In patients with advanced OC, it is possible to detect TAMs in the primary lesion as well as in the ascitic fluid, and are associated with worst prognosis and tumor dissemination in the peritoneal cavity (Reinartz et al., 2014).

As in other cancers, TAMs are the most abundant leukocytes cells infiltrating in human ovarian tumors. Pro-tumor TAMs expressing pro- and anti-inflammatory markers such as CD163 and CD206 are recruited from circulating monocytes by ovarian tumors that express chemoattractant factors CCL2 and CSF1 (Colvin, 2014). CCL2 is overexpressed in ovarian tumor cells, but not in TAMs, also CSF1 expression is higher in malignant cells. Indeed there is a strong correlation between the number of infiltrating TAMs and the malignancy of OC. Likewise, peripheral blood monocytes and ascitic TAMs in

women with ovarian cancer have a dedifferentiated phenotype compared to cells from healthy. The expression of M2-markers or cytokines produced by TAMs are prognostic factors of poorer prognosis in human ovarian cancer. Thus, both CD163 and IL10 are correlated with progression-free survival and higher tumor grade (Colvin et al., 2014).

TAMs form spheroids and secrete cytokines that promote the lymphangiogenesis process (Zhang and Thian, 2014; Yin et al., 2016). Co-culture experiments or culture with conditioned medium have shown that ovarian tumor cells can polarize macrophages towards an M2-protumoral phenotype, while TAMs can modulate ovarian cancer cells to more aggressive and chemoresistant phenotype, indicating the importance of this relation tumor cell-TAM in ovarian cancer progress (Lengyel, 2010; Colvin, 2014). Altogether, this evidence prompted me to use ovarian cancer as the experimental model for my PhD project.

Ovarian Cancer models

In xenograft cancer models, cells are injected into immunocompromised mice such as nude, SCID or NOD/SCID to enable the cells to engraft without being eliminated by the immune system (Bobbs et al., 2015). However, this model has some disadvantages, as it does not reflect what happens in clinical practice since the tumor is not located on the same site or in contact with peritoneal microenvironment, and immune response cannot be studied.

Patient derived xenografts (PDX) models use human tumor engrafted in immunodeficient mice. This model offers a powerful tool to recapitulate woman ovarian cancer patient histotype with whole genome expression and evaluate accurately treatment response. Nevertheless PDX has the drawback that require the use of immunodeficient mice where it is not possible to study the role of the immune system and the tumor-

stroma crosstalk, it is difficult to achieve tumor engraftment and it is more costly and time-consuming than other models (Siolas and Hannon, 2013).

Some of these disadvantages can be overcome in syngeneic models, which use immunocompetent mice where mouse ovarian surface epithelial (MOSE) cells are isolated from the ovaries of wild-type normal mice then cultured *in vitro* for a prolonged period until to be spontaneously transformed or by inserting genetic modifications in healthy cells. These transformed cells are injected into recipient mice and will be able to form tumors. This model provides the opportunity to study the tumor microenvironment, tumor-stromal cells crosstalk, tumor-secreting factors and immune cell infiltration. Likewise, some syngeneic models use genetically modified cells and highly metastatic cell lines stably expressing luciferase for monitoring disease (Fong and Kakar, 2009). Overall, syngeneic models present tumors with similar histopathologic characteristics those observed in women with ovarian cancer as also development of closely resembling human disease. Roby et al. (2000) isolated and culture MOSE cells, which spontaneously were transformed *in vitro* with repeated passages. This is the origin of ID8 cell line that has been widely used as an experimental mouse model of ovarian cancer as it resembles the late metastatic stage of human HGSC (Roby et al., 2000). Like in human HGSC, ID8 tumor deposits are highly infiltrated with immune cells, mainly macrophages.

This ID8 model is particularly useful to study of interactions between tumor cells and their microenvironment, ID8 injected into the ovarian bursa of C57BL/6 mice showed that interaction between tumor cells and the ovarian stroma results in increased expression of proliferative and survival markers, including phosphorylated Akt, proliferating cell nuclear antigen, and Bcl-2 (Greenaway et al., 2008). *In vivo* passages of ID8 cells into naive mice increased their aggressiveness as defined by a shorter lag to develop both tumor and ascites and enhanced morbidity (Cai et al., 2015). Both studies highlight the interplay between tumor cells and their microenvironment in the modulation of tumor cell properties.

OBJECTIVES

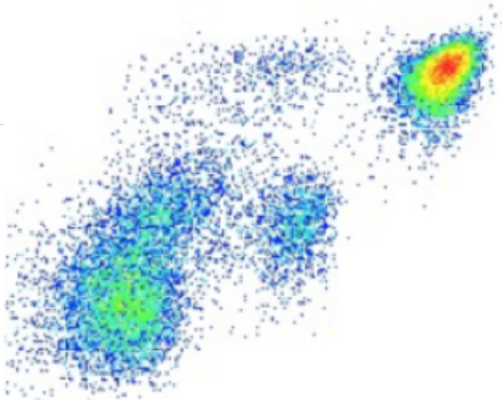

This dissertation aimed to study the role of ZEB1 in macrophages and had two specific objectives:

1. Characterize the expression and function of ZEB1 in macrophages during monocyte-macrophage differentiation and in macrophage homeostasis and activation.

2. Characterize the expression and function of ZEB1 in tumor-associated macrophages and in their crosstalk with cancer cells.

To address these goals, I used a wide number of techniques, namely, high throughput analysis (RNA sequencing) and different functional assays in a transgenic mouse model harboring the deletion one *Zeb1* allele [*Zeb1* (+/-)] and the ID8 syngeneic mouse model of ovarian cancer.

METHODS

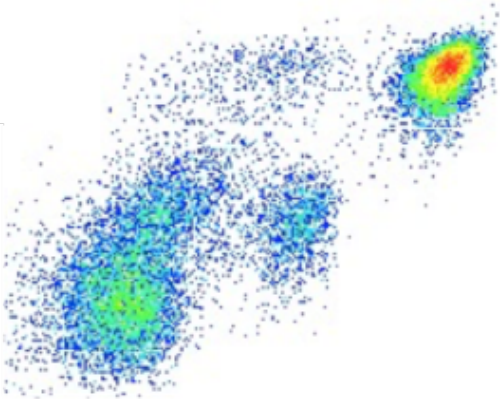

Antibodies

Antibodies used in this article originated as follows: anti-human/mouse ZEB1 (Clones H-102 and E-20, Santa Cruz Biotechnology, Dallas, TX, USA), anti-mouse β-Actin (Clone C4, Santa Cruz Biotechnology), anti-mouse F4/80 conjugated to APC (clone BM8, reference 17-4801; Bioscience Inc., San Diego, CA, USA), anti-mouse CD11b conjugated to PE (clone M1/70.15, reference 22159114; Immuno Tools GmbH, Friesoythe, Germany), anti-mouse CD45 conjugated to PerCP/Cy5.5 (clone 30-F11, reference 103131; BioLegend, San Diego, CA, USA), anti-human ZEB1 (clone HPA027524, Sigma-Aldrich, St. Louis, MO, USA), anti-human CCL2 (clone 2D8, Invitrogen, Thermo Fisher, Carlsbad, CA, USA), anti-human CD163 (clone 10D6, Leica Biosystems, Newcastle Upon Tyne, UK), anti-human CCR2 (clone 48607, R&D Systems, Minneapolis, MN, USA) and anti-human MMP9 (clone E-11, sc-393859, Santa Cruz Biotechnology).

In addition, the study used the following secondary antibodies peroxidase-AffiniPure donkey anti-Mouse IgG (H+L) (reference 715-035-151), peroxidase-AffiniPure goat Anti-Rabbit IgG (H+L) (reference 111-035-144) and mouse gamma globulin (reference 015-000-002), all purchased from Jackson ImmunoResearch Europe (Newmarket, UK).

Mouse models

Wild-type C57BL/6J and *Lyz2Cre* mice were obtained from Jackson Laboratories (Bar Harbor, ME, USA). Mice heterozygous for *Zeb1* (*Zeb1* (+/-) mice) were obtained from Dr. Douglas S. Darling (University of Louisville, KY, USA) and Dr. Y. Higashi (Institute for Development Research, Kasugai-shi, Aichi, Japan) (Takagi et al., 1998). $Socs3^{f/f}$ and $Socs2^{-/-}$ mice were obtained from D.J. Hilton (Royal Melburne Hospital, Victoria, Australia). All animal procedures were approved by Animal Experimentation Ethics Research Committee at the University of Barcelona.

Isolation and culture of normal mouse primary cells

Bone marrow total cells (BMTCs) were obtained from 6-8 weeks-old C57BL/6 wild-type and *Zeb1* (+/-) mice (Takagi et al., 1998) and differentiated into macrophages as described (Zhang et al., 2008). Briefly, femur and tibia bone marrows were flushed with Phosphate buffered saline (PBS) and BMTCs collected were centrifuged and resuspended fin Dulbecco's modified Eagle Medium (DMEM) (Lonza, Basel, Switzerland) supplemented with 10% FBS (Sigma-Aldrich. St. Louis, MO), and 1% penicillin-streptomycin (Pen/Strep) (Lonza), medium hereafter referred as complete medium. To generate bone marrow–derived macrophages (BMDM), BMTCs were cultivated with 20 ng/ml of recombinant M-CSF (ImmunoTools GmbH, Friesoythe, Germany) during 6 days. Every 2 days, half of the medium was replaced with fresh medium supplemented with M-CSF. Identical results were obtained when BMTCs were cultivated with 40% of supernatant from L929 culture cells (ATCC, Manassas, VA, USA) stably transfected with M-CSF expression vectors.

Peritoneal macrophages were isolated from 6-8 week-old *Zeb1* (+/+) and *Zeb1* (+/-) mice as per standard protocols (Zhang et al., 2008). Briefly, mice were euthanized and the peritoneal cavity was washed twice with 6 ml of ice-cold PBS supplemented with 3% FBS. Cells from the peritoneal lavage were centrifuged at 400 x g for 10 min at 4ºC and erythrocytes in the cell suspension were osmotically lysed by incubation with Red Blood Cell Lysis Buffer (Sigma-Aldrich), followed by washing with PBS and resuspension in PBS or complete medium. Peritoneal cells were then sorted for F4/80 and CD11b cell surface expression and isolated cells were then either examined for mRNA or cell surface markers expression or tested for the indicated functional assays.

Isolation and culture of human primary cells

Use of human samples was approved by the Ethics Committee for Clinical Experimentation at Hospital Clinic of Barcelona (Barcelona, Spain). Peripheral blood

mononuclear cells were obtained from buffy coats extracted from healthy donors and were separated by density gradient centrifugation with Lymphocyte Separation Medium (Lonza, Basel, Switzerland). Monocytes were purified from total PBMCs by magnetic cell sorting with Dynabeads® CD14 (Dynal®, Thermo Fisher, Waltham, MA, USA). Purified human monocytes (> 92% $CD14^+$) were cultured for 7 days in RPMI 1640 (Lonza) supplemented with 10% FBS (Sigma-Aldrich. St. Louis, MO), 1% penicillin-streptomycin (Pen/Strep) (Lonza) and 20 ng/ml of human recombinant M-CSF/CSF1 (ImmunoTools) or human recombinant GM-CSF/CSF2 (ImmunoTools GmbH).

Flow cytometry analysis and sorting (FACS)

Cells were first blocked for Fc receptors with mouse gamma globulin (Jackson ImmunoResearch Europe). Cells were then incubated in PBS with 2% FCS for 45 min at 4˚C with the corresponding fluorochrome-labeled antibodies. Expression of cell surface proteins was assessed in a BD FACSCanto™ II analyzer (BD Biosciences, San Jose, CA, USA). Wherever indicated, cells were sorted for specific subpopulations in a FACS Aria™ II cell sorter (BD Biosciences) for subsequent experimentation. The acquired data were analyzed using FlowJo for Windows, version 7.6.1 (FlowJow, Ashland, OR, USA).

RNA extraction and quantitative real time PCR

Total RNA was extracted with RNAzol® RT reagent (Sigma-Aldrich) or TRIzol® (Life Technologies, Thermo Fisher Scientific) and reverse transcribed with oligodT using High-Capacity cDNA Reverse Transcription Kit (Life Technologies, Thermo Fisher Scientific). mRNA levels were then determined by quantitative real-time PCR (qRT-PCR) at 60 ºC using GoTaq® qPCR Master Sybr Green Mix (Promega Corp., Madison, WI, USA). Results were analyzed using Opticon Monitor 3.1.32 software (Bio-Rad,

Hercules, CA, USA) by ΔΔCt method and normalizing values with respect to mouse *Gapdh* or human *GAPDH* housekeeping gene. DNA primers used in qRT-PCR were purchased from Sigma-Aldrich and their sequences are described in Table 1. The nomenclature for mouse and human genes adheres to MGI (Mouse Genome Informatics, http://www.informatics.jax.org/) and HGNC (HUGO Gene Nomenclature Committee, http://www.genenames.org/), respectively.

Target gene	**Forward 5' → 3'**	**Reverse 5' → 3'**	**Ref**
Aldh1a1	GACAGGCTTTCCAG ATTGGCTC	AAGACTTTCCCACC ATTGAGTGC	Levi et al.,2009
Ccl2	GGGATCATCTTGCT GGTGAA	AGGTCCCTGTCATG CTTCTG	Aurora et al., 2014
Ccr2	AGCACATGTGGTGA ATCCAA	TGCCATCATAAAGG AGCCA	Kitamoto et al., 2013
Cd163	TGTATGCCCTTCCTG GAGTC	TGTGCAGTGTCCAA AAGGAG	Li et al., 2015
Cdh1	AGACTTTGGTGTGG GTCAGG	ATCTGTGGCGATGA TGAGAG	Lin et al., 2012
Gapdh	CGACTTCAACAGCA ACTCCCACTCTTCC	TGGGTGGTCCAGGG TTTCTTACTCCTT	De Freitas et al., 2012
Il1b	TGACGTTCCCATTA GACAACTG	CCGTCTTTCATTACA CAGGACA	Arnold et al., 2007
Cxcl15/Il8	AGAGGCTTTTCATG CTCAACA	CCATGGGTGAAGGC TACTGT	Zhang et al., 2017
Il10	TGTCAAATTCATTC ATGGCCT	ATCGATTTCTCCCCT GTGAA	Kwon et al., 2014
Kit	GACGCAACTTCCTT ATGATC	TGGTTTGAGCATCTT CACGG	Leong et al., 2008
Mdr1	TCCACAGAAAGCAA GACCAAGAG	CCAGAGGCACATCT TCATCCA	Rankin et al., 2006
Mmp9	TAAGGACGGCAAAT TTGGTT	CTTTAGTGGTGCAG GCAGAG	Nakasone et al., 2012
Mrc1	AAGGCTATCCTGGT GGAAGAA	AGGGAAGGGTCAGT CTGTGTT	Colegio et al., 2014
Nfkb1	GAACGATAACCTTT GCAGGC	TTTCGATTCCGCTAT GTGTG	Eisele et al., 2013
Retnla	GCTGATGGTCCCAG TGAATAC	CCAGTAGCAGTCAT CCCAGC	Arranz et al., 2012
Tnf	TTTCGATTCCGCTAT GTGTG	CCACCACGCTCTTCT GTCTAC	Eisele et al., 2013
Vegf	AATGCTTTCTCCGCT CTGAA	GATCATGCGGATCA AACCTC	Wei et al., 2015
Vim	CCAACCTTTTCTTCC CTGAA	TGAGTGGGTGTCAA CCAGAG	Olmeda et al., 2007
Zeb1	AACTGCTGGCAAGA CAAC	TTGCTGCAGAAATT CTTCCA	Siles et al., 2013
hZEB1	AGCAGTGAAAGAGA AGGGAATGC	GGTCCTCTTCAGGT GCCTCAG	Sanchez Tillo et al., 2011

hGAPDH	TGCACCACCAACTG CTTAGC	GGCATGGACTGTGG TCATGAG	Sanchez Tillo et al., 2011
hCD163	AGGATGCTGGAGTG ATTTGC	CCAGCCGTCATCAC ATATTG	Medina et al., 2011
hWNT5A	CTTGGTGGTCGCTA GGTATG	TCGGAATTGATACT GGCATT	Keller et al., 2008

Table 1. Primers used in qRT-PCR assays

RNA interference and stable transfection of mouse and human primary cells

Mouse and human macrophages were transfected with 200 nM of either siRNA control or siRNAs specific against mouse *Zeb1* or human *ZEB1* with Lipofectamine® RNAimax (Thermo Fisher, Waltham, MA) as per manufacturer's instructions. siRNA oligonucleotide duplexes were purchased from Sigma-Aldrich and their sequences are detailed in Table 2.

Zeb1 was overexpressed in peritoneal macrophages by transduction of lentiviral particles generated from a plasmid encoding for mouse *Zeb1* (LP-Mm05622-Lv103-0200-P) (Tebu-bio, Le-Perray-en-Yvelines, France) kindly provided by Dr D.C. Dean (University of Louisville, Louisville, KY, USA).

siRNA	Gene Targeted	Sense strand sequence	Reference
siCtl	N/A	UAUAGCUUAGUUCGUA ACCTT	Siles et al., 2013
si*Zeb1*-A	Mouse *Zeb1* & Human ZEB1	AACUGAACCUGUGGAU UAUTT	Siles et al., 2013
si*Zeb1*-B	Mouse *Zeb1*	GACCAGAACAGUGUUC CAUGUUUAATT	Siles et al., 2013

Table 2. siRNA oligonucleotide sequences

RNA sequencing and data analysis

Peritoneal macrophages ($CD45^+$, $CD11b^+$, $F4/80^+$) from *Zeb1* (+/-) and *Zeb1* (+/-) 6-to-8-weeks old female mice—6 for each genotype—were isolated and their RNA extracted using RNAzol® RT reagent (Sigma-Aldrich) as per manufacturer's instructions. RNA was quantified and its quality (RNA integrity numbers ≥ 8.5) assessed on a Agilent 2100 Bioanalyzer (Agilent, Santa Clara, CA, USA). Part of the RNA samples were reverse transcribed as described above to examine *Zeb1* expression. To obtain at least 1 µg of RNA required in the preparation of libraries in triplicate, two samples from each genotype were pooled.

Libraries construction and RNA sequencing was performed at the Centro Nacional de Regulacion Genomica (Barcelona, Spain). Libraries were prepared from total RNA with the TruSeq®Stranded mRNA LT Sample Prep Kit (Illumina Inc., San Diego, USA Rev.E, October 2013). Briefly, 0.5 µg of total RNA was used for poly-A based mRNA enrichment with oligo-dT magnetic beads. The mRNA was fragmented (resulting RNA fragment size was 80-250nt, with the major peak at 130nt) and the first strand cDNA synthesis was done by random hexamers and reverse transcriptase. The second strand cDNA synthesis was performed in the presence of dUTP instead of dTTP, to achieve the strand specificity. The blunt-ended double stranded cDNA was 3´adenylated and Illumina indexed adapters were ligated. The ligation product was enriched with 15 PCR cycles and the final library was validated on an Agilent 2100 Bioanalyzer with the DNA 7500 assay. Libraries were sequenced on HiSeq2000 (Illumina, Inc) in paired-end mode with a read length of 2 x 76bp using TruSeq SBS Kit v3-HS.

Over 20 million paired-end reads were generated for each sample in a fraction of a sequencing flowcell lane, following the manufacturer's protocol. Image analysis, base calling and quality scoring of the run were processed using the manufacturer's software Real Time Analysis (RTA 1.13.48) and followed by generation of FASTQ sequence files by CASAVA. Reads were mapped against the mouse reference genome (GRCm38) with STAR (Dobin and Gingeras, 2015) using the ENCODE parameters for long RNA. Gene

quantification was performed with RSEM (Li and Dewey, 2011) with default options and gencode version 11 mouse annotation. Normalization and differential expression analysis was done with edgeR (Robinson et al., 2010) with default options. GO and KEGG enrichment analyses were performed with the beta version of DAVID database (http://david.ncifcrf.gov/).

All 412 differentially expressed (DE) genes were grouped in a Hierarchical clustering with Genesis software (http://genome.tugraz.at, Sturn et al. 2002) and some of them were examined using the gene-gene and gene-protein network tool GeneMANIA plataform (Mostafavi et al., 2008).

Western blot

Peritoneal macrophagess were harvested, washed with ice-cold PBS and resuspended in RIPA lysis buffer (150 mM NaCl, 50 mM Tris pH 8, 1 % NP40, 0.5 % SDS, 2 mM EDTA) containing protease inhibitors (10 μg/ml aprotinin, leupeptin, pepstatin A and PMSF) as previously described (Sánchez-Tilló et al., 2011). Lysates were sonicated in an Ultrasonic Liquid Processor (Misonix Inc.), clarified by centrifugation and quantified by Bradford assay. Lysates were then boiled and loaded onto 10 % polyacrylamide gels and transferred to a PVDF membrane (Immobilon-P, Millipore, Bedford, MA, USA). Membranes were blocked with 5% non-fat milk and blotted with the indicated primary antibodies overnight at 4 ºC. Detection was done after incubation with HRP-conjugated secondary antibodies. Reaction was developed with SuperSignal West Pico Chemilluminescent Substrate (Thermo Fisher Scientific).

In vivo phagocytosis assay

5×10^6 ID8-GFP cells or ID8 labeled with CFSE cells were injected into the peritoneal cavity of *Zeb1* (+/+) and *Zeb1* (+/-) mice. Mice were euthanized 3-4 h later and peritoneal exudate cells were collected by lavage with 6 ml of ice-cold PBS supplemented with 3% FBS twice. Cells were then analyzed in a BD FACSCanto™ II analyzer (BD Biosciences) and *in vivo* phagocytosis was determined by the percentage of GFP^+ cells out of the total of those previously gated as positive for F4/80.

In vitro macrophage migration

In vitro migration of macrophages was assessed through two approaches. First, using a wound-healing assay. Briefly, 1 x 10^6 peritoneal macrophages in complete medium were seeded in 6-well plates and incubated overnight. A defined wound field was then created with a pipette tip and cell migration across the gap was monitored by light microscopy (Olympus, Hicksville, NY) for up to 24 h.

Secondly, macrophage migration was examined with a Transwell® migration assay. Briefly, 0.5 x 10^6 peritoneal macrophages were labeled with 5 mM Carboxy-fluorescein diacetate succinimidyl ester (CFSE, Sigma-Aldrich). After washing once with complete medium and thrice with PBS, cells were resuspended in 200 µl of DMEM supplemented with 2.5% FBS and added on top of 6.5 mm diameter/8 µm pore polycarbonate Transwell® inserts (Corning Inc., Tewksbury, MA, USA), which in turn were placed over a 24-well plate. The lower chamber was filled with 0.6 ml of complete medium containing 80 ng/ml mouse recombinant CCL2 (mrCCL2) (ImmunoTools GmbH).

After 2 hrs, macrophage migration was assessed by the CFSE fluorescence signal measured in a Modulus II GloMax®-Multi-Detection System microplate reader

(Promega Corp., Madison, WI, USA). Macrophage migration was then expressed as relative fluorescence units (RFU) with respect to a 100% value represented by the fluorescence of the cell suspension initially loaded on top of the Transwell® insert. RFU values are expressed as the mean with their standard errors of five mice for each genotype.

In vivo migration

Briefly, for *in vivo* migration of myeloid precursors and macrophages, bone marrow total cells (BMTCs) or bone marrow-derived macrophages (BMDMs) from *Zeb1* (+/+) and *Zeb1* (+/-) mice were first labeled with CFSE. Wild-type mice were then injected i.p. with 1 ml of 3% thioglycollate (Sigma-Aldrich) before either 2-3 x 10^7 CSFE-labeled BMTCs or 5-6 x 10^6 CSFE-labeled BMDMs were then injected i.v. into these *Zeb1* (+/+) recipients. After 48 h mice were sacrificed and the mobilization and recruitment of these cells into the peritoneal cavity was then assessed by CSFE expression in peritoneal lavage cells by FACS analysis.

In vivo monocyte maturation

In vivo monocyte maturation was carried out as described (Tsou et al., 2007). Briefly, bone marrow total cells (BMTCs) from *Zeb1* (+/+) and *Zeb1* (+/-) mice were first labeled with CFSE. 2-3 x 10^7 CSFE-labeled BMTCs were inoculated i.v. into *Zeb1* (+/+) recipients. For *in vivo* mobilization and differentiation of myeloid precursors into macrophages, either 1 ml of conditioned medium from L929/M-CSF cells or 1 μg of recombinant CCL2 (Peprotech) were inoculated i.p. into 6-8 weeks-old *Zeb1* (+/+) and *Zeb1* (+/-) mice. The mobilization of monocytes into the peritoneal cavity and their maturation into macrophages was followed up at different time points up to 7 h by FACS analysis.

Endotoxic shock and tolerance susceptibility

Zeb1 (+/+) and *Zeb1* (+/-) mice, weighing ~20 g each (6–10 weeks old. A single high dose of LPS (*Escherichia coli* 055:B5**,** Sigma-Aldrich), 0.5 mg LPS x 25g mouse was used and given i.p. and survival was monitored for 72 h. For induction of Endotoxin Tolerance were used two doses, 1st dose LPS: 100μg LPS x 25g mouse and a 2nd dose 24 h Later: 200 μg LPS x 25 g mouse. i.p., and survival was monitored for 120 h.

Isolation and culture of tumor associated macrophages

To generate conditioned medium (CM) from peritoneal macrophages and TAMs, both cells types were sorted by flow cytometry and 5 x 10^5 cells cultured on ultra-low attachment 6-well plates (Costar, Corning) during 24 h in 2 ml DMEM supplemented with 2% FBS. The CM was then collected and dialyzed overnight against PBS. Wherever indicated the CM was concentrated in a high retention dialysis tubing (Sigma-Aldrich) with poly-ethylene glycol 20,000 mw (Thermo Fisher Scientific) as per standard protocols.

Chromatin Immunoprecipitation Assays

Chromatin immunoprecipitation (ChIP) assays were performed using EpiQuick ChIP kit (Epigentek Group Inc, NY, USA) as per manufacturer's instructions. Briefly, 1.5 x 10^7 bone-marrow derived macrophages were incubated during 10 min with 1% formaldehyde solution (Electron Microscopy, PA, USA) at room temperature followed by incubation with 1.25 mM glycine. Lysates were sonicated as described elsewhere (Sanchez-Tillo et al., 2011). Goat anti-mouse/human ZEB1 (E-20) and its corresponding normal goat IgG (Jackson ImmunoResearch) were used.

Identification of DNA binding sequences for ZEB1 and design of primers for qRT-PCR was conducted using MacVector software (MacVector Inc, Apex, NC, USA). DNA fragments were quantified by qRT-PCR as detailed above using the primers detailed in Table 3. In all qRT-PCRs, values shown represent relative binding in relation to input and are the average of at least three independent ChIP experiments, each one performed in triplicate.

Promoter Region	Forward 5' → 3'	Reverse 5' → 3'
Ccr2 promoter ZEB1 binding site (-868 bp &-818bp) (-868/-772 bp)	CAGGTGCCAATGGA GTTCAAA	CCCAAGTTGATTTC CTATACCC
Ccr2 promoter Non ZEB1 binding sites (NBS) (574/-422 bp)	AGAATGCTTTTGGGT ACAATGAA	GTGTAGCATAGGCT TTATGCTTGG

Table 3. Primers used in qRT-PCR for ChIP assays

Culture of ID8 cells with conditioned medium, soluble factors, drugs and inhibitors

The C57BL/6 mouse ovarian carcinoma cell line ID8 was obtained from K. Roby, (University of Kansas, Kansas City, KS, USA) and T. Lawrence (CIML, Marseille, France) (Roby et al., 2000) and cultured in complete medium. ID8-GFP cells were obtained by stable transfection of ID8 cells with pEGFP-C1 (Clontech Laboratories Inc., Mountain View, CA, USA). ID8-luc cells, harboring the luciferase gene obtained from T. Lawrence (CIML, Marseille, France) have been previously described (Hagemann et al., 2008). In selected experiments, 0.5 x 10^6 ID8-luc cells were plated onto 6-well plates with 2 ml of complete medium and supplemented with 100-200 µl of concentrated CM from peritoneal macrophages or TAMs during 16-24 h.

Inhibition of MMP9 in the CM from TAMs was conducted as follows. First, the CM from 5 x 10^5 TAMs isolated from 13-weeks ID8 tumor-bearing *Zeb1* (+/+) or *Zeb1* (+/-) mice was collected and concentrated as detailed above. Then, concentrated CM was diluted 30 times in complete medium (30 µl of concentrated CM in 1 ml of complete medium) and incubated during 45 min with 20 µM of MMP9 inhibitor dissolved in DMSO (MMP-9 PEX Inhibitor 444293, Calbiochem, Millipor, DC, USA) or the corresponding volume of DMSO (1 µl of MMP9 inhibitor or DMSO per 1 ml of diluted CM). Lastly, 0.3 x 10^6 ID8-luc cells were plated on 12-wells plates and incubated during 16 h with 1 ml diluted CM (with or without MMP9 inhibitor) before cells were processed for gene expression by qRT-PCR. In experiments using rmMMP9, 0.3 x 10^6 ID8luc cells were plated in 12-wells plates with in 1 ml complete medium supplemented with 1 mg/ml of rmMMP9 (590502, Biolegend) during 36 hours.

Blocking of CCR2 signaling in co-cultures of ID8-luc cells with CM from TAMs was carried out as follows. First, six *Zeb1* (+/+) and six *Zeb1* (+/-) mice were inoculated i.p. with 5 x 10^6 ID8RI cells. After 72 h, mice for each genotype were divided into two cohorts and injected i.p. every 12 hours during 3 days with either PBS or 2.5 mg/kg of a small molecule CCR2 inhibitor (RS 504393, Tocris) before being sacrificed. The CM from TAMs for each mice and cohort were collected as detailed above. The CM was diluted twice in complete medium and 1 ml of the diluted CM was added onto ID8-luc cells for an additional 72 h before being assessed for *Ccl2* expression by qRT-PCR. The effect of cisplatin on ID8 cells was examined through two different approaches. In a first approach, 5 x 10^6 ID8-luc were injected in *Zeb1* (+/+) and (+/-) mice and allowed to grow in these mice for 8 weeks. At this point, (ID8RI) cancer cells were sorted out by FACS and 5 x 10^4 ID8RI cells were plated onto 96-well plates and incubated for 24 h in the absence (only complete medium) or presence of 50 µg/ml of cisplatin (Pharmacia Nostrum, Madrid, Spain).

In the second set of experiments, 5 x 10^6 ID8-luc were injected in *Zeb1* (+/+) and *Zeb1* (+/-) mice and TAMs were then sorted out 96 h after. TAMs were then cultured for 24 h as described above to generate CM. 5 x 10^4 ID8-luc cells were then plated in 96-well plate and culture for 24 h in the absence (only complete medium) or presence 50 µg/ml

of cisplatin and the CM from *Zeb1* (+/+) and *Zeb1* (+/-) TAMs. In both cases, the response of ID8 cancer cells to cisplatin was examined through an MTT assay. Briefly, 15 µl of a 5 mg/ml MTT solution (Sigma-Aldrich) was added to each well for 3 hours at 37ºC. Then, 100 µl of DMSO was added to each well, incubated for 15 min under dark and the absorbance at 590 nm was read with a reference filter 750 in Glomax microplate reader (Promega).

ID8 syngeneic mouse model and bioluminescence imaging

Either 5×10^6 ID8, ID8-GFP or ID8-luc cells were resuspended in 500 µl of PBS and injected i.p. into 8 week-old *Zeb1* (+/+) and *Zeb1* (+/-) female mice. At the indicated periods, mice were euthanized and ID8 cells and total macrophages ($CD11b^+F4/80^+$) were sorted and processed for experimentation. At the end of each protocol, the abdominal perimeter, ascites volume and tumor deposits on the peritoneal lining were assessed. In selected experiments, tumor progression was followed up over time by bioluminescent imaging as described elsewhere (Evans et al., 2014). Briefly, mice were injected i.p. with 1.5 mM of CycLuc1 substrate (Calbiochem®, EMD Millipore, Billerica, MA, Spain) in 100 µl of PBS. Ten min later mice were anesthetized with 2.5% isofluorane and the photon flux signal was collected in a charge-coupled ORCA-2BT imaging system (Hamamatsu Photonics, Hamamatsu City, Japan).

Bioluminescence data was analyzed with Wasabi! Imaging Software (Hamamatsu Photonics) and represented as the total photon flux/sec/cm^2 signal emitted from the abdominal cavity. In ID8 reinoculation experiments, ID8-luc cells that had been injected in *Zeb1* (+/+) and *Zeb1* (+/-) mice were isolated from the ascites after 13 weeks and re-inoculated into *Zeb1* (+/+) recipients. As ID8RI cells accelerate tumor progression (Cai et al., 2015), mice were euthanized 6 weeks post-inoculation and peritoneal cells were isolated for subsequent analysis.

Adoptive transfer of bone marrow-derived macrophages into mice tumor-bearing mice

Adoptive transfer of macrophages into ID8 tumor-bearing mice was performed as in (Hageman et al., 2008). Female *Zeb1* (+/+) mice were injected with 1 x 10^6 ID8RI-luc cells previously inoculated in *Zeb1* (+/+) female mice during 13 weeks. Twenty-three days after re-inoculation of ID8RI-luc cells, mice were inoculated with 3-4 x 10^6 BMDM from *Zeb1* (+/+) and *Zeb1* (+/-) mice. Tumor progression was monitored by bioluminescence imaging as described above. Mice were euthanized 7 days after BMDM inoculation and peritoneal cells were isolated for subsequent analysis.

Human samples

For correlations between relevant protein expression, a series of 18 cases of different stages of serous ovarian carcinomas were obtained from the Hospital Clinico San Carlos (Madrid, Spain). In case of survival plots correlating ZEB1 expression in TAMs and ovarian carcinoma patients survival, 18 cases of grade III and IV with complete surgery were obtained from the Hospital Clinico San Carlos (Madrid, Spain). Use of human samples was approved by the corresponding local Ethics Research Committees.

Immunohistochemistry of human ovarian carcinomas

Immunohistochemistry of formalin-fixed, paraffin-embedded human samples of a series of 35 cases of human ovarian carcinomas was carried out as follows. Slides were deparaffinized and rehydrated before being subjected to antigen retrieval with 10 mM sodium citrate pH 6.0 for 5 min. Slides were then incubated with a non-specific binding blocking solution (5% donkey/goat normal serum plus 4% BSA in PBS, 0.5% Tween 20) followed by the corresponding primary and HRP-conjugated secondary antibodies (see

above for the source of antibodies). Staining was performed mannually except for CD163 that was performed automatically in a Bond-Max automatic stainer (Leica Biosystems, clone 10D6).

The primary antibodies used were as follows: ZEB1: 1/250 dilution overnight at 4ºC; CCL2: 1/50 dilution overnight at 4ºC; CCR2: 1/100 dilution overnight at 37ºC; MMP9: 1/50 dilution overnight at room temperature; and CD163: 1/3000 dilution 1 h at room temperature. Secondary antibodies were incubated at 1/100 during 1 h at 37ºC, except for ZEB1 (1/200, 1 h at 37ºC) and CD163 (1/200, 30 min at room temperature). For CD163, automated staining was conducted as follows. Antigen retrieval was carried out with low pH Bond ER2 Buffer Solution® (Vision Biosystems, Leica, Wetzlar, Germany) for 30 min, followed by incubations with CD163 antibody (30 min, room temperature) and Bond Refine Polymer (Vision Biosystems) (20 min, room temperature). The immunohistochemistry reaction was developed with a DAB substrate kit (Vector Labs, Burlingame, CA) before slides were counterstained with hematoxylin and mounted in Di-N- butylPhthalate in Xylene solution (DPX, Sigma-Aldrich).

The number of positive cells was scored by microscopic analysis at 400X magnification. Statistical analyses of immunohistochemistry data was as follows. The percentage of tumor cells and TAMs expressing each protein was determined and cases were then segregated by their expression of ZEB1—in tumor cells or in TAMs—below or above the median. The means for CCL2 expression in tumor cells (n = 18), the percentage of TAM infiltration—determined by expression of CD163—(n = 18), and the expression of CCR2 (n = 15) and MMP9 (n =15) in TAMs was calculated for the low and high ZEB1 cohorts and the significance of their difference was assessed by a Mann-Whitney U test. Correlations between relevant protein expression pairs in tumor cells and/or TAMs in serious ovarian carcinomas (n = 15) were assessed by a Spearman's correlation coefficient (r). Their significance is represented by the p value.

Survival plots of women ovarian cancer patients

Correlation between the expression of *ZEB1* and *CCL2* and progression-free survival was examined in published array databases of ovarian carcinoma. Only datasets publishing survival data with a mean follow-up of at least 2 years and using the Affymetrix Human Genome chips were considered to avoid platform differences when using different gene arrays. After MAS5 normalization in the R statistical environment, the probe set 212758_s_at was used for *ZEB1* and the probe set 216598_s_at was used for *CCL2*. The four datasets included in the study are GSE15622 (Ahmed et al., 2007), GSE26193 (Mateescu et al. 2011), GSE30161 (Ferriss et al., 2012), and GSE26712 (Bonome et al., 2008). Datasets were processed separately and assembled into a single final database. Cox proportional hazards regression analysis was performed and Kaplan-Meier survival plot was generated to compare survival of patients displaying high and low expression of the genes in the R statistical environment as described previously (Mihály et al., 2013).

Statistical analysis

Statistical analysis of all the data in this dissertation was performed using Prism for Mac version 5.0a (GraphPad Software Inc., La Jolla, CA, USA). Statistical significance was assessed with a non-parametric Mann-Whitney U test except in Kaplan Meier survival plots of ovarian cancer patients where a Cox proportional hazard regression was used. Error bars in all figures represent standard errors of means. Histogram bars represent the means with standard errors and relevant comparisons of conditions were labeled as either significant at the $p \leq 0.001$ (***), $p \leq 0.01$ (**) or $p \leq 0.05$ (*) levels, or non-significant (ns) for values of $p > 0.05$.

RESULTS

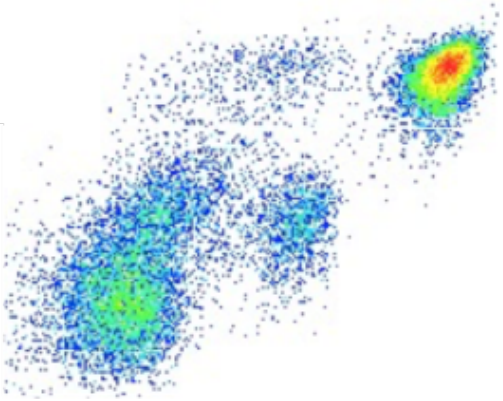

Chapter I : Role of ZEB1 in macrophage differentiation and polarization

1. Zeb1 expression and function during monocyte-macrophage differentiation

As ZEB1 inhibits the terminal differentiation, I first examined the expression of *Zeb1* during monocyte-to-macrophage differentiation in mouse. Then, wild-type C57BL/6 mice were treated with M-CSF and the mRNA expression of *Zeb1* was examined in bone marrow total cells (BMTCs) and in mononuclear myeloid cells in the peritoneal cavity, an easily accessible source of macrophages (Zhang et al., 2008). I found that expression of *Zeb1* was higher in monocytes ($CD11b^{+}F4/80^{-}$) than in macrophages ($CD11b^{+}F4/80^{+}$) (Figure 4).

As noted earlier, expression of F4/80 antigen distinguishes those macrophages that originated from peripheral blood monocytes ($CD11b^{+}F4/80^{low}$ macrophages) from those that have differentiated from embryonic precursors ($CD11b^{+}F4/80^{high}$ macrophages). Peritoneal $CD11b^{+}F4/80^{high}$ macrophages are larger in size—and referred as large peritoneal macrophages (LPM)—and represent the largest fraction in basal conditions but disappear upon bacterial lipopolysaccharide (LPS) or thioglycolate (TG) stimulation. In turn, $CD11b^{+}4/80^{low}$ are smaller—and consequently referred as small peritoneal macrophages (SPM)—express high levels of MHCII and are the main population following LPS or TG stimulation that increases monocyte migration and macrophage yields. LPM and SPM also differ in the functionally, LPM exhibit greater phagocytic activity than SPM (Goshn et al 2010; Rei et al 2014). As shown in Figure 4, *Zeb1* was almost exclusively expressed in $CD11b^{+}F4/80^{low}$ SPM.

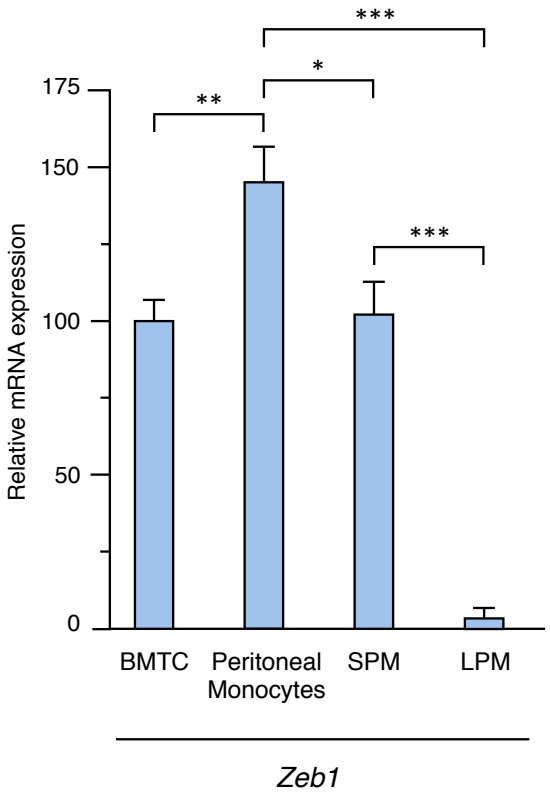

Figure 4. Wild-type C57BL/6 mice were injected i.p. with M-CSF and 4 h later bone marrow total cells (BMTC) and peritoneal cells were harvested and, in the case of peritoneal cells, sorted for CD11b and F4/80. *Zeb1* relative mRNA expression with respect to *Gapdh* was then assessed in BMTC, peritoneal monocytes ($CD11b^{+}F4/80$), small peritoneal macrophages (SPMs, $CD11b^{+}F4/80^{low}$) and large peritoneal macrophages (LPMs, $CD11b^{+}F4/80^{high}$) by quantitative real time PCR (qRT-PCR).

Next, I characterized *Zeb1* expression and function in macrophages under homeostatic, since they begin to develop from bone marrow pluripotent cell until to reach macrophage state. Using mice with heterozygous deletion of *Zeb1* [*Zeb1* (+/-)]—null *Zeb1* (-/-) are embryonic lethal— I characterized *Zeb1* expression and function in macrophages under homeostatic and activation conditions, since they begin to develop from bone marrow pluripotent cell until to reach mature macrophage state. Bone marrow cells treated *in vitro* with either GM-CSF or M-CSF render cells with a gene expression profile closer to macrophages than to dendritic cells but the former generates cells secreting more inflammatory cytokines and less anti-inflammatory cytokines (M1-like macrophages) than the later (Fleetwood et al., 2007; Lacey et al., 2008). Bone marrow myeloid cells from wild type *Zeb1* (+/+) and heterozygous *Zeb1* (+/-) mice were derived into

macrophages by incubation with GM-CSF or M-CSF. As shown in Figure 5, expression of CD11b and F4/80 was similar in *Zeb1* (+/+) and *Zeb1* (+/-) bone marrow-derived macrophages suggesting that *Zeb1* is dispensable for precursor myeloid cells differentiation into macrophages.

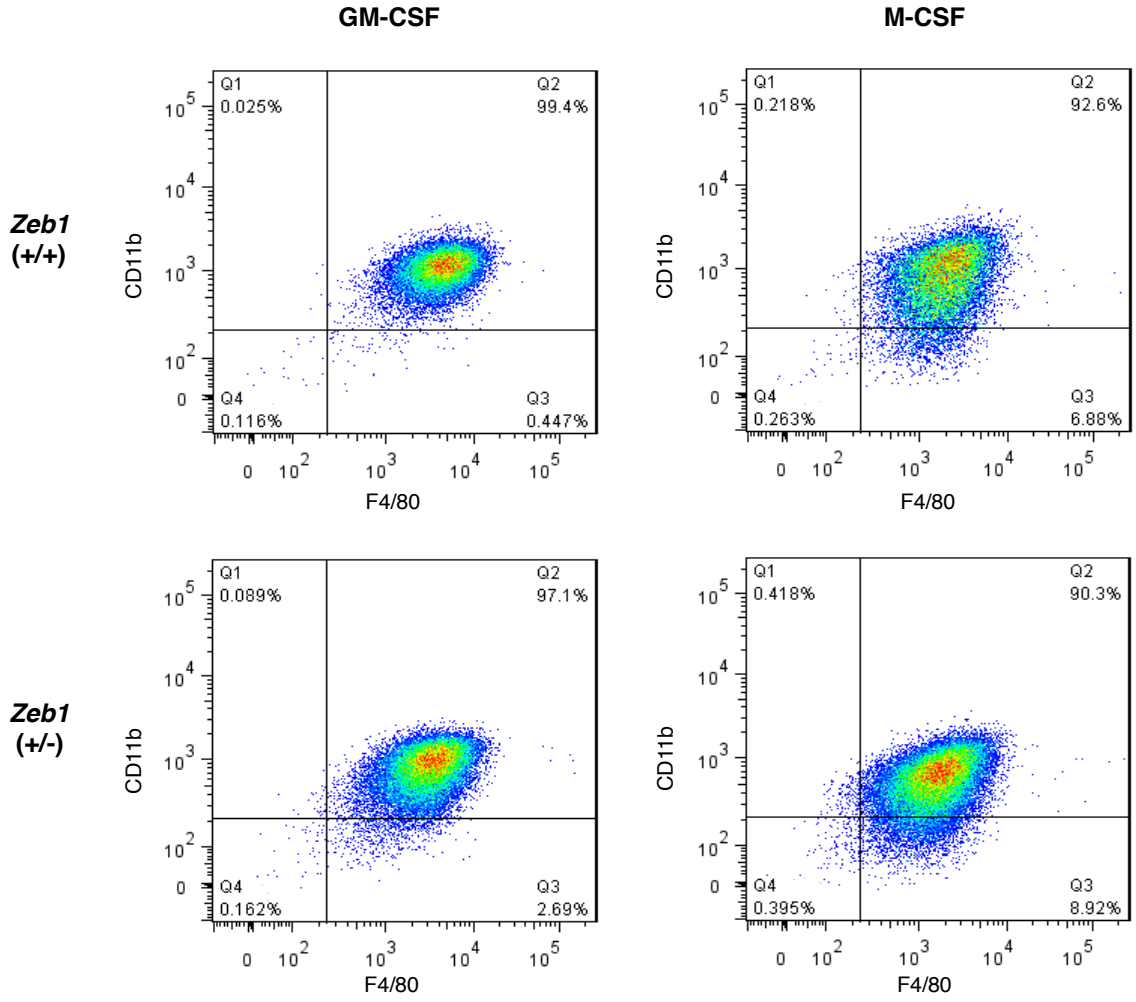

Figure 5. Bone marrow total cells (BMTCs) from *Zeb1* (+/+) and *Zeb1* (+/-) mice were derived into macrophages by incubation with GM-CSF or M-CSF as described in Materials and Methods and the distribution of macrophage subpopulations determined by CD11b and F4/80 expression by FACS.

I also investigated whether *Zeb1* plays a role in peritoneal macrophage homeostasis. I found that the number of macrophages, as the percentage of $CD11b^{+}F4/80^{+}$ cells in the peritoneal exudate, was significantly higher in *Zeb1* (+/-) mice than in *Zeb1* (+/+) mice.

At the same time, the ratio F4/80^{high} *vis-à-vis* F4/80^{low} macrophages was significantly larger in *Zeb1* (+/-) mice (Figures 6, 7 and 8). Thus, *Zeb1* modulates the total number of macrophages and the ratio of F4/80^{high} and F4/80^{low} macrophages populations as *Zeb1* deficient mice have higher levels of F4/80^{high}.

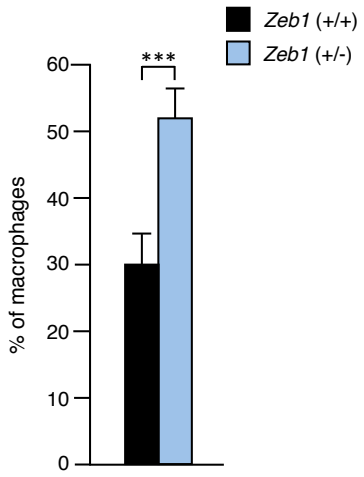

Figure 6. Six animals for each genotype *Zeb1* (+/+) and *Zeb1* (+/-) mice were analyzed for the percentage of macrophages (CD11b+F4/80+) out total peritoneal exudate cells

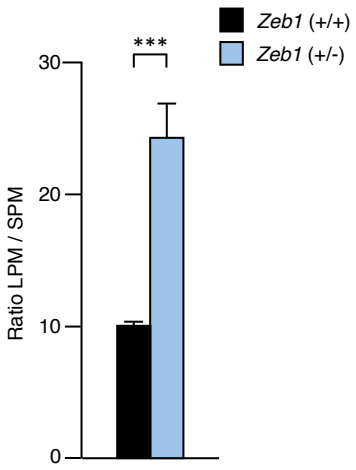

Figure 7. Peritoneal macrophages from *Zeb1* (+/+) and *Zeb1* (+/-) mice were examined by FACS for CD11b and F4/80 expression. Graphic shows F4/80^{high} to F4/80^{low} ratio values are means with standard errors of six mice for each genotype.

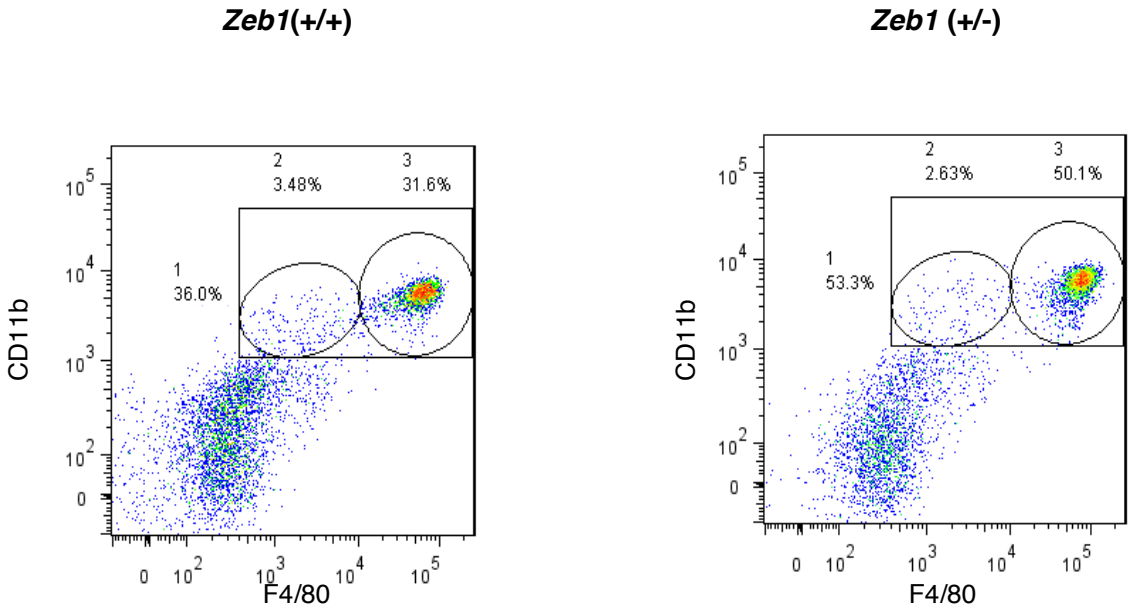

Figure 8. A representative plot for each genotype is shown. Gates numbering corresponds to total macrophages (1), SPMs (2) and LPMs (3).

2. Zeb1 modulates genes related to inflammation and SPM subpopulation

The results above indicated that ZEB1 is dispensable for the development of macrophages but, in turn, it modulates the distribution of subpopulations of macrophages, which differ in ontogeny, polarization profile and function. Consequently, I evaluated whether *Zeb1* has a role in macrophage polarization profile. First I characterized this activation state through their gene related polarization expression in both subpopulations in macrophages from wild-type mice. As expected, SPM and LPM subpopulations present different activation profile. LPMs have a reduced expression of several pro-inflammatory markers compared to SPM that have a pro and anti-inflammatory mixed phenotype (Figure 9).

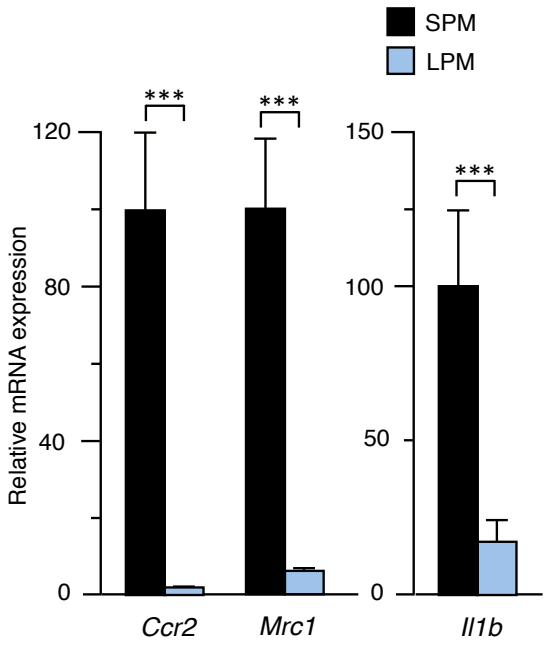

Figure 9. Gene expression of *Ccr2*, *Mrc1* and *Il1b* in LPM and SPM subpopulations from three wild-type mice was analyzed by qRT-PCR.

I then next investigated whether *Zeb1* expression regulates the expression of these and other genes associated to either classical or alternative activation in macrophages in wild type peritoneal macrophages where *Zeb1* expression had been knockdown by siRNA. *Zeb1* (+/+) peritoneal macrophages were transfected with either a siRNA control (siCtl) or siRNA against *Zeb1* (si*Zeb1*), which specificity has been previously shown (Siles et al., 2013). The expression of M2- and/or TAM-associated genes as *Ccr2, Cxcl15, Cd163, Mrc1* and *Retnla* were lower in *Zeb1* knocked down macrophages than in macrophages transfected with siCtl. Conversely, expression of the M1-associated gene *Socs3* was higher in macrophages interfered with si*Zeb1* than in those transfected with siCtl (Figure 10).

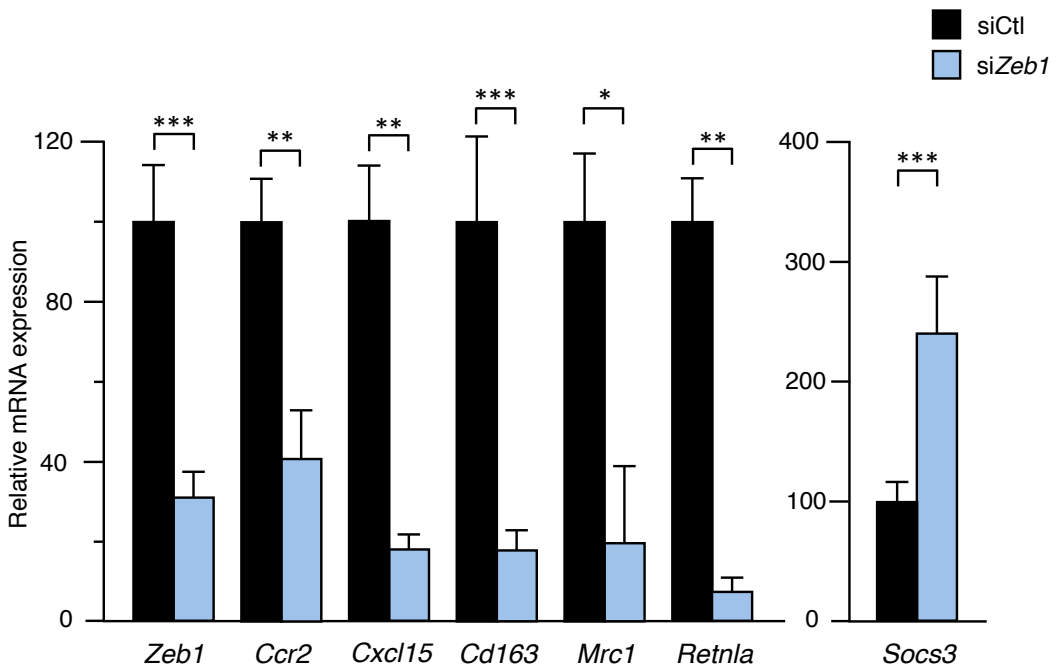

Figure 10. Gene expression analysis in wild-type and *Zeb1*-deficient peritoneal macrophages interfered with a specific siRNA against mouse *Zeb1* (si*Zeb1*) or a siRNA control (siCtl). Data represent at least three independent experiments.

Zeb1 was also interfered with si*Zeb1* in mouse bone marrow cells. As shown in Figure 11 expression of *Cd163* and *Wnt5a* is also downregulated. It is known the association of Wnt5a overexpression with tumor aggressiveness. Wnt5a is produced by monocytes and monocyte-derived macrophages and regulates VEGF-C production and macrophage immunotolerant phenotype (Sessa et al., 2016).

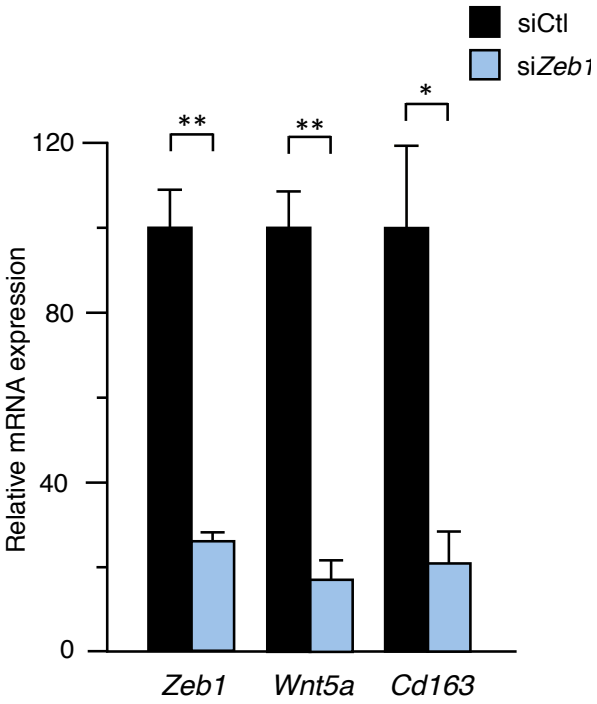

Figure 11. Expression of *Zeb1, Wnt5a* and *Cd163* in bone marrow total cells (BMTCs) interfered with siCtl or si*Zeb1*.was assessed by qRT-PCR for the expression of *Wnt5a* and *Cd163*, along with *ZEB1* as control, with reference to *Gapdh.*

I also examined if the role of ZEB1 in human macrophages is parallel that I found in mouse counterparts. Human $CD14^{+}$ peripheral blood monocytes were treated with either M-CSF (CSF1) or GM-CSF (CSF2) to generate macrophages that were then interfered with either a siCtl or a siRNA against human ZEB1 (siZEB1) (Sanchez-Tillo et al., 2011). As shown in Figure 12, *ZEB1* interference also resulted in the downregulation of *CD163* and *WNT5A*. Altogether, the results above indicated that ZEB1 activates the expression of genes in macrophages associated to their activation.

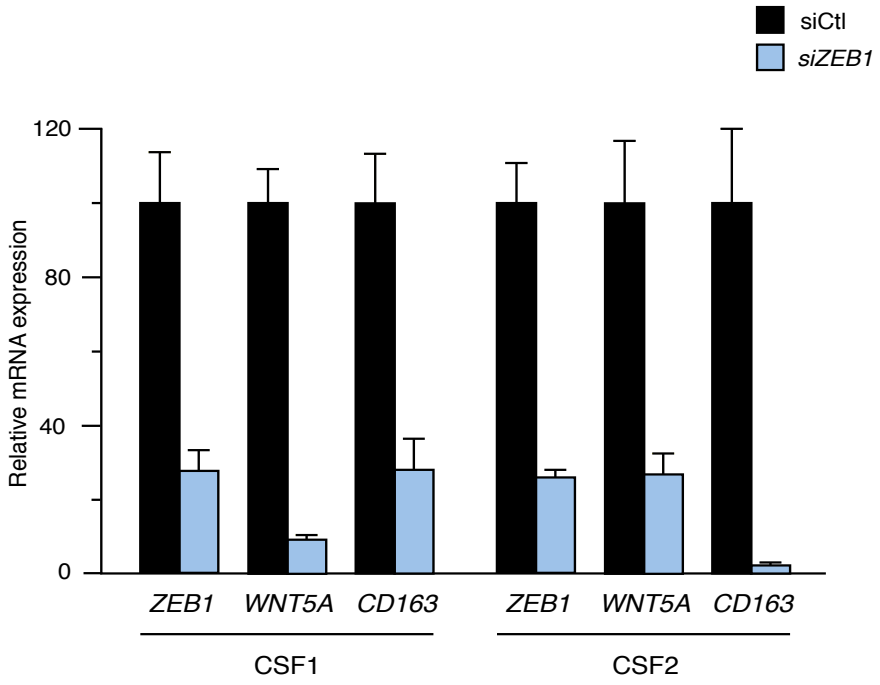

Figure 12. Human macrophages derived from peripheral blood CD14+ monocytes treated with either recombinant human M-CSF (CSF1) or GM-CSF (CSF2) and interfered with a specific siRNA against human *ZEB1* (si*ZEB1*) or a siRNA control (siCtl) and were assessed by qRT-PCR for the expression of *WNT5A* and *CD163*, along with *ZEB1* as control, with reference to *GAPDH*. Data show two independent experiments.

Lastly, I also analyzed if *Zeb1* activates genes that are associated to inflammation in peritoneal macrophages from *Zeb1* (+/+) and *Zeb1* (+/-) mice. In line with my results above, compared to their wild-type counterparts, peritoneal macrophages from *Zeb1* (+/-) mice expressed reduced mRNA levels of a number of both pro-inflammatory and anti-inflammatory genes. Thus, *Zeb1* (+/-) macrophages expressed lower levels of *Ccr2, Nfkβ1, Il1β, Cxcl15/Il8, Il10, Cd163*, *Cd206/Mrc1, Retnla* and *Mmp9, o*n the other hand, expression of *Gata6* which expression is associated to LPMs was higher in *Zeb1* (+/-) macrophages (Figure 13). Interestingly, all of these genes are related with SPM subpopulation. Therefore, *Zeb1* not only modulates the distribution of LPM and SPM populations and increases the latter, but it also activates SPM-associated genes.

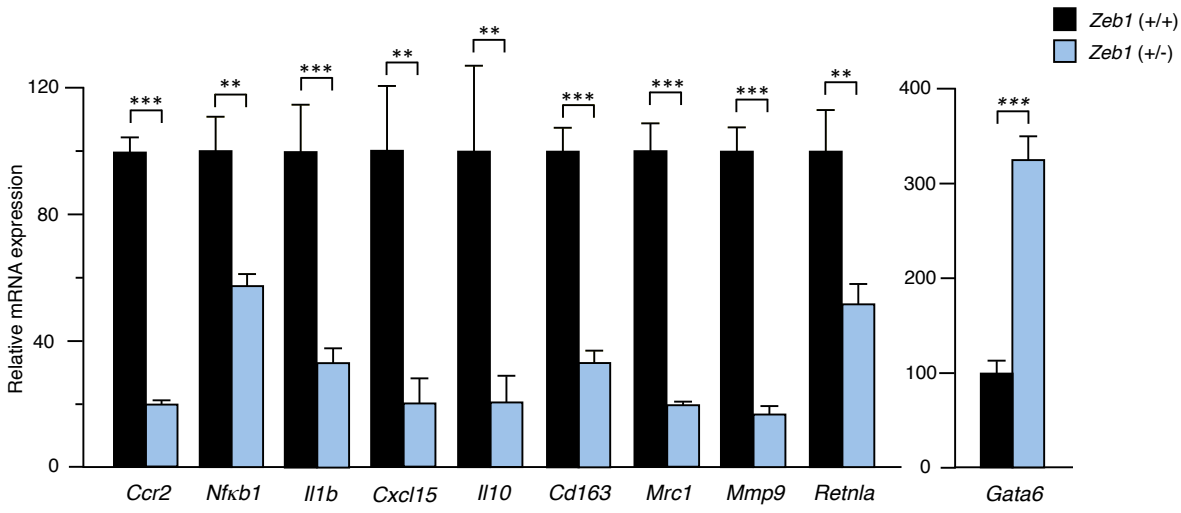

Figure 13. Peritoneal macrophages from 6-8 week-old *Zeb1* (+/+) and *Zeb1* (+/-) mice, four mice for each genotype, were assessed for the indicated genes with respect to *Gapdh* by qRT-PCR.

3. Gene expression analysis using RNA-Sequencing data

I decided to study the gene signature associated to *Zeb1* in peritoneal macrophages. To that effect, RNA transcripts from *Zeb1* (+/+) and *Zeb1* (+/-) peritoneal macrophages were compared by RNAseq technology that was performed at the Centro Nacional de Análisis Genómico (Barcelona). The gene signature in the three samples for each condition was very similar as shown in the MDS plot (Figure 14).

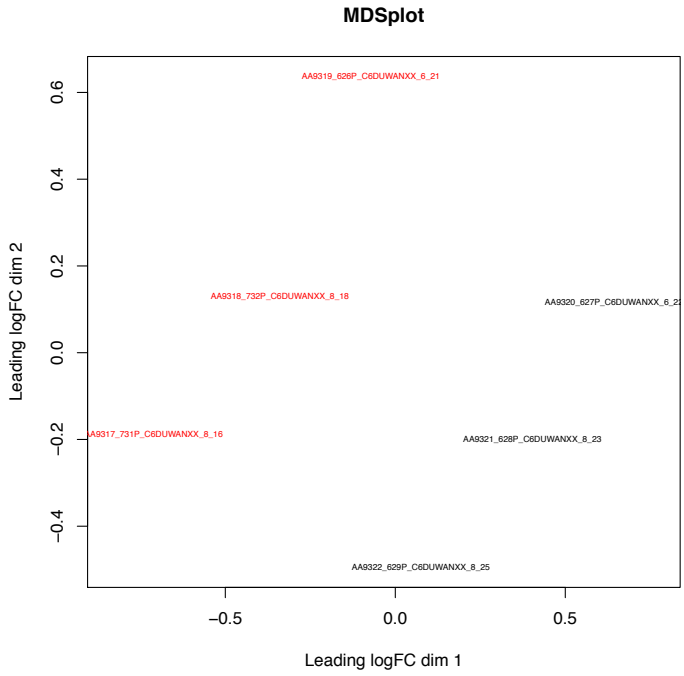

Figure 14. Multidimensional scaling (MDS) plot of digital gene expression profiles for the RNAseq data obtained from mRNA libraries of peritoneal macrophages from *Zeb1* (+/+) (black) and *Zeb1* (+/-) (red) mice. MDS plot show the relations between the samples in two dimensions and distances on the plot represent the biological coefficient of variation of expression between samples.

For all samples, hierarchical clustering was performed using Genesis software as shown in Figure 15 normalizing rows of data for similar distribution. Samples could be separated in 2 groups according their genotype, where *Zeb1* (+/-) samples form A and *Zeb1* (+/+) samples form B group. Of the 12,877 genes that yielded the RNAseq, 412 were significantly differentiantly expressed (DE) between both groups. Genes were grouped in order their correlation in six clusters.

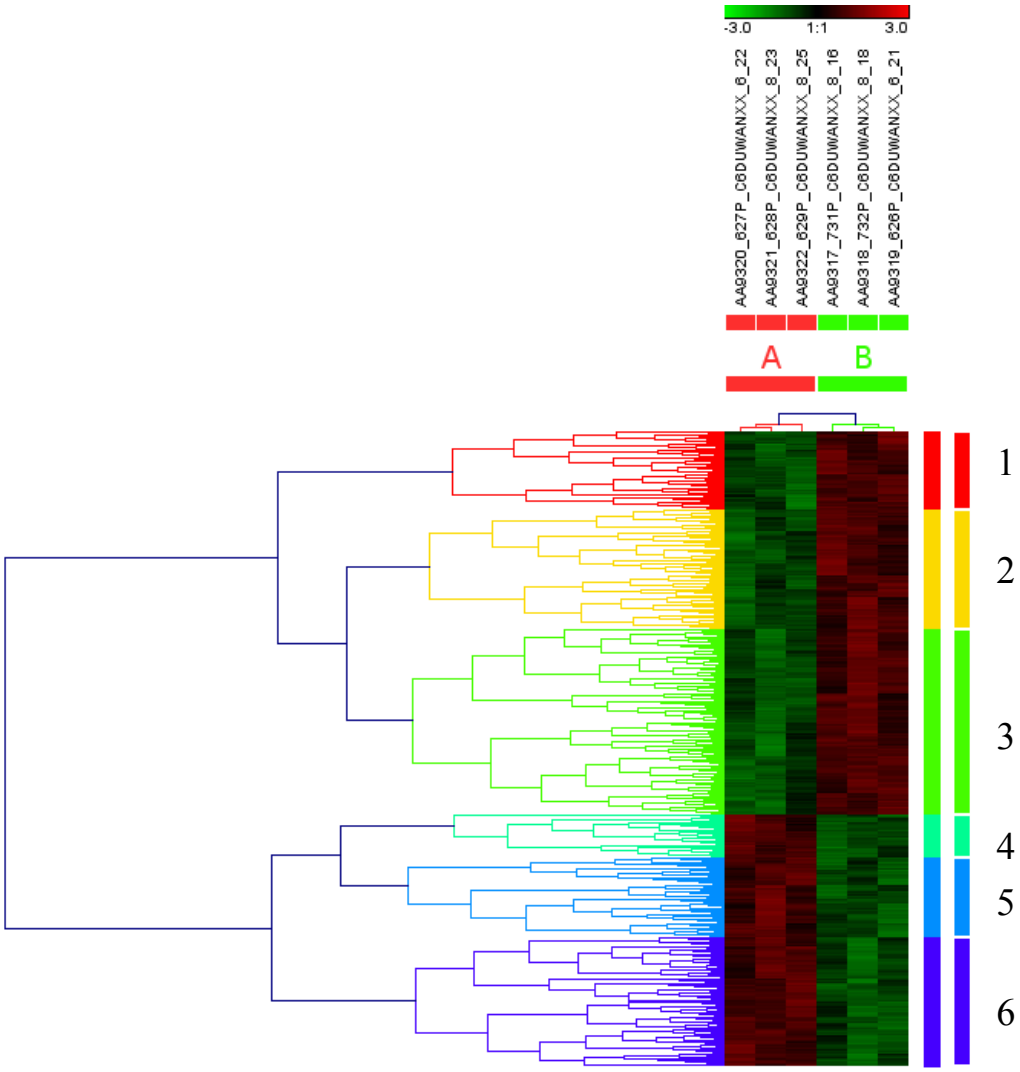

Figure 15. Hierarchical clustering of 412 differentially expressed genes in peritoneal macrophages from *Zeb1* (+/+) and *Zeb1* (+/-) mice. Each row represents a gene and each column a sample. The color scale ranges from saturated red for upregulated genes to green for downregulated genes.

A Gene Ontology (GO) and an enriched KEGG pathways functional analysis of DE genes were performed. These bioinformatics analyses revealed that most DE genes were associated to immune system processes and hematopoietic cell lineage functions (Tables 4 and 5).

Biological Process	Count	%	p value
GO:0002376 immune system process	34	6,60	6,21E-10
GO:0006954 inflammatory response	25	4,85	8,52E-06
GO:0019886 antigen processing and presentation of exogenous peptide antigen via MHC class II	6	1,16	1,60E-05
GO:0001816 cytokine production	7	1,36	2,82E-05
GO:0007155 cell adhesion	29	5,63	3,92E-05
GO:0006874 cellular calcium ion homeostasis	12	2,33	4,11E-05
GO:0019882 antigen processing and presentation	8	1,55	3,78E-04
GO:0050853 B cell receptor signaling pathway	8	1,55	4,24E-04
GO:0031623 receptor internalization	7	1,36	4,45E-04
GO:0002250 adaptive immune response	12	2,33	6,73E-04
GO:0042113 B cell activation	6	1,16	6,96E-04
GO:0007568 aging	14	2,71	7,67E-04
GO:0000082 G1/S transition of mitotic cell cycle	8	1,55	8,84E-04
GO:0006164 purine nucleotide biosynthetic process	5	0,97	0,001115
GO:0002504 antigen processing and presentation of peptide or polysaccharide antigen via MHC class II	4	0,77	0,001171
GO:0006955 immune response	19	3,69	0,001241
GO:0009615 response to virus	9	1,74	0,001298
GO:0007399 nervous system development	21	4,07	0,001345
GO:0031589 cell-substrate adhesion	5	0,97	0,001367
GO:0034113 heterotypic cell-cell adhesion	5	0,97	0,001367
GO:0016337 single organismal cell-cell adhesion	10	1,94	0,001673
GO:0007157 heterophilic cell-cell adhesion via plasma membrane cell adhesion molecules	7	1,35	0,001833
GO:0021785 branchiomotor neuron axon guidance	4	0,78	0,002216
GO:0030335 positive regulation of cell migration	14	2,72	0,002217
GO:0010628 positive regulation of gene expression	21	4,08	0,002836
GO:0006816 calcium ion transport	11	2,13	0,002937
GO:0071353 cellular response to interleukin-4	5	0,97	0,003234
GO:0035556 intracellular signal transduction	21	4,08	0,003261
GO:0007166 cell surface receptor signaling pathway	14	2,72	0,003601
GO:1902287 semaphorin-plexin signaling pathway involved in axon guidance	4	0,78	0,003701

Table 4. Gene Ontology (GO) functional enrichment of genes differentially expressed (DE) between *Zeb1* (+/+) and *Zeb1* (+/-) peritoneal macrophages. Only the top 30 biological process with value $p<0.05$ are shown. The first column refers to the GO term and the description of the biological process. The second and third columns indicate the number of genes and the share (in percentage) out all genes, respectively. The fourth column shows the p value

Biological Process	Count	%	p value
mmu04514: Cell adhesion molecules (CAMs)	18	3,74	6,11E-06
mmu04640: Hematopoietic cell lineage	12	2,49	5,97E-05
mmu03010: Ribosome	12	2,49	1,02E-04
mmu05416: Viral myocarditis	11	2,28	7,22E-04
mmu04662: B cell receptor signaling pathway	10	2,07	8,87E-04
mmu04672: Intestinal immune network for IgA	7	1,45	0,006840
mmu00562: Inositol phosphate metabolism	7	1,45	0,006840
mmu04070: Phosphatidylinositol signaling system	8	1,66	0,009271
mmu04510: Focal adhesion	14	2,91	0,009809
mmu03320: PPAR signaling pathway	8	1,66	0,012185
mmu05310: Asthma	5	1,03	0,019538
mmu04612: Antigen processing and presentation	8	1,66	0,024827
mmu05200: Pathways in cancer	18	3,74	0,026591
mmu04650: Natural killer cell mediated cytotoxicity	9	1,87	0,039307
mmu04512: ECM-receptor interaction	7	1,45	0,047312

Table 5. Kyoto Encyclopedia of Genes and Genomes (KEGG) analysis of genes differentially expressed (DE) between *Zeb1* (+/+) and *Zeb1* (+/-) peritoneal macrophages. The first column refers to the KEGG term and the description of the biological process. The second and third columns indicate the number of genes and the share (in percentage) out all genes, respectively. The fourth column shows the p value.

Interestingly, many of the DE genes are implicated in macrophage activation/polarization and/or are associated to F4/80^{high} and F4/80^{low} phenotypes (e.g. *Cd163, Mrc1, Retnla*), corroborating my findings above about a potential role of *Zeb1* in macrophage activation (Figure 16).

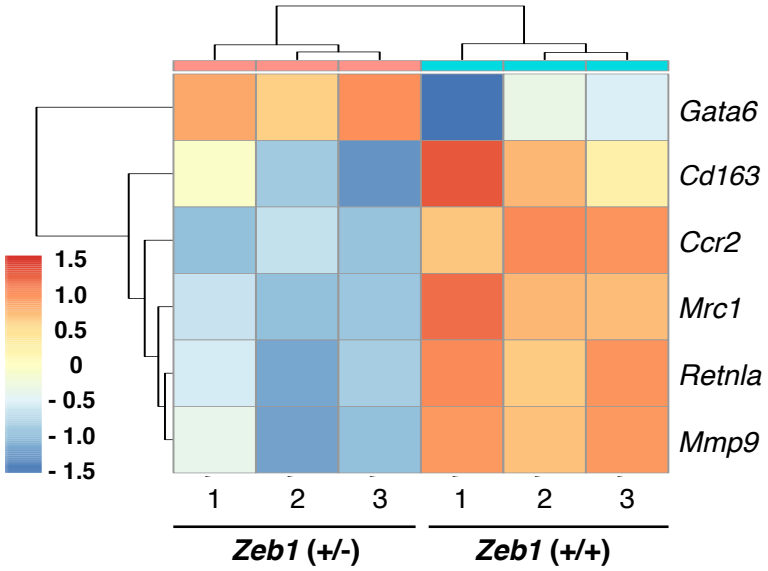

Figure 16. Hierarchical clustering of some of top DE genes up and downregulated.

Use of the GENEMANIA platform allowed me to elaborate a network weighting for some DE genes of the RNA-seq. Figure 17 shows the network established by the coexpression of *Mrc1, Ccr2, Mmp9, Cd163* and *Retnla*. It is interesting to note that other TAM-related genes as *Csf1, Il10* and *Nfkb* are coexpressed with the DE genes obtained in the RNAseq,

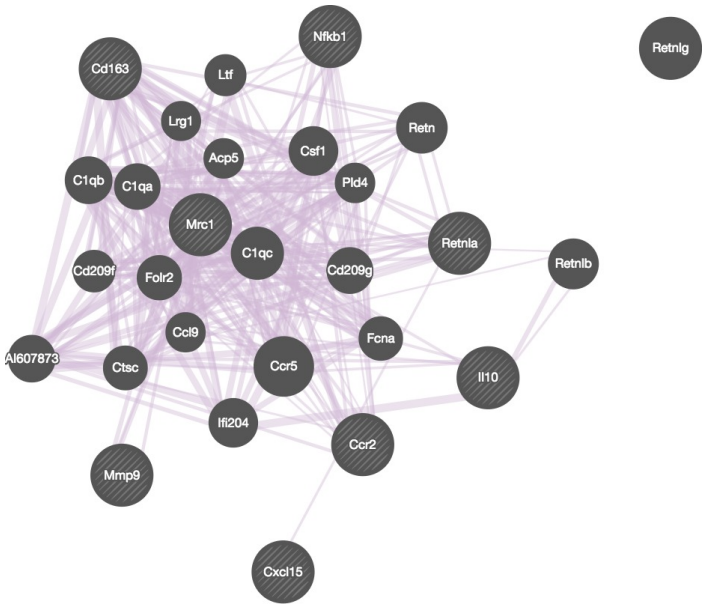

Figure 17. Gene network extracted from GENEMANIA, describing the genetic relation for some inflammatory DE genes from RNA-seq. The arrows in purple represent co-expression of determined genes.

4. Socs3 is involved in Zeb1 regulation

All of these data indicate that *Zeb1* regulates macrophage phenotype and SPM distribution, and both anti and pro-inflammatory markers. This led me to explore other mouse models involved in the activation and distribution of peritoneal macrophages, including genes with could have common pathways with *Zeb1* and study how it is modulating macrophage activation and try to revert *Zeb1* deficiency through an *in vivo* model. Therefore, I used mice deficient for either *Socs2* or *Socs3* genes.

In order to inquire whether *Zeb1* regulates macrophage polarization through cross-regulation of *Socs2* or *Socs3* and if macrophage polarization is restored or enhanced, I crossed *Socs2* (-/-) and $Socs3^{Lyz2cre}/Zeb1$ (+/+) with *Zeb1* (+/-) mice. I analyzed the peritoneal exudate from these different mice and examined changes in macrophage distribution by FACS. I did not observe clear differences in peritoneal macrophage subpopulations between $Socs3^{Lyz2cre}/Zeb1$ (+/+) and $Socs3^{Lyz2cre}/Zeb1$ (+/-) mice (Figure 18).

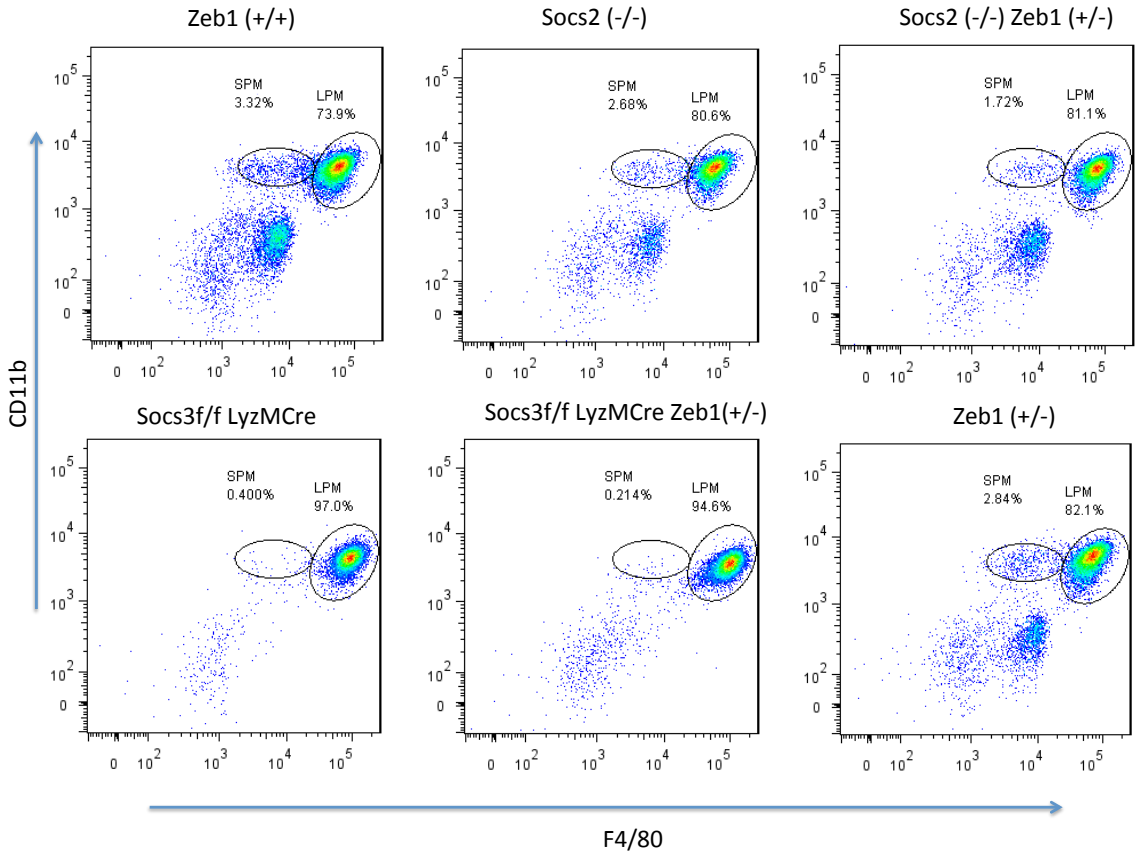

Figure 18. Flow cytometric dot plot of cells to peritoneal lavage cells from *Zeb1* (+/+), *Socs3*^{Lyz2cre}*/Zeb1* (+/+), *Socs3*^{Lyz2cre}*/Zeb1* (+/-), and *Zeb1* (+/-) mice. There are variations in F4/80^{high} and F4/80^{low} populations as is known in these mice, but there is not difference between *Socs3*^{Lyz2cre}*/Zeb1* (+/+) *Socs3*^{Lyz2cre}*/Zeb1* (+/-) mice.

Next, I analyzed the expression of *Zeb1* and other polarization-associated genes in peritoneal macrophages from these mice and found a similar patron in gene expression in macrophages from *Socs3*^{Lyz2cre}*/Zeb1* (+/+) and *Socs3*^{Lyz2cre}*/Zeb1* (+/-) mice (Figure 19). Based on the gene expression profile, I concluded that *Socs2* did not alter the polarization, nor have direct relationship with *Zeb1*.

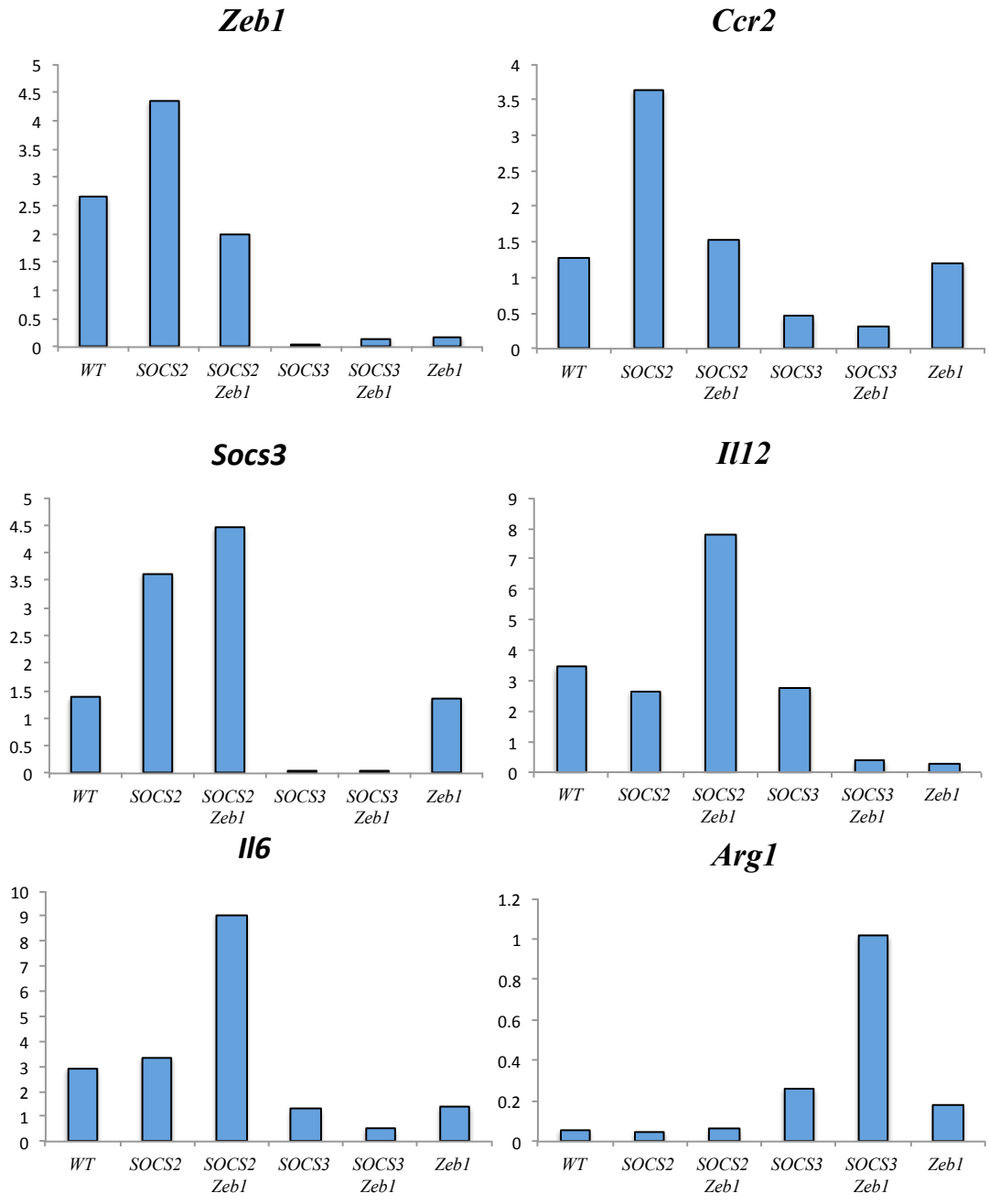
Zeb1
5
4.5
4
3.5
3
2.5
2
1.5
1
0.5
0
WT
SOCS2
SOCS2 Zeb1
SOCS3
SOCS3 Zeb1
Zeb1
Ccr2
4
3.5
3
2.5
2
1.5
1
0.5
0
WT
SOCS2
SOCS2 Zeb1
SOCS3
SOCS3 Zeb1
Zeb1
Socs3
5
4.5
4
3.5
3
2.5
2
1.5
1
0.5
0
WT
SOCS2
SOCS2 Zeb1
SOCS3
SOCS3 Zeb1
Zeb1
Il12
9
8
7
6
5
4
3
2
1
0
WT
SOCS2
SOCS2 Zeb1
SOCS3
SOCS3 Zeb1
Zeb1
Il6
10
9
8
7
6
5
4
3
2
1
0
WT
SOCS2
SOCS2 Zeb1
SOCS3
SOCS3 Zeb1
Zeb1
Arg1
1.2
1
0.8
0.6
0.4
0.2
0
WT
SOCS2
SOCS2 Zeb1
SOCS3
SOCS3 Zeb1
Zeb1

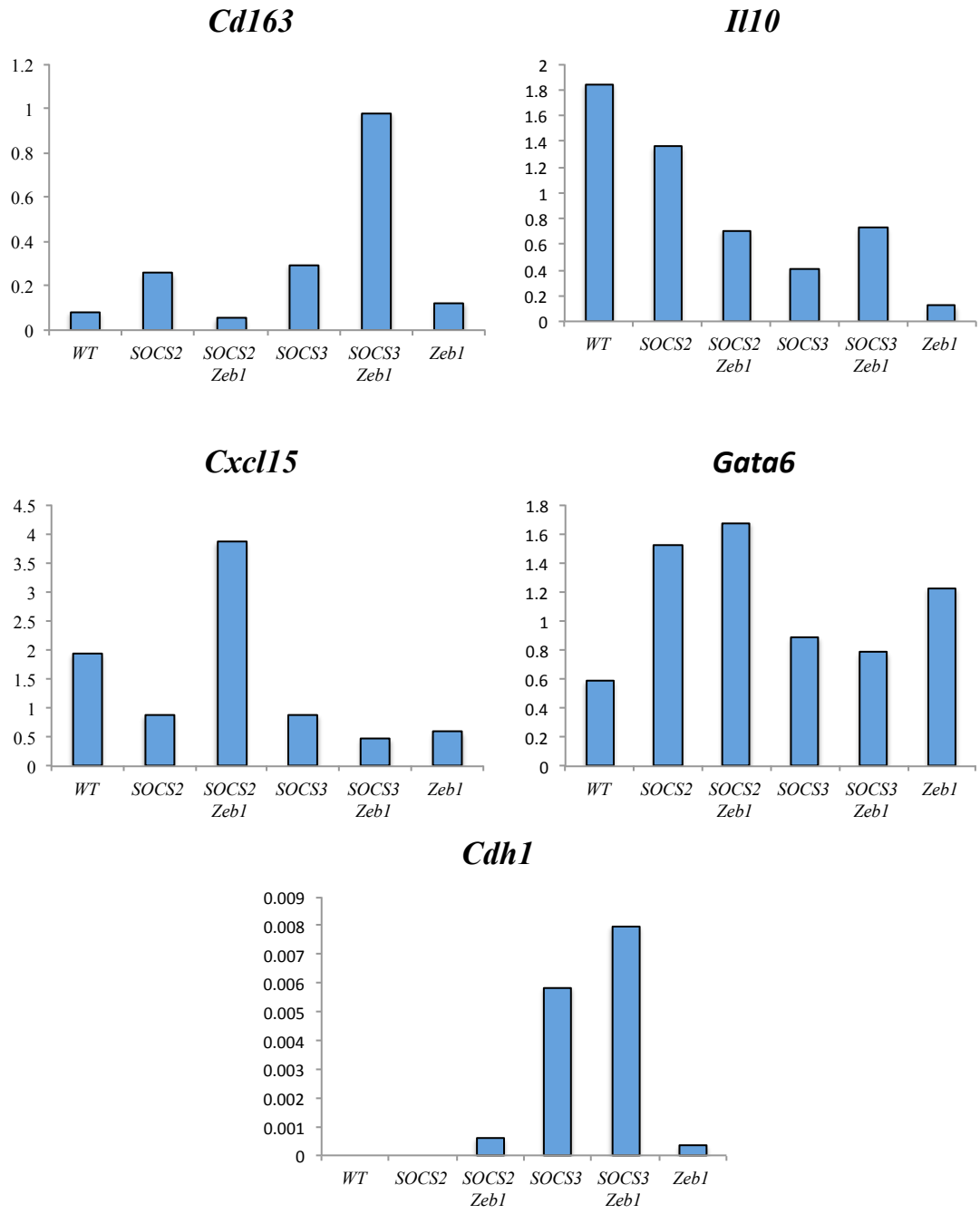

Figure 19. Gene expression analysis by qRT-PCR (relative to *Gapdh* mRNA levels) in peritoneal macrophage from *Zeb1* (+/+) (*WT*), *Socs2*$^{-/-}$ (*SOCS2*) Socs2$^{-/-}$*Zeb1*(+/-) (*SOCS2 Zeb1*) *Socs3*^{Lyz2cre} (*SOCS3*) *Socs3*^{Lyz2cre}*/Zeb1* (+/-) (*SOCS3 Zeb1*) and *Zeb1* (+/-) (*Zeb1)* mice.

Surprisingly, *Socs3*^{Lyz2cre}*/Zeb1* (+/+) mice express non-detectable mRNA or protein levels of Zeb1 (Figures 19, 20 and 21). In addition, I found that *Socs3* expression was upregulated in *Zeb1* (+/-). Likewise, classical ZEB1 target genes in epithelial tissues, like E-cadherin, were overexpressed in *Socs3*^{Lyz2cre}*/Zeb1* (+/+) mice (Figure 20). These results indicated that *Zeb1* and *Socs3* modulate each other expression in peritoneal macrophages.

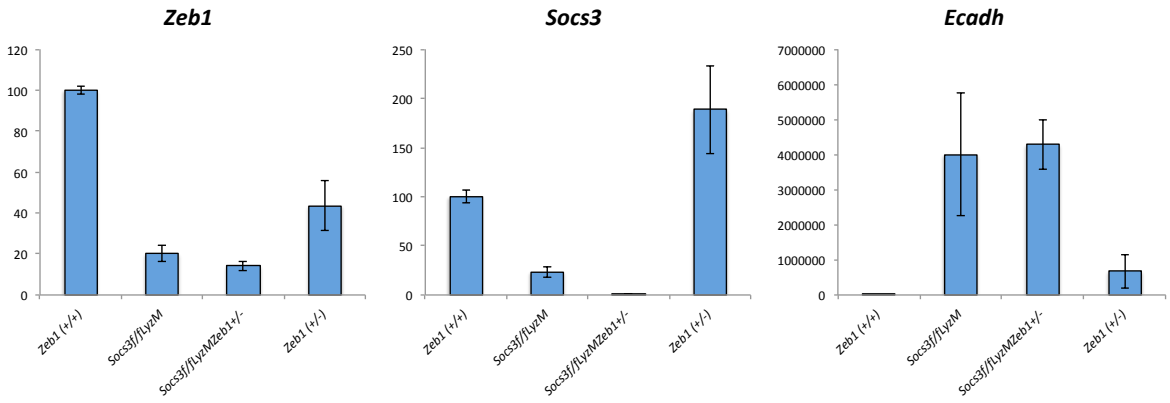

Figure 20. Gene expression analysis by qRT-PCR (relative to *Gapdh* mRNA levels) in peritoneal macrophage from different mice. Histogram show average of two independent experiments.

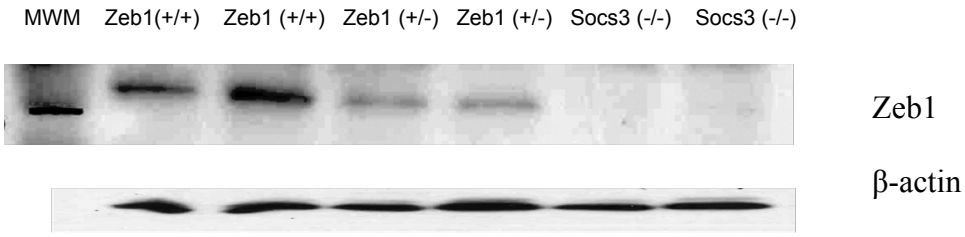

Figure 21. Western blot for ZEB1 protein expression. β-Actin was used as a control.

Next, I sought to investigate the molecular mechanism of this mutual regulation between *Zeb1* and *Socs3*. To that effect, *Zeb1* was overexpressed in peritoneal macrophage using lentivirus that carries the mouse *Zeb1* gene fused to GFP. Transduced cells were analyzed for *Zeb1* expression and GFP. Peritoneal macrophages showed high transduction efficiencies as scored by FACS with over >50% of cells positive for GFP (Figure 22). These transduced cells I assessed by qRT-PCR for the expression of different genes associated to polarization as well as *Zeb1* and *Socs3 t*arget genes. Genes like *Ccr2* displayed a similar expression pattern in normal macrophages and in $Socs3^{f/f}Lyz2cre^{+/-}$ macrophages when overexpressed *Zeb1*. In both situations levels were higher when *Zeb1* was overexpressed, independently of *Socs3* levels. Nevertheless, other genes like *Gata6* or *Il6* displayed different regulation as shown in Figure 23. These data indicate that some genes are regulated for *Socs3* in independently of *Zeb1*.

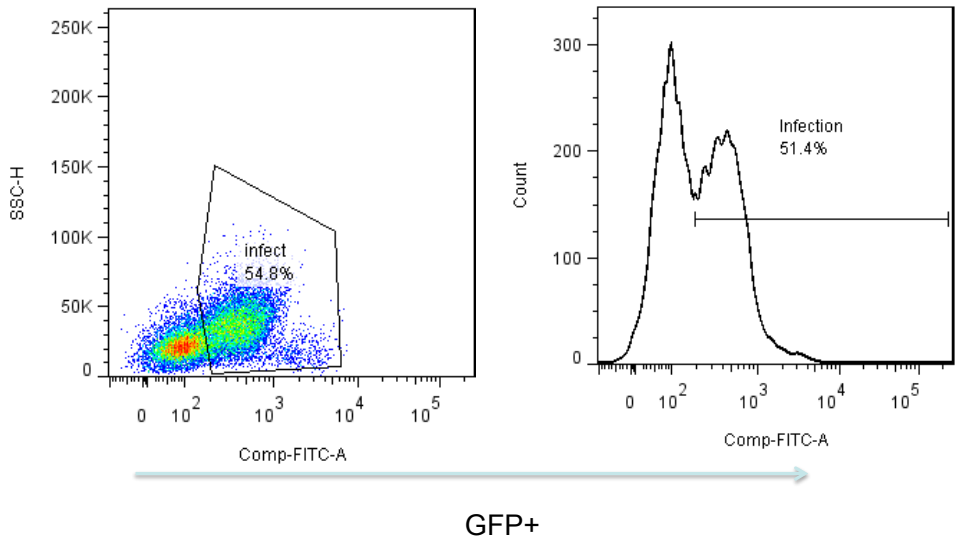

Figure 22. FACS dotplot and histogram showing peritoneal macrophages from *Zeb1* (+/+) (n=2) and $Socs3^{Lyz2cre}$ (n=2) mice transduced with a lentiviral *Zeb1* expression vector co-expressing eGFP, or a control vector expressing eGFP only are shown.

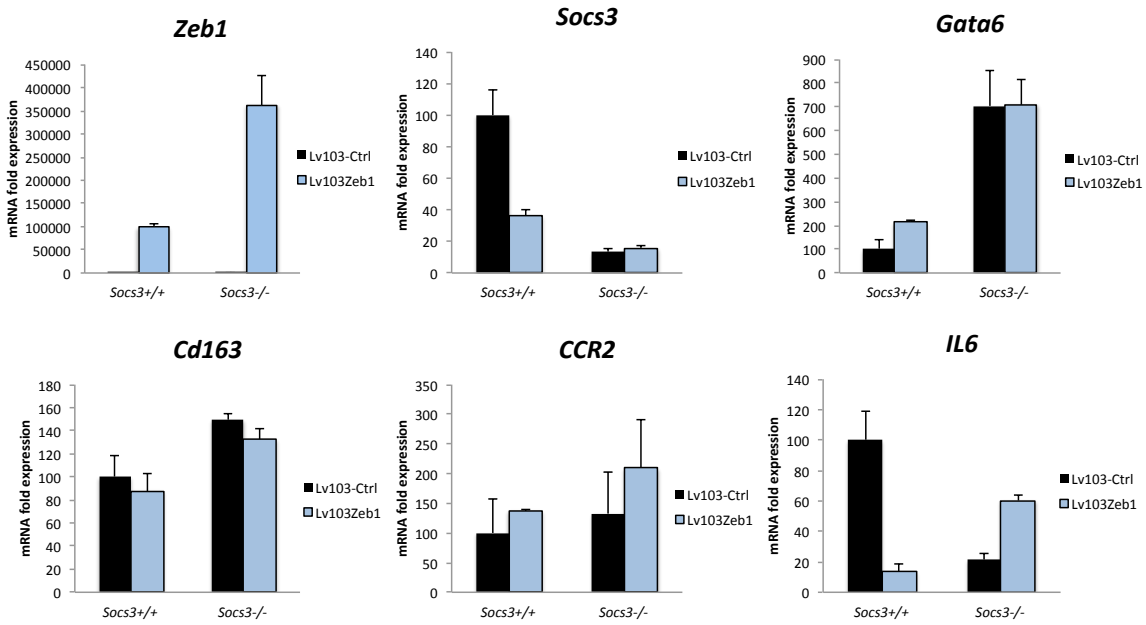

Figure 23. mRNA expression levels for *Zeb1* and other *Zeb1* and *Socs3*-related genes with respect to *Gapdh* were analyzed by qRT-PCR 96 h after transduction. Data show two independent experiments.

Chapter II : Role of ZEB1 in macrophage function

1. *Zeb1 expression impairs macrophage phagocytosis*

Macrophages are specialized phagocytes that remove pathogens and clear dead and malignant cells. $CD11b^{+}F4/80^{high}$ LPMs display higher phagocytic capacity than $CD11b^{+}F4/80^{low}$ SPMs (Cain et al., 2013). Since my results above indicate that *Zeb1* (+/-) mice have a larger $CD11b^{+}F4/80^{high}$ LPM subpopulation, I studied the phagocytic capacity of peritoneal *Zeb1* (+/+) and *Zeb1* (+/-) macrophages. To that effect, I used the ID8 syngeneic murine ovarian cancer model. Intraperitoneal (i.p.) injection of ID8 cancer cells results in their rapid growth and development of ascites with abundant infiltration of immune cells, mostly TAMs (Hagemann et al., 2006; Hagemann et al., 2008).

I stably transfected ID8 cells with an expression vector encoding GFP and injected them or ID8 CFSE-labeled i.p. into *Zeb1* (+/+) and *Zeb1* (+/-) mice. The peritoneal exudate was harvested after 3 h and phagocytosis of ID8-GFP cells by F4/80 macrophages was assessed by FACS. I found that peritoneal macrophages from *Zeb1* (+/-) displayed higher phagocytic capacity than their *Zeb1* (+/+) counterparts (Figure 24).

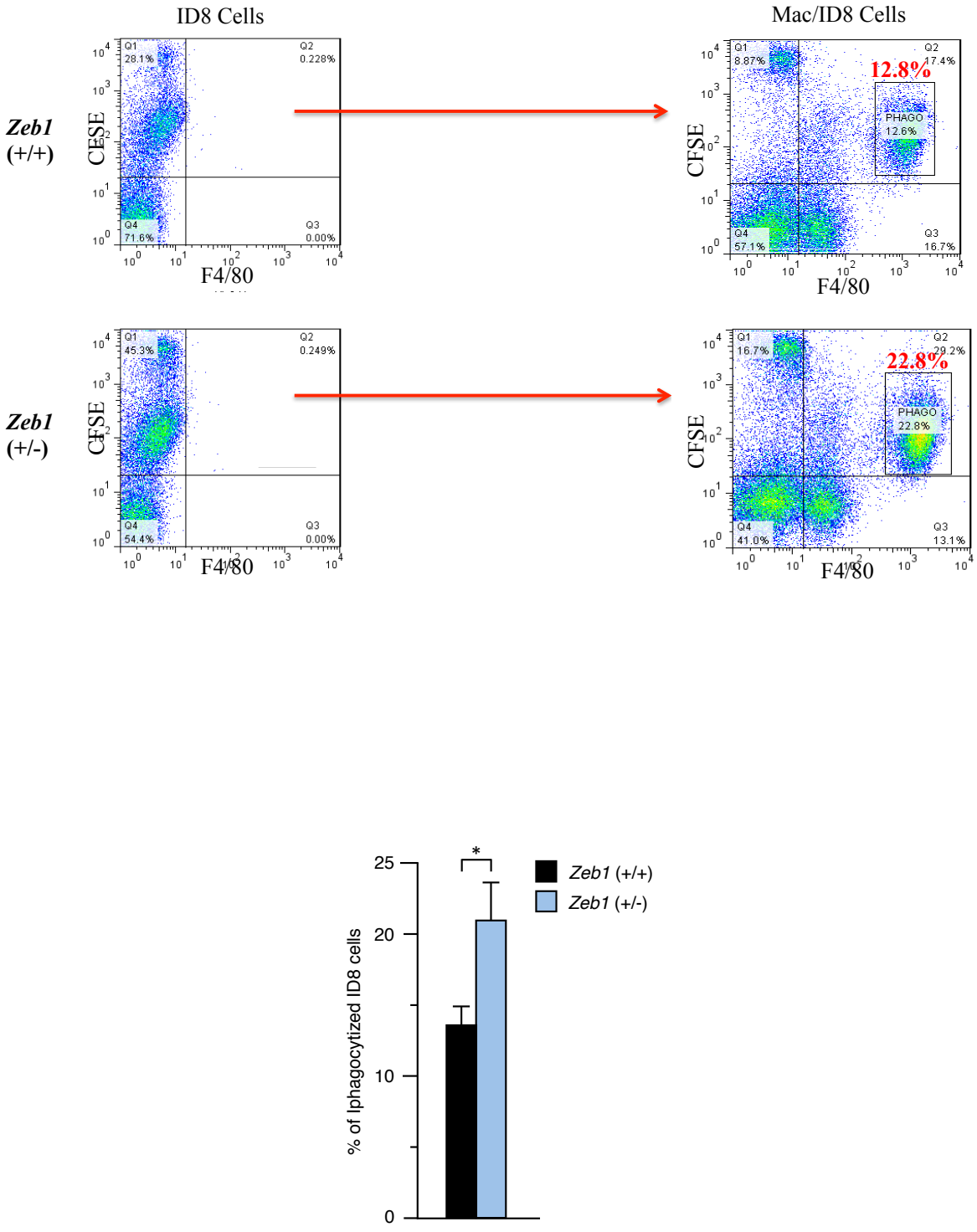

Figure 24. *Upper panel: Zeb1* (+/-) macrophages display increased phagocytic capacity. *Zeb1* (+/+) and *Zeb1* (+/-) mice were injected i.p. with ID8-GFP cells and 3 h later mice were euthanized and *in vivo* phagocytosis was assessed by FACS as $F4/80^{+}$ cells that were also GFP^{+} (gate 1). *Lower panel*: The histogram shows the percentage of ID8 cells phagocyted in relation to the total peritoneal cells.

2. *ZEB1 expression promotes macrophage migration*

ZEB1 enhances the invasive behavior in cancer cells. Consequently, I sought to investigate whether *Zeb1* also regulates migration in macrophages. First, I analyzed the basal motility of *Zeb1* (+/+) and *Zeb1* (+/-) peritoneal macrophages in an *in vitro* wound healing assay. In the absence of chemotactic stimuli, *Zeb1*-deficient macrophages showed a slower closure of the scratch wound than wild-type macrophages (Figure 25).

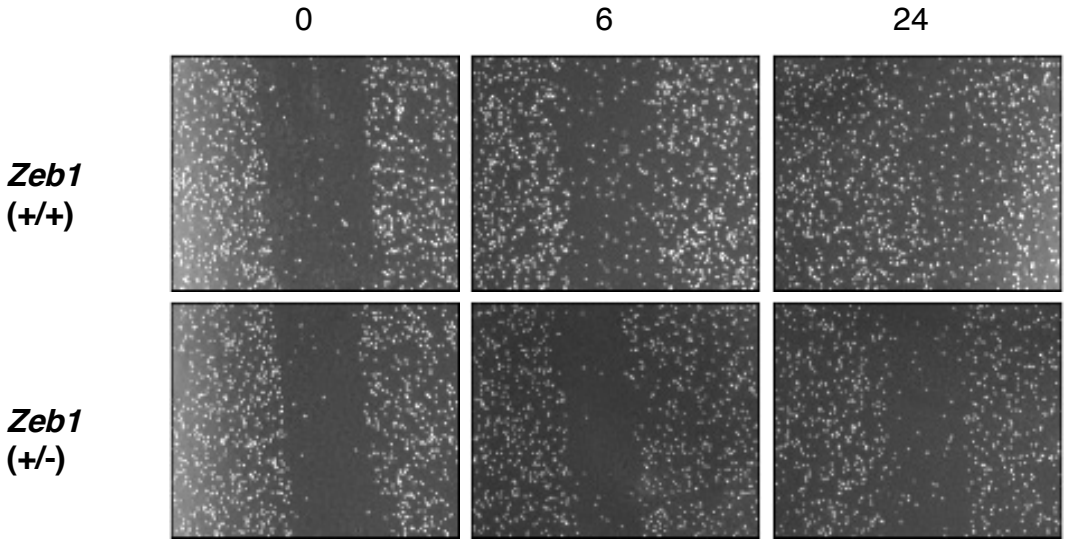

Figure 25. *Zeb1* (+/+) peritoneal macrophages migrated more than *Zeb1* (+/-) ones in a wound healing assay. Images shown are representative of at least four different mice for each genotype.

In addition to its role in the recruitment of circulating monocytes into the tumor microenvironment, CCL2 is required for the mobilization of pro-inflammatory CCR2+ monocytes into inflammatory and infection foci (Serbina and Palmer, 2006; Si et al., 2010). I examined the chemotaxis of macrophages from both genotypes to CCL2 in a Transwell® migration assay and found that *Zeb1* (+/-) macrophages migrated less efficiently to mouse recombinant Ccl2 (mrCcl2) than their wild-type counterparts (Figure

26). These data indicate that *Zeb1* promotes macrophage motility both under basal and chemotactic conditions.

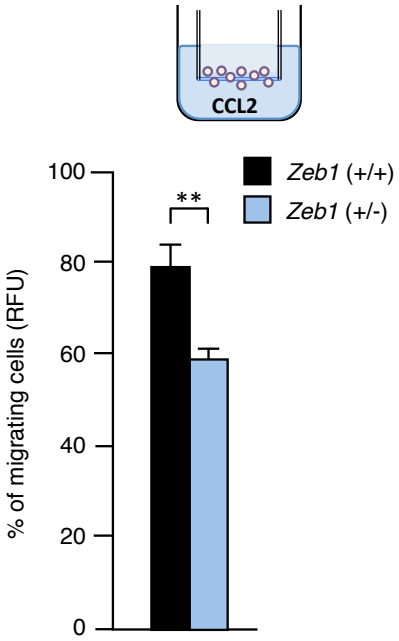

Figure 26. Transwell® chemotaxis assay for CFSE-labeled peritoneal macrophages from *Zeb1* (+/+) and *Zeb1* (+/-) mice under the stimulus of recombinant mouse Ccl2. Values are the means of relative fluorescence units (RFU) of five mice for each genotype with standard errors.

The lower migratory capacity of *Zeb1* (+/-) macrophages was then assessed *in vivo* by examining the adoptive transfer of BMTC and BMDM into wild-type mice. BMTC and BMDM from *Zeb1* (+/+) and *Zeb1* (+/-) mice were labeled with the fluorescent cell tracer carboxyfluorescein succinimidyl ester (CFSE) and injected intravenously (i.v.) in *Zeb1* (+/+) mice. A control cohort of *Zeb1* (+/+) mice was injected with PBS. In the case of BMTCs mice received a thyoglicolate i.p. injection after BMTCs i.v. injection and peritoneal exudates were collected and analyzed for $CFSE^+$ cells 72 hours after, and for BMDM peritoneal exudate was analyzed 24-48 hours after inoculation. In line with my *ex vivo* results above, BMDMs and BMTCs from *Zeb1* (+/+) migrate more efficiently than their *Zeb1* (+/-) counterparts (Figures 27 and 28).

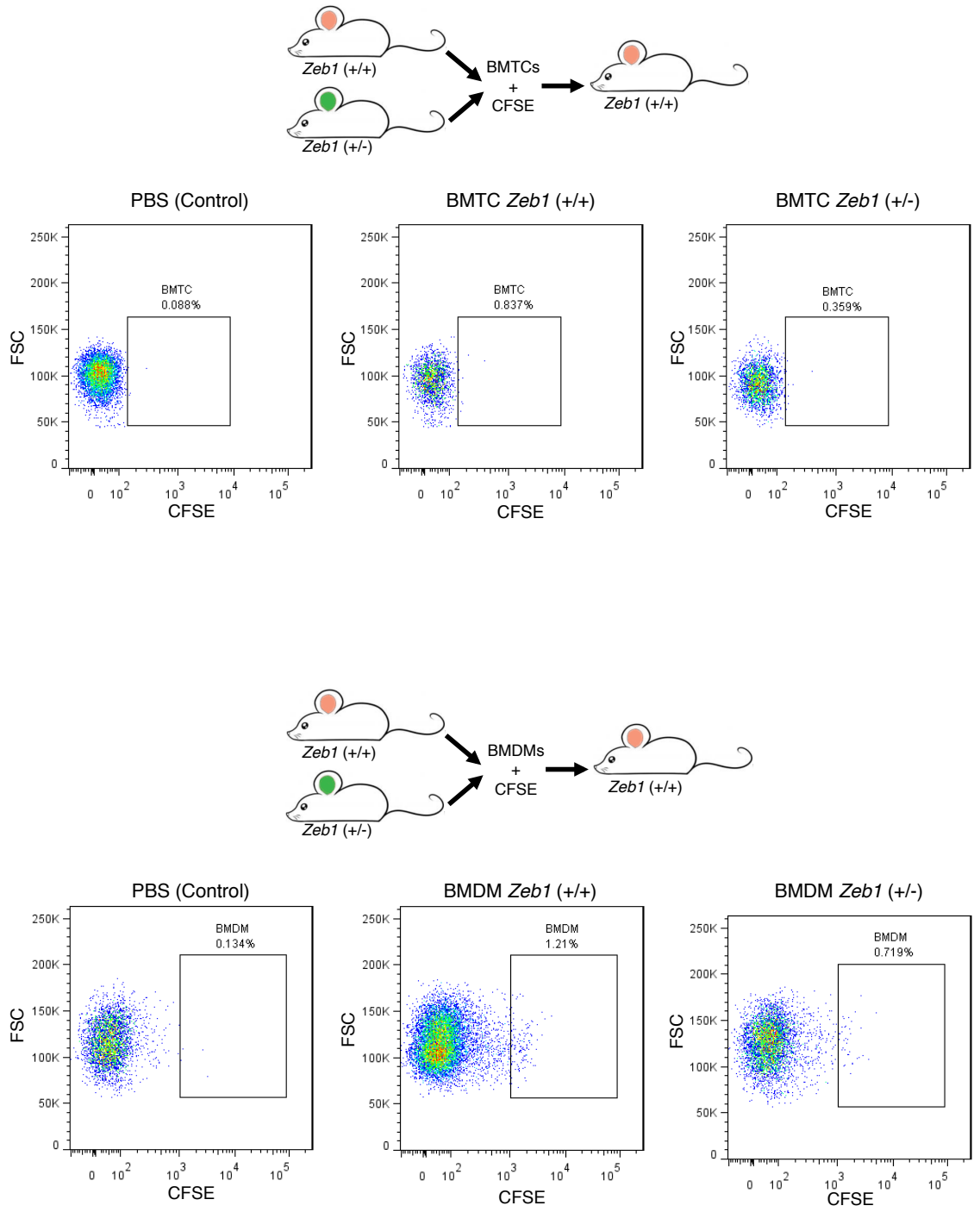

Figures 27 and 28. Increased *in vivo* migration of *Zeb1* (+/-) BMTCs and BMDMs in adoptive transfer assays. CFSE-labeled BMTCs and BMDMs from *Zeb1* (+/+) and *Zeb1* (+/-) mice were inoculated into *Zeb1* (+/+) mice and their BMTC/BMDM *in vivo* migration into the peritoneal cavity was examined 24-72 h later as described in Materials and Methods**.**

3. Zeb1 expression impairs macrophage maturation to LPM subpopulation

I next explored whether *Zeb1* regulates bone marrow mobilization of monocytes *in vivo* by chemotactic stimuli such as M-CSF, CCL2 or by ID8 tumor cells. Intraperitoneal injection of M-CSF or CCL2 in *Zeb1* (+/-) mice failed to elicit the mobilization and peritoneal infiltration of monocytes and the reduction in LPMs that is observed in *Zeb1* (+/+) mice after only 3 h (Figures 29 and 30), the same phenomena occurs using ID8 tumor cells as chemotactic stimulus after 72 hours (Figure 29).

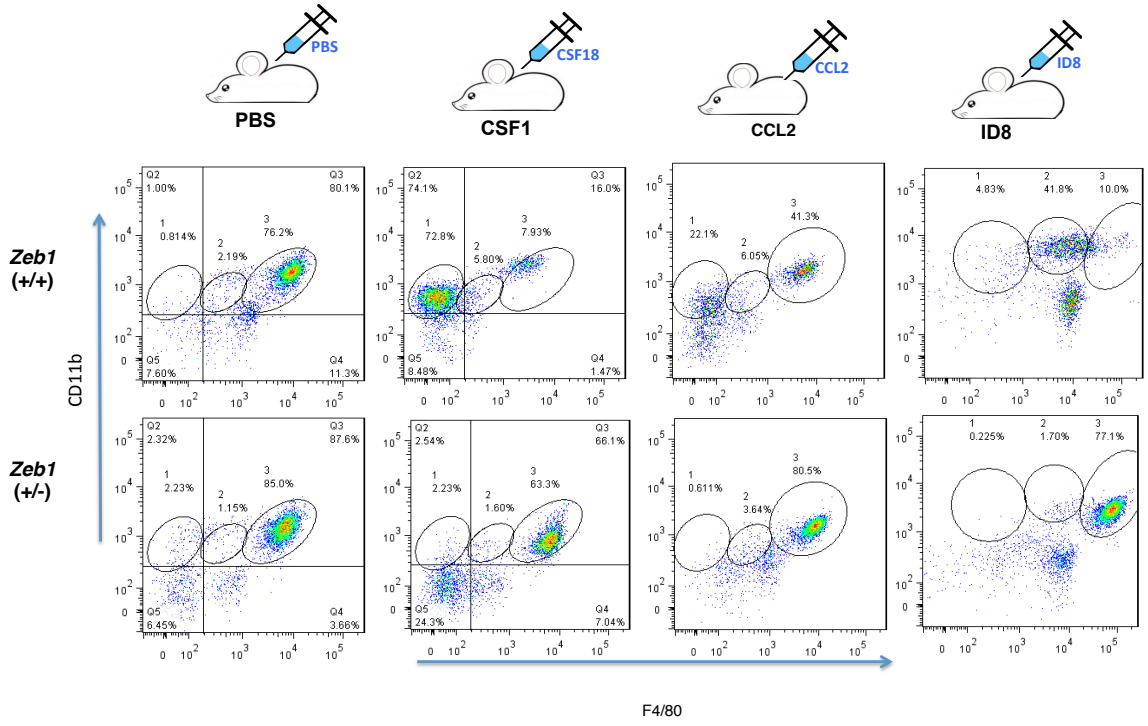

Figure 29. *Zeb1* (+/+) and *Zeb1* (+/-) mice were injected i.p. with PBS, CSF1, CCL2 for 3 hours or ID8 cells for 72 hours, and cells were analyzed by FACS

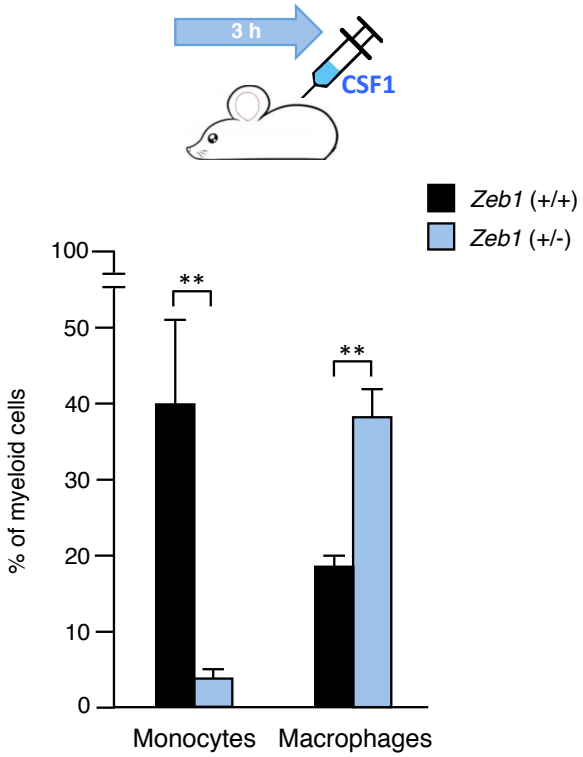

Figure 30. Four *Zeb1* (+/+) and four *Zeb1* (+/-) mice were injected i.p. with PBS or CSF1 and monocyte chemotaxis into the peritoneum and maturation into macrophages was examined after 3 h.

After 7 hours, SPM and LPM subpopulations almost recovered to basal conditions in *Zeb1* (+/+) but not in *Zeb1* (+/-) mice (Figure 31). Altogether, these results indicate a deficient mobilization of monocytes-macrophages in *Zeb1* (+/-) mice.

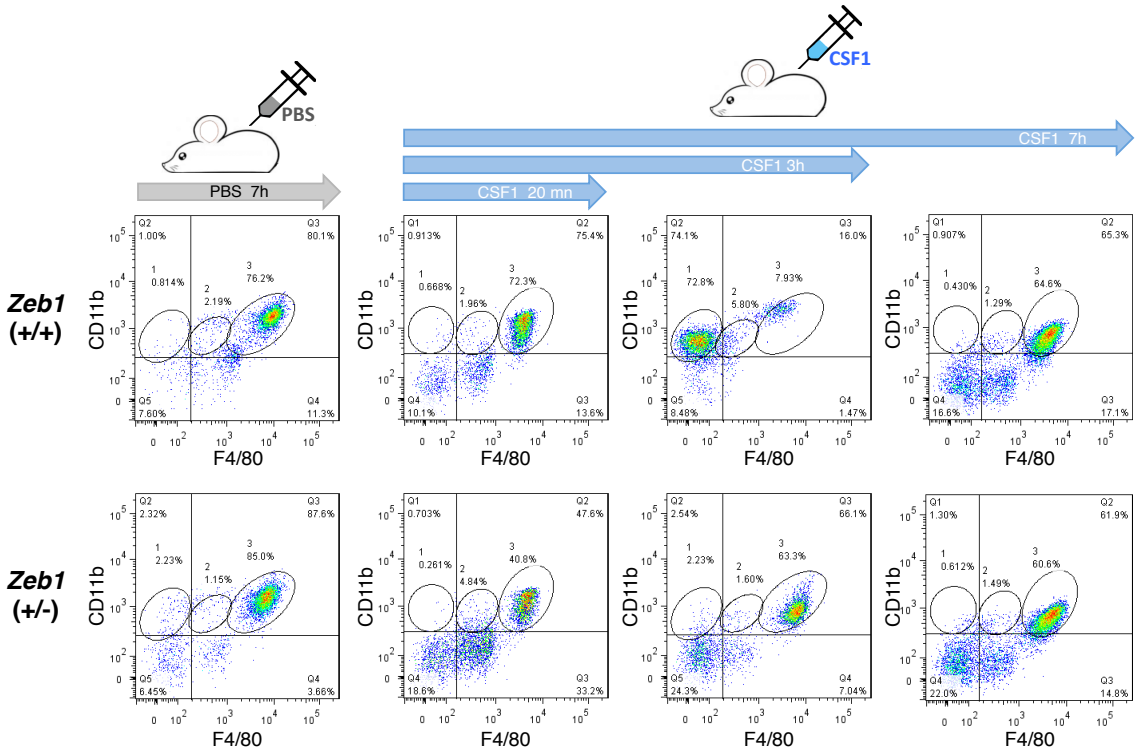

Figure 31. *Zeb1* (+/+) and *Zeb1* (+/-) mice were treated with CSF1 and the peritoneal myeloid subpopulation assessed by FACS as in Figure 22 over time (20 min-7h).

Next, I investigated whether the wild-type or *Zeb1*-deficient microenvironment background influences the migration of monocytes into the peritoneal cavity and their subsequent maturation into macrophages. To that effect, BMTCs from *Zeb1* (+/+) and *Zeb1* (+/-) mice were labeled with CFSE and injected i.v. and M-CSF i.p. into a *Zeb1* (+/+) recipient background. After only 4 h, a larger share of *Zeb1* (+/-) BMTCs [BMTC (+/-)] than wild-type ones [BMTC (+/+)] had differentiated toward macrophages (Figure 32). At later times (7 h), virtually all macrophages originated from BMTC (+/-), but only a small fraction of those originated from BMTC (+/+), were F4/80^{high} LPMs.

Altogether, these results indicate that BMTC (+/-) differentiate into macrophages more efficiently than wild type BMTCs and that *Zeb1* blocks monocyte-to-macrophage

differentiation. In addition, these results allow me to conclude that the failure of BMTC (+/-) to generate F4/80^{low} SPMs is independent of the microenvironment background of the recipient host—whether *Zeb1* (+/-) or (+/+)—but it is rather intrinsic to the *Zeb1*-deficiency of BMTCs.

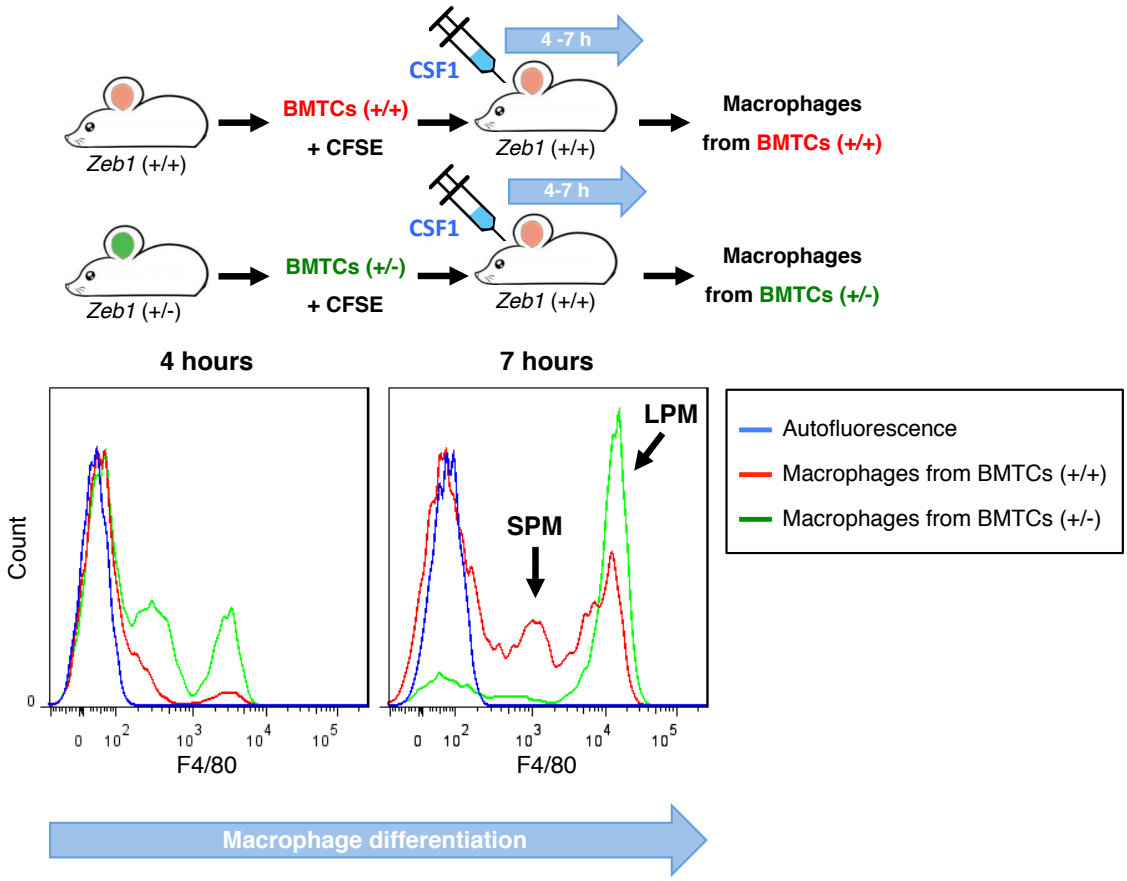

Figure 32. CFSE-labeled BMTCs from *Zeb1* (+/+) (BMTC (+/+)) and *Zeb1* (+/-) (BMTC (+/-)) mice were inoculated into wild-type mice. Mice were then injected i.p. with CSF1 and myeloid cell mobilization was assessed at 3 h and 7 h.

4. Zeb1 in response to LPS-induced endotoxic shock and tolerance

In light of the results above indicating that *Zeb1* regulates key pro-inflammatory and anti-inflammatory genes, I examined whether *Zeb1* modulates LPS-induced endotoxic shock and tolerance responses. Injection of LPS into mice triggers a strong pro-inflammatory macrophage-induced and NFκB-mediated response with high secretion of *Tnfa*, *Il1β*, *Il6*, and *Cox2*, which could eventually lead to death (Benoit et al., 2008). However, when mice are subjected to repeated doses of LPS, they developed a protective adaptive response (endotoxin tolerance) characterized by the inability of macrophages to produce pro-inflammatory cytokines and their switch to an anti-inflammatory phenotype (*Il10, Tgfβ1, Il1ra*) (Biswas and Lopez-Collazo, 2009; Pena et al., 2011). Since my results above indicate that *Zeb1* regulates key pro-inflammatory and anti-inflammatory genes, I examined whether *Zeb1* modulates LPS-induced endotoxic shock and tolerance responses.

Zeb1 (+/+) and *Zeb1* (+/-) mice were injected i.p. with a single lethal dose of LPS and their survival followed over time. I found that *Zeb1*-deficient mice have improved survival rates to LPS-induced shock compared than *Zeb1* (+/+) mice (Figure 33). This is in line with Figure 13 showing that *Zeb1* (+/-) macrophages produce lower levels of *Il1b, Nfkb1/p50* and *Il8*.

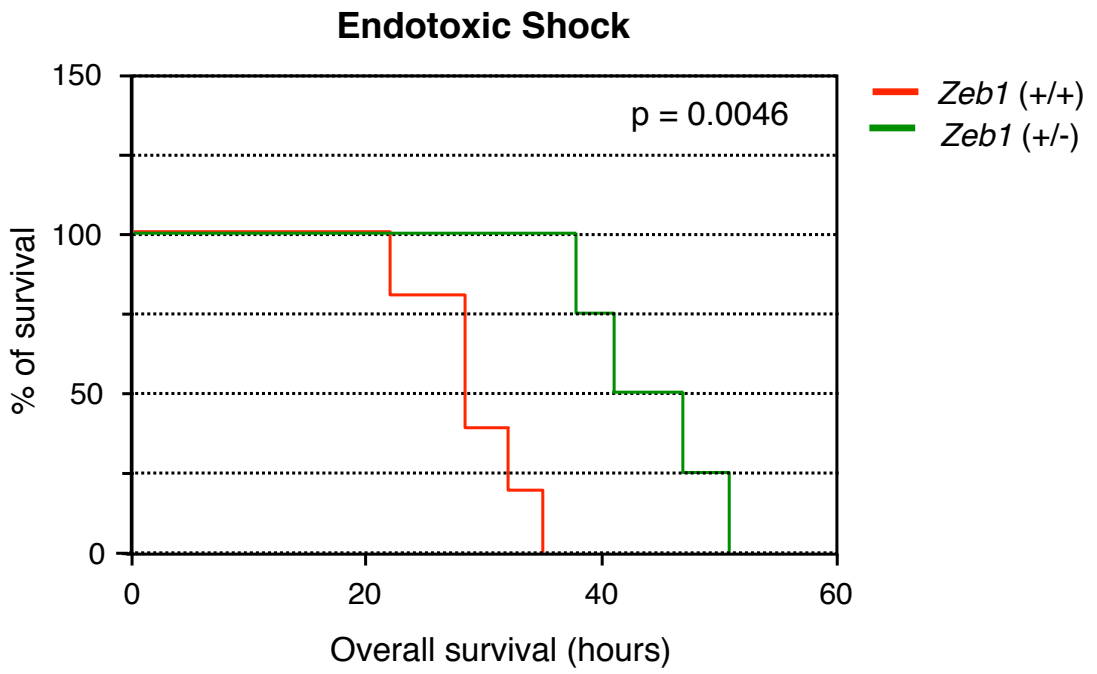

Figure 33. Kaplan Meier survival plots of *Zeb1* (+/+) and *Zeb1* (+/-) mice treated with a single lethal dose of LPS (endotoxic shock).

Next, mice from both genotypes were injected with a single sub-lethal dose of LPS followed by a lethal dose of LPS. Under these conditions, the opposite pattern was observed; *Zeb1* (+/-) mice died throughout the protocol, while all *Zeb1* (+/+) mice survived, indicating that *Zeb1* conferred strong protection against secondary endotoxin re-challenge (Figure 34). These data are also consistent with Figure 13, where *Zeb1* (+/-) macrophages failed to shift to an anti-inflammatory state and displayed lower levels of *Il10*. Altogether, these results indicate that *Zeb1* enhances not only the *in vivo* inflammatory response to LPS-induced endotoxic shock but also the tolerance response to secondary LPS stimulation.

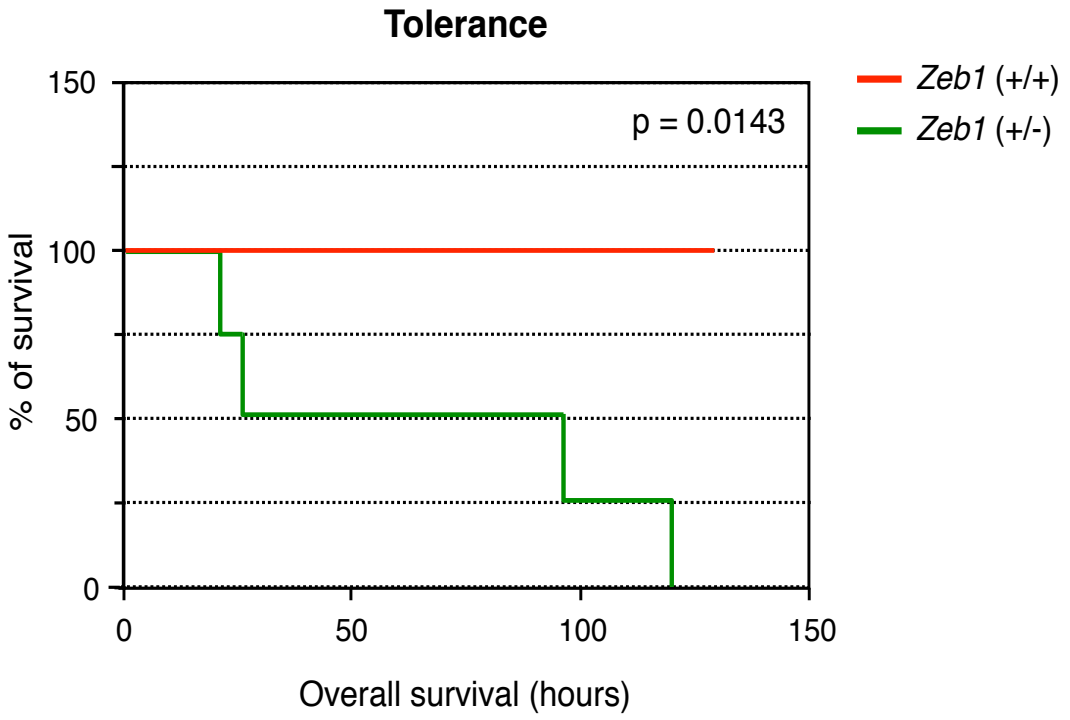

Figure 34. Kaplan Meier survival plots of *Zeb1* (+/+) and *Zeb1* (+/-) mice treated with a sub-lethal dose of LPS followed a lethal one (tolerance).

Next, I sought to investigate whether the response of *Zeb1* (+/-) mice to endotoxin shock or tolerance translated in a differential pattern of cytokine expression. Peritoneal macrophages from *Zeb1* (+/+) and *Zeb1* (+/-) mice were treated *ex vivo* with either a single dose or subsequent doses of LPS to mimic *in vivo* settings. Macrophages were then assessed for their expression of *Tnfa* (encoding TNF*a*) and *Il10,* the prototypical pro-inflammatory and anti-inflammatory cytokines responsible for the septic shock and tolerance, respectively (Sanchez-Tilló et al., 2007; Biswas and Lopez-Collazo, 2009). In line with *in vivo* results of Figure 33 and 34, I found that *Zeb1* (+/-) macrophages expressed lower levels of *Tnfa* in response to septic shock and had lower expression of *Il10* in response to tolerance (Figure 35).

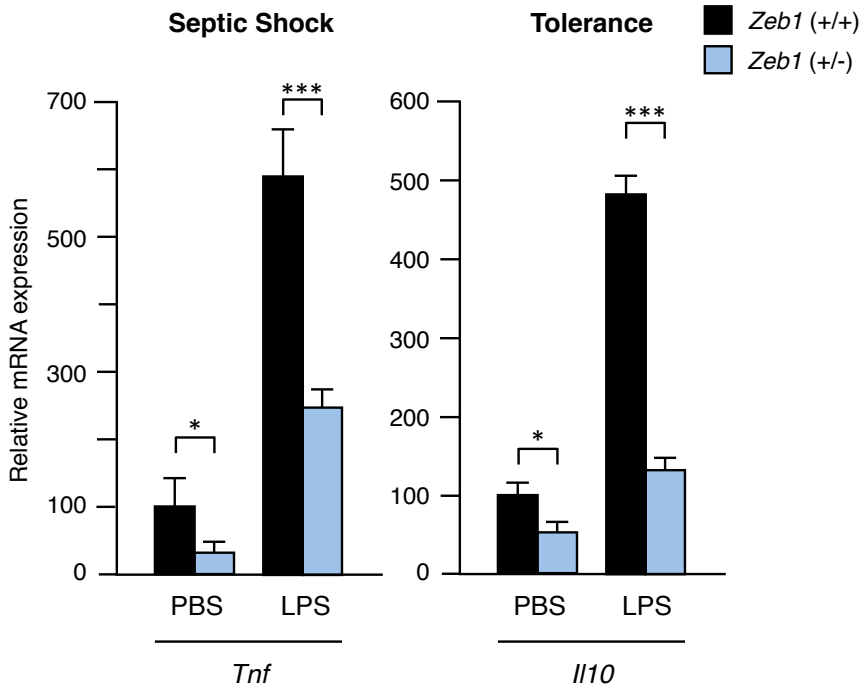

Figure 35. Peritoneal macrophages from *Zeb1* (+/+) and *Zeb1* (+/-) mice were treated with either a single doses or subsequent doses of LPS. Expression of *Tnf* and *Il10* were determined by qRT-PCR.

Chapter III : Role of *Zeb1* in the tumor microenvironment

1. Zeb1 is upregulated in TAMs increasing SPMs and a pro-tumor profile

My results above show that *Zeb1* (+/-) macrophages display lower levels of SPM-associated markers that are known to be also expressed by TAMs. Consequently, I first examined whether *Zeb1* expression in peritoneal macrophages was modulated by the presence malignant cells. To that effect, I used again the ID8 ovarian carcinoma model.

In wild-type mice, I found that *Zeb1* expression was much higher in peritoneal TAMs obtained from mice that had been injected with ID8 cells during 13 weeks than in basal peritoneal macrophages mice that had never been exposed to tumor cells (Figure 36). Similar upregulation of *Zeb1* was observed in peritoneal TAMs vis-à-vis normal peritoneal macrophages in *Zeb1* (+/-) mice (Figure 36). Importantly, these results indicate that *Zeb1* expression is activated by the presence of cancer cells and support a role for *Zeb1* in the regulation of a TAM phenotype.

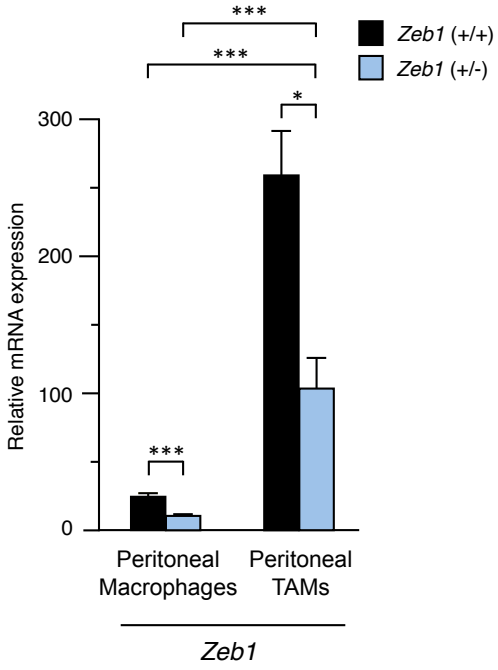

Figure 36. *Zeb1* expression increases during activation of peritoneal macrophages into TAMs. *Zeb1* mRNA levels were determined by qRT-PCR in peritoneal macrophages from *Zeb1* (+/+) and *Zeb1* (+/-) mice either under homeostasis conditions (peritoneal macrophages) or 13 weeks after injection of ID8 carcinoma cells (peritoneal TAMs).

I next explored whether or not expression of *Zeb1* by macrophages affects their activation towards TAMs. *Zeb1* (+/+) and *Zeb1* (+/-) mice were injected with ID8 cells during 8 weeks and the resulting peritoneal TAMs were examined for the expression of genes associated with a TAM phenotype. I found that expression of *Ccr2, Nfkb1/p50, Il1b, Il10, Cd163, Mrc1, Mmp9, and Vegf* was significantly lower in peritoneal *Zeb1* (+/-) TAMs than in their wild-type counterparts (Figure 37). Interestingly, the archetypal M1 *Nos2* and M2 *Arg1* genes—that displayed similar levels in both genotypes under homeostasis—were upregulated and downregulated, respectively, in *Zeb1* (+/-) TAMs (Figure 37). The above data indicate that *Zeb1* promotes the *in vivo* differentiation/activation of macrophages into TAMs, a process that is compromised in *Zeb1* (+/-) mice.

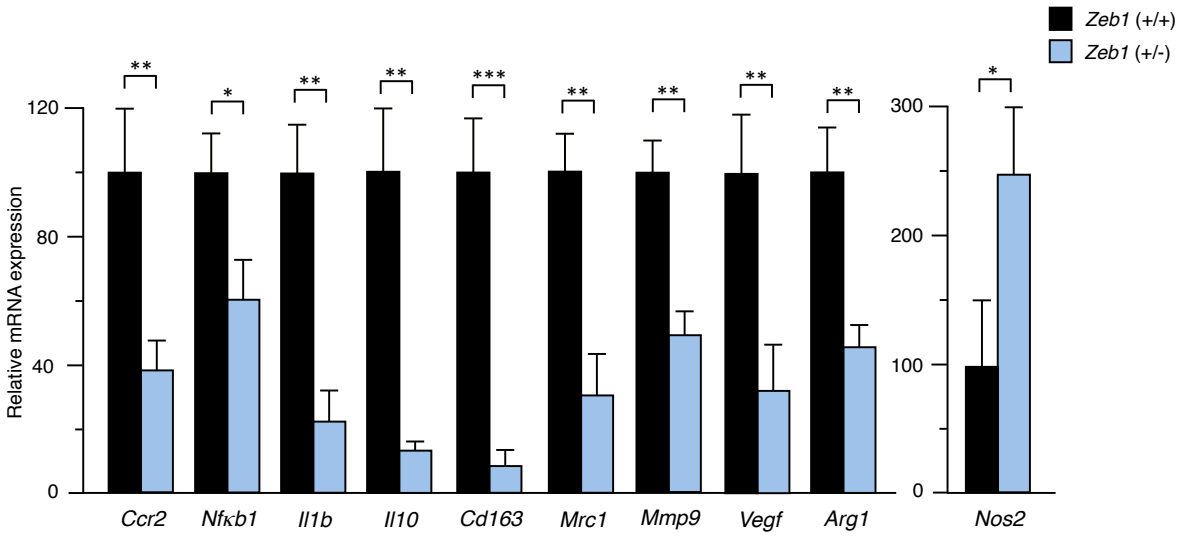

Figure 37. *Zeb1* (+/+) and *Zeb1* (+/-) mice were injected with ID8 cells and 6 weeks later peritoneal TAMs were isolated and assessed for gene expression by qRT-PCR.

In the ID8 ovarian cancer model, peritoneal TAMs with low expression of F4/80 (F4/80^{low}) (SPM-TAMs) display a strong pro-inflammatory and pro-angiogenic phenotype (e.g., high levels of *Vegf, Il1b, Il6*) that promotes ID8 cell proliferation (Hagemann et al., 2006; Cain et al., 2013; Rei et al., 2013). We examined the F4/80^{low} (SPM-TAMs) and F4/80^{high} (LPM-TAMs) subpopulations in the peritoneal exudate of *Zeb1* (+/+) and *Zeb1* (+/-) mice that had been injected with ID8 carcinoma cells for 6 weeks. I found that, compared to wild-type mice, the F4/80^{high} LPM-TAM subpopulation was expanded in *Zeb1* (+/-) mice (Figure 38). Likewise, the ratio F4/80^{high} to F4/80^{low} in *Zeb1* (+/-) TAMs was also higher than in *Zeb1* (+/+) TAMs (Figures 38 and 39). Of note, this ratio was even higher in TAMs than in the normal macrophages shown in Figures 7 and 8. The lower share of F4/80^{low} in *Zeb1* (+/-) TAMs reflects a deficient recruitment of circulating monocytes into the tumor microenvironment in *Zeb1* (+/-) mice, which parallels the lower *Ccr2* expression in *Zeb1* (+/-) macrophages and TAMs (Figures 13 and 37).

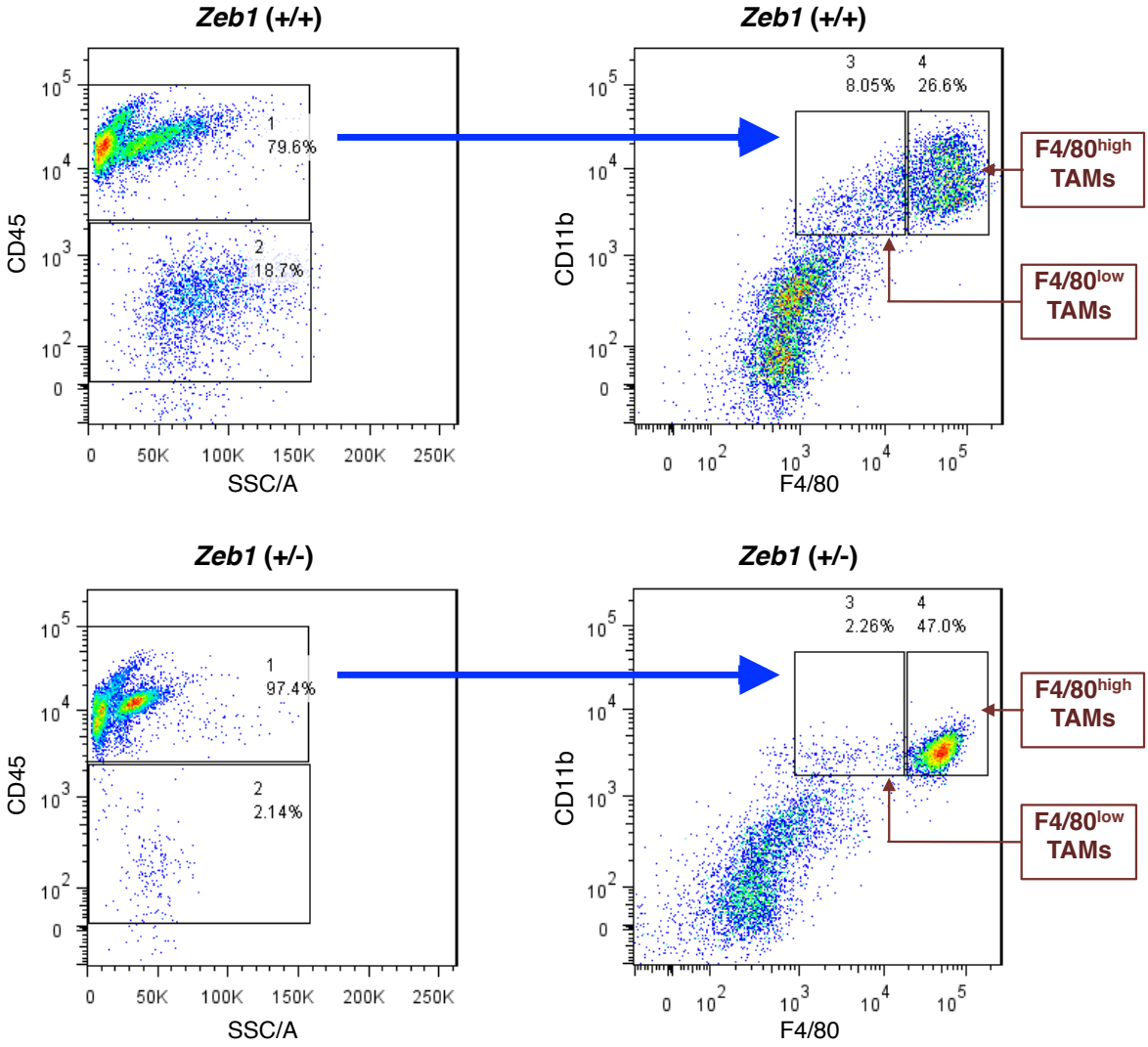

Figure 38. *Left panels*: *Zeb1* (+/+) and *Zeb1* (+/-) mice were injected with ID8 cells and the distribution of ID8 tumor ($CD45^-$) and immune ($CD45^+$) cells in peritoneal exudates was examined 6 weeks post-inoculation. *Right panels*: CD45+ cells were then analyzed for CD11b and F4/80 expression to determine the distribution of SPM ($F4/80^{low}$) and LPM ($F4/80^{high}$) TAM subpopulations. On the left panels, gates represent total leukocytes (1) and ID8 tumor cells (2). On the right panels, gates represent SPMs (3) and LPMs (4) from gate (1).

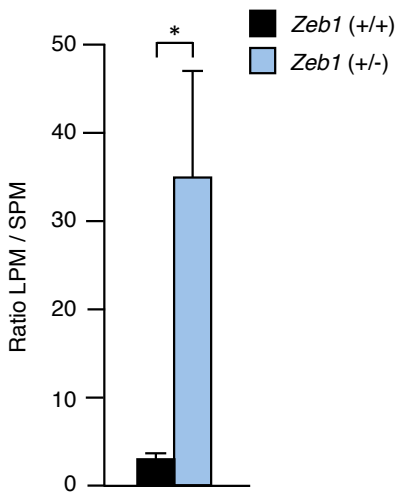

Figure 39. As in Figure 38, expression of F4/80 was assessed in TAMs from *Zeb1* (+/+) and *Zeb1* (+/-) mice 6 weeks upon injection with ID8 carcinoma cells.

The above results indicate that *Zeb1* upregulates *Ccr2* expression in macrophages and TAMs. I therefore investigated whether ZEB1 regulates *Ccr2* by direct binding to its promoter. ZEB1 binds to a subset of E-box and E-box-like sequences in the regulatory regions of its target genes (Brabletz and Brabletz, 2010).

Examination of the first 2 kb of the mouse *Ccr2* promoter revealed the existence of at six ZEB1 high-affinity binding sequences (Figure 40). The ability of endogenous *Zeb1* to directly bind to the *Ccr2* promoter was tested for two of these sites (-868 bp and -818 bp) by chromatin immunoprecipitation (ChIP) assay in BMDMs from wild-type mice. It was found that an antibody against *Zeb1*, but not its respective host matched control IgG, immunoprecipitated a region of the mouse *Ccr2* promoter containing both of these sites but not a region lacking consensus binding sites for *Zeb1* (Figure 40).

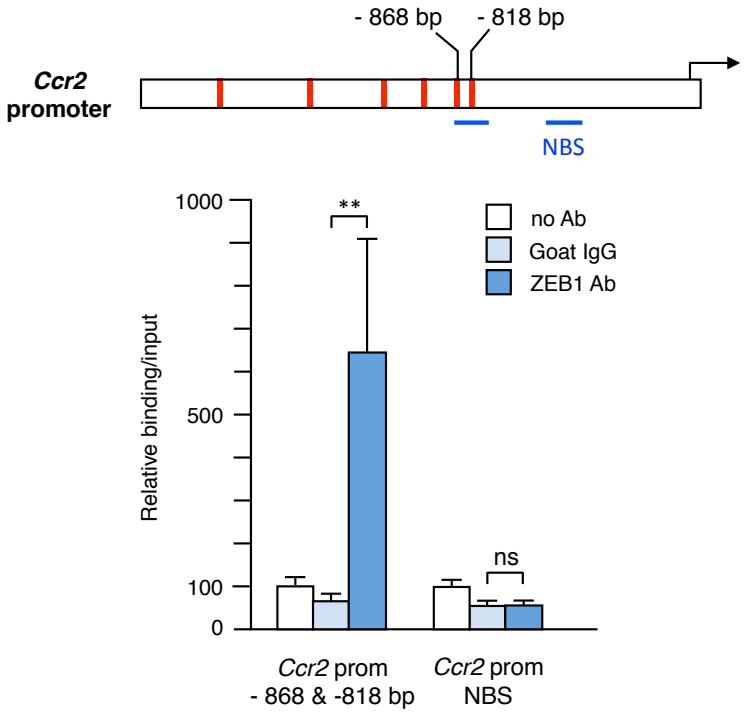

Figure 40. ZEB1 binds to the mouse *Ccr2* promoter. *Upper panel*: Scheme of 2 kb of the *Ccr2* promoter. Consensus binding sites for ZEB1 in the first -2 kb of the *Ccr2* promoter include six high affinity sequences (red boxes) at -1713 bp (CAGCTG), -1398 bp (CACCTG), -1136 bp (CAGCTG), -984 bp (CACGTA), -868 bp (CAGGTG), and -818 bp (CAGGTG). The regions examined by ChIP assay are represented by blue bars (see below). *Lower panel*: DNA from BMDM immunoprecipitated with antibodies against ZEB1 (E-20X) or goat IgG serum control was amplified by qRT-PCR for two regions of the *Ccr2* promoter, one containing a consensus ZEB1 binding sites at – 868 bp and -818 bp (-868/-772 bp) and another lacking consensus binding sites for ZEB1 (non-binding site, NBS, -574/-422 bp) (blue bars in the upper panel). A condition without antibody is also shown. For each promoter fragment, the condition without antibody was equaled to 100.

2. Expression of Zeb1 in F4/80^{low} TAMs promotes tumor progression

Within TAMs, those with F4/80^{low} (SPM-TAMs), have a stronger pro-tumor effect by supporting cancer cell survival and tumor angiogenesis (Ostuni et al., 2015; Rei et al., 2014). I therefore explored whether the smaller fraction of F4/80^{low} SPM-TAM in *Zeb1* (+/-) mice affects tumor progression.

Zeb1 (+/+) and *Zeb1* (+/-) mice were injected with ID8 cells and sacrificed 6 weeks later to examine tumor growth. I found that the number of ID8 cells in the peritoneal exudate of *Zeb1* (+/-) mice—assessed as the percentage of $CD45^-$ cells—was drastically lower than in *Zeb1* (+/+) mice (*Left panel* Figure 38 and Figure 41). These results indicate that *Zeb1* expression in TAMs promotes tumor growth. I then investigated whether the more differentiated phenotype of ID8 cells when they have been injected in *Zeb1* (+/-) mice than in *Zeb1* (+/+) mice translated into a less aggressive tumor behavior. Indeed, compared to wild-type mice, there were not only lower number of ID8 cells in *Zeb1* (+/-) mice, but I also detected fewer tumor deposits in the peritoneal lining of these mice (Figure 42).

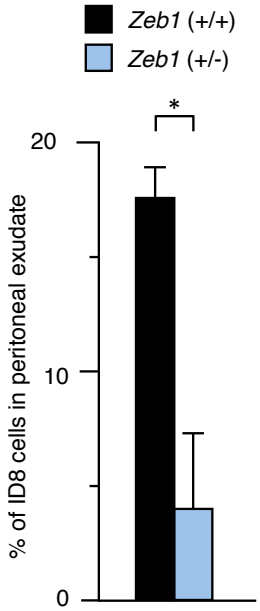

Figure 41. Reduced tumor growth of ID8 cells in *Zeb1* (+/-) mice. As in the the percentage of ID8 cells in the peritoneal cavity of *Zeb1* (+/+) and *Zeb1* (+/-) mice was assessed by FACS 6 weeks after injection.

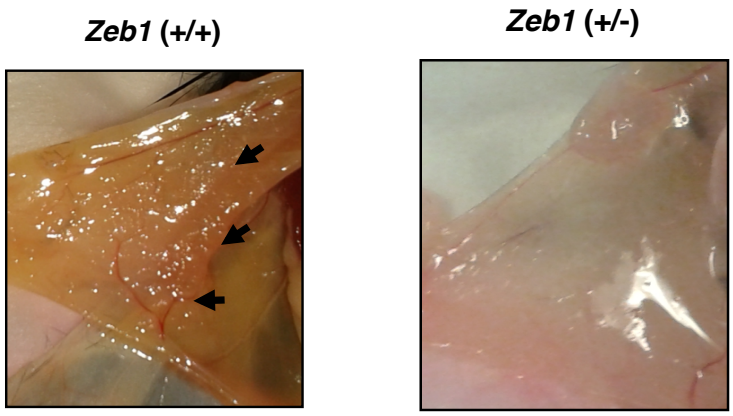

Figure 42. Representative images of the peritoneal lining of *Zeb1* (+/+) and *Zeb1* (+/-) mice 13 weeks after i.p. injection with ID8 carcinoma cells are shown.

Also tumor progression of the ID8 tumor model in *Zeb1* (+/+) and *Zeb1* (+/-) mice was also followed over time by bioluminescence imaging. Mice from both genotypes were injected with ID8 cells that carried the luciferase-2 gene (ID8-luc) followed by administration of the cycLuc1 luciferase substrate. As shown in Figures 43 and 44, tumor load was lower in *Zeb1* (+/-) mice than in *Zeb1* (+/+) counterparts, confirming once again a faster tumor progression in a wild-type microenvironment.

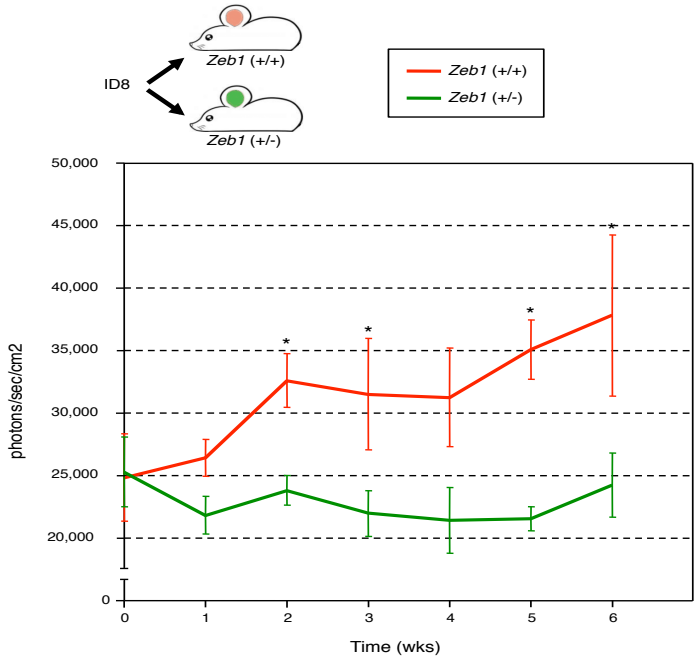

Figure 43. A *Zeb1* (+/-) background suppresses tumor growth. *Zeb1* (+/+) and *Zeb1* (+/-) mice were injected with ID8-luc cells and tumor load progression was followed up over time by bioluminescence imaging. Tumor load in *Zeb1* (+/+) was significantly larger than in *Zeb1* (+/-) with a $p \leq 0.05$ (*) at the indicated time points. Five mice of each genotype were included.

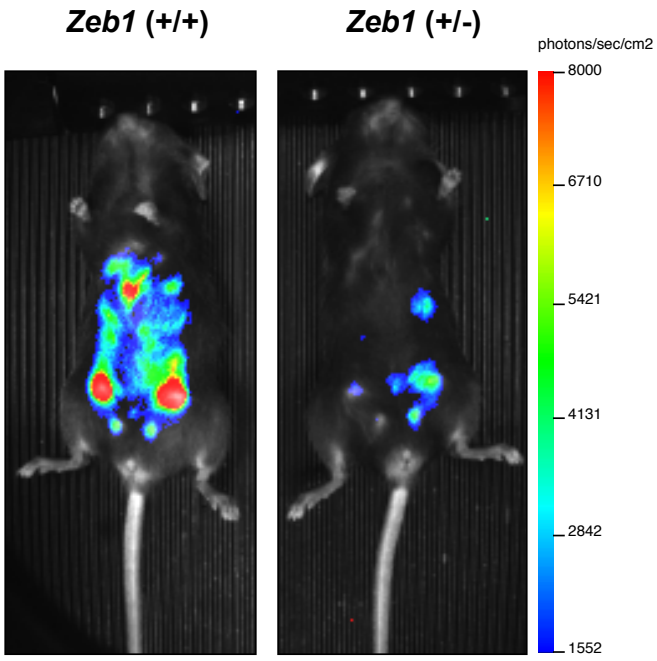

Figure 44. Representative pictures of the bioluminescence signal of mice for each genotype at week 6.

Next, I investigated whether the smaller proportion of F4/80^{low} TAMs in *Zeb1* (+/-) mice alters the phenotype of the injected ID8 tumor cells. The expression of an epithelial phenotype in carcinomas, including E-cadherin, is associated with a less aggressive behavior (Perl et al., 1998; Sawada et al., 2008; and reviewed in Nieto et al., 2016). Mice from both genotypes were injected with ID8 cells and after 13 weeks they were sacrificed and ID8 cells were examined for the expression of a panel of genes, namely: *Zeb1* itself, whose expression determines worse prognosis in most cancers; E-cadherin (*Cdh1*) and vimentin (*Vim*), the archetypal epithelial and mesenchymal markers, respectively (Nieto et al., 2016); *Aldh1a1* and *Kit*, two cancer stem cell markers whose expression is associated with tumor progression and poorer prognosis in most carcinomas, including ovarian (Ginestier et al., 2007; Silva et al., 2011; Chau et al. 2013); and *Mdr1/Abcb1*, an efflux drug transporter whose expression is associated to chemotherapy resistance (Gottesman et al., 2002).

Interestingly, I found that expression of *Zeb1* was higher in the ID8 cells isolated from peritoneal cavity of *Zeb1* (+/+) mice than in those from *Zeb1* (+/-) mice (Figure 45). In that line, expression of *Vim, Aldh1a1*, *Kit* and *Mdr1* were also higher in ID8 cells recovered from *Zeb1* (+/+) mice while *Cdh1* was lower (Figure 45). Two conclusions can be raised from the above results: first, *Zeb1* (+/+) TAMs elicit a greater tumor response than *Zeb1* (+/-) counterparts, and second, *Zeb1* expression in TAMs alters the functional phenotype of malignant cells triggering a mesenchymal, stem-like EMT phenotype and chemotherapy resistance.

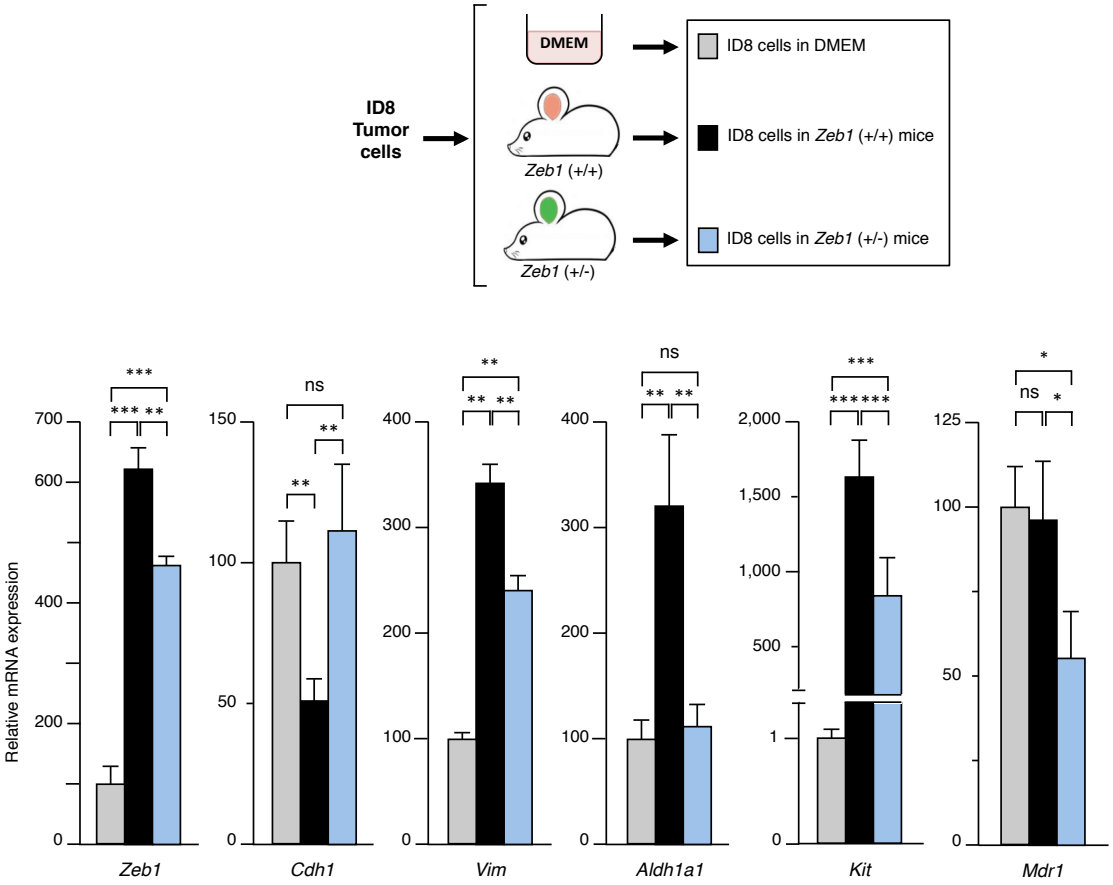

Figure 45. ID8 cells were either cultured *in vitro* (DMEM) or injected i.p. during 13 weeks into *Zeb1* (+/+) and *Zeb1* (+/-) mice. ID8 cells for the three conditions were assessed by qRT-PCR for the expression of the indicated genes in reference to *Gapdh*.

TAM infiltration associates with higher tumor cell resistance to chemotherapy (De Palma and Lewis, 2013). Therefore, I examined whether expression of *Zeb1* in TAMs affected the response of ID8 cells to cisplatin. I found that ID8 cells isolated from *Zeb1* (+/-) mice displayed higher sensitivity to cisplatin than ID8 isolated from wild-type counterparts (Figure 46). Likewise, incubation of ID8 cells with CM from wild-type TAMs, but not with CM from *Zeb1*-deficient TAMs, rendered cancer cells more resistant to cisplatin (Fig. 47). I can thus conclude that for TAMs to enhance resistance to cisplatin they have to express full levels of *Zeb1*.

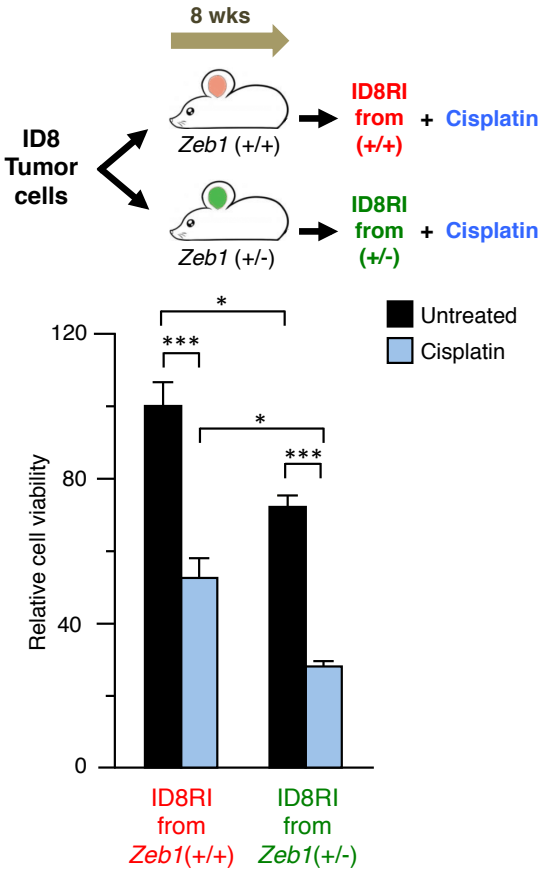

Figure 46. ID8 cells isolated from mice of both genotypes 8 weeks after injection were culture in complete medium or in the presence of 50 μg/ml of cisplatin and their viability assessed by an MTT assay.

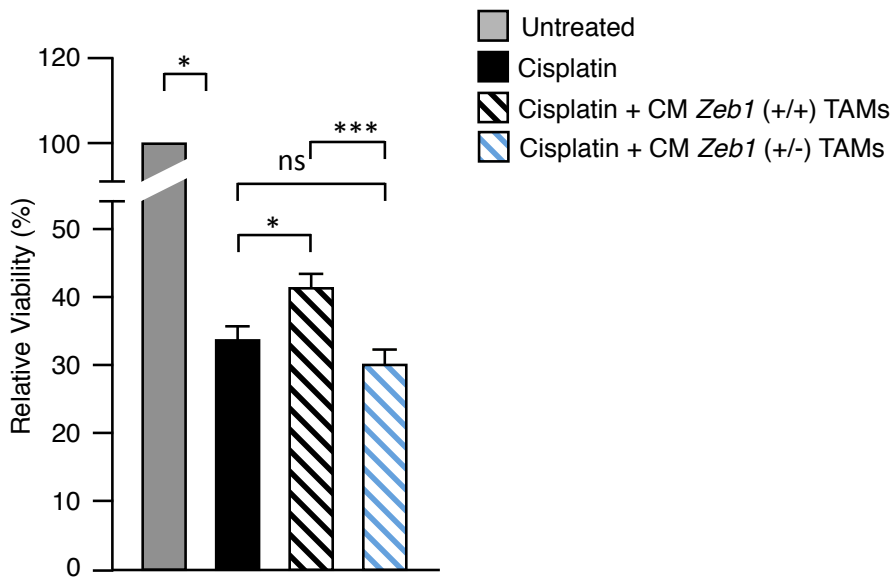

Figure 47. ID8 cells were cultured in complete medium or treated with 50 µg/ml of cisplatin and then either incubated with CM from *Zeb1* (+/+) or *Zeb1* (+/-) TAMs.

3. Zeb1 activates a Ccr2-Mmp9-Ccl2 loop between TAMs and cancer cells

Growth of ID8 cancer cells in the peritoneal cavity of a mouse activates the Src/Akt/Erk pathways and confers them with enhanced tumor aggressiveness (Cai et al. 2015). Thus, when ID8 cells are isolated from a mouse ascites and are reinjected into a new recipient mouse, these new ID8 cells—renamed hereafter as ID8RI—accelerate the onset and progression of tumor growth and ascites formation further (Cai et al., 2015). This indicates that the tumor microenvironment provided by the mouse peritoneal cavity modulates the functional phenotype of ID8 cells previously grown *in vitro*. I next tested the expression of *Zeb1* and *Ccl2* in ID8RI cells and found that, ID8RI cells that had grown in the peritoneal cavity of mice expressed higher levels of both genes than ID8 cells (Figure 48).

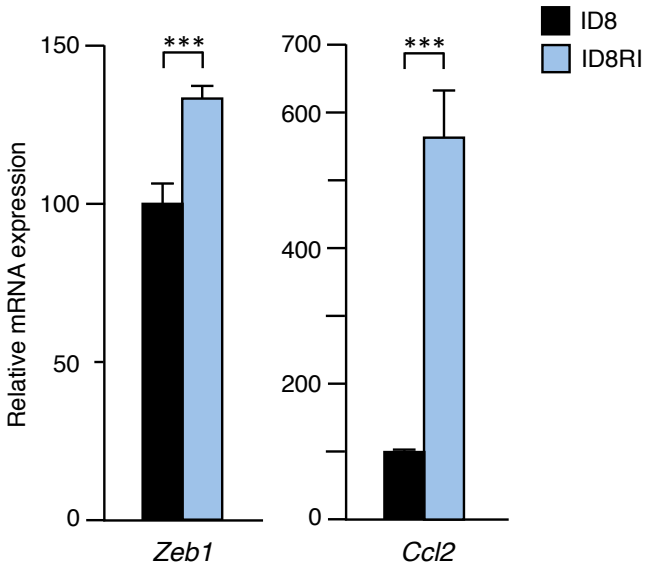

Figure 48. ID8RI cells express higher levels of *Zeb1* and *Ccl2* than parental ID8 cells. ID8 and ID8RI cells were assessed for gene expression by qRT-PCR with respect to *Gapdh*.

I next explored whether this higher expression of *Ccl2* by ID8RI cells was modulated specifically by the expression of *Zeb1* in TAMs. Since I found that ID8 cells that had been injected into *Zeb1* (+/+) during 13 weeks expressed higher levels of *Ccl2* than those that were injected in *Zeb1* (+/-) mice (Figure 49 left panel). In fact, the ID8 cells that were injected in *Zeb1* (+/-) mice display similar expression of *Ccl2* than were not injected in mice and rather maintained in DMEM medium. I therefore cultivated ID8 cells with conditioned medium (CM) collected from either normal peritoneal macrophages or TAMs from both genotypes. I found that *Ccl2* expression was higher in ID8 cells incubated with CM from *Zeb1* (+/+) macrophages or TAMs than in ID8 cells cultured with CM from *Zeb1* (+/-) counterparts (Figure 49, center and right panels, respectively). Importantly, these results indicate that *Zeb1* not only upregulates *Ccr2* in TAMs (Figure 37) but also induces the expression of *Ccl2* in cancer cells (Figure 49). By triggering this positive *Ccr2*-*Ccl2* loop between TAMs and cancer cells, *Zeb1* regulates the crosstalk between tumors and their microenvironment that contributes to tumor progression.

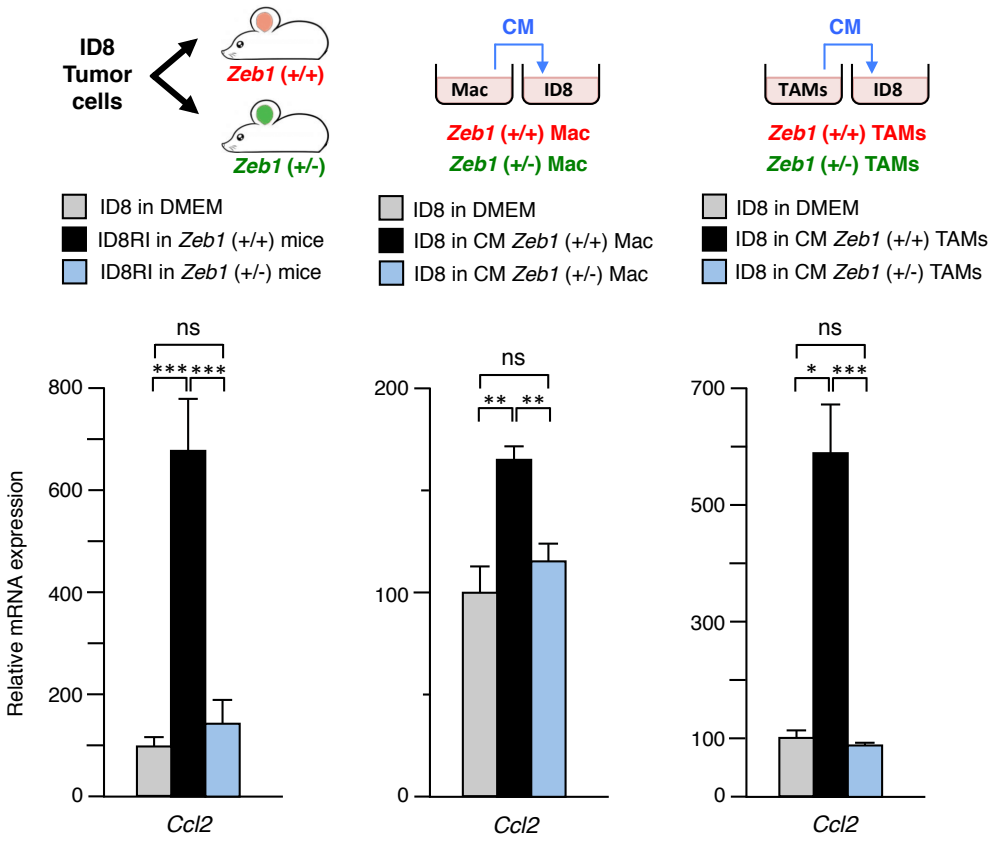

Figure 49. The expression of *Ccl2* was examined by qRT-PCR in ID8 cells cultured *in vitro* in complete medium (DMEM), from 13 weeks tumor-bearing mice or co-cultured with conditioned medium (CM) from either *Zeb1* (+/+) and *Zeb1* (+/-) peritoneal macrophages (central panel) or with CM from *Zeb1* (+/+) and *Zeb1* (+/-) peritoneal TAMs (right panel).

Production of the metalloproteinase MMP9 by tissue macrophages and TAMs is not only required for their migration and infiltration but it also promotes invasiveness and metastasis of malignant cells and tumor angiogenesis (Hiratsuka et al., 2002; Giraudo et al., 2004; Gong et al., 2008). I therefore explored whether the lower *Mmp9* expression I observed in *Zeb1*-deficient macrophages and TAMs (Figures 13 and 37) participates in the more differentiated phenotype of ID8 cancer cells when injected in *Zeb1* (+/+). I first examined whether the MMP9 produced by TAMs affected *Ccl2* expression in ID8 cells. ID8 cells were incubated with CM from *Zeb1* (+/+) and *Zeb1* (+/-) TAMs in the presence of absence of an MMP9 allosteric inhibitor. Upregulation of *Ccl2* in ID8 cells by CM from *Zeb1* (+/+) TAMs was reduced by the MMP9 inhibitor (Figure 50). In contrast, *Ccl2* expression was not altered by CM from *Zeb1* (+/-) TAMs nor by the MMP9 inhibitor (Figure 50).

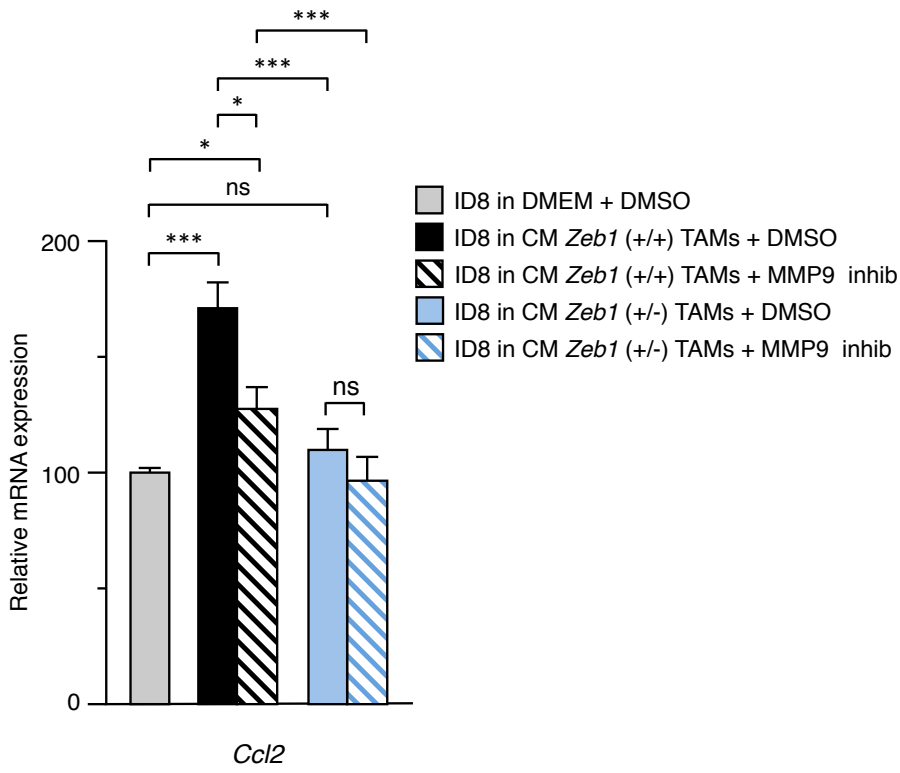

Figure 50. ID8 cells were incubated with CM from *Zeb1* (+/+) and *Zeb1* (+/-) TAMs in the presence of absence of an MMP9 as described in Materials and Methods.

This positive regulation of *Ccl2* in ID8 cells by MMP9 was corroborated with recombinant mouse MMP9 (Figure 51) in ID8 cells and mouse recombinant CCL2 in peritoneal macrophages (Figure 52). Altogether these results indicate that lower MMP9 production by *Zeb1* (+/-) TAMs contributes, at least in part, to the lower induction of *Ccl2* found in tumor cells that had grown in a *Zeb1*-deficient microenvironment. CCL2 promotes tumor progression mainly by its effects on macrophages but CCL2 also has direct effects on tumor cells where it enhances cancer cell survival and motility, in part through the induction of MMP9 (Dagouassat et al., 2010; Fang et al., 2012).

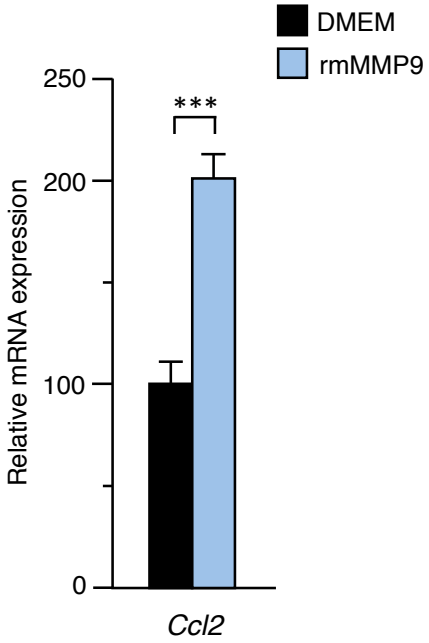

Figures 51. Recombinant mouse MMP9 (rmMMP9) upregulated *Ccl2* in ID8-luc cells. Data show three independent experiments.

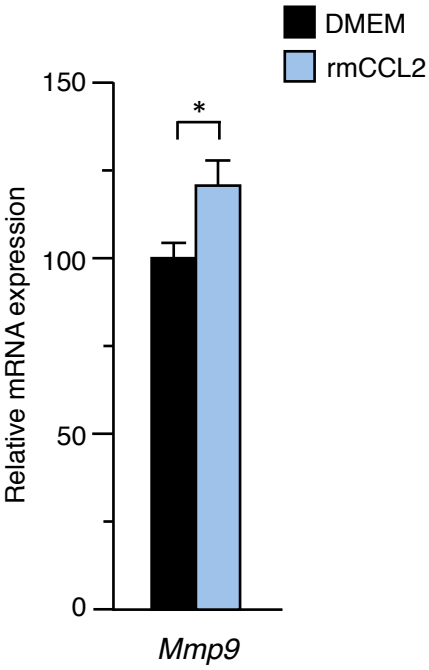

Figures 52. Recombinant mouse CCL2 (rmCCL2) induces MMP9 in peritoneal macrophages. Data show three independent experiments.

Blockade of CCL2-CCR2 signaling in macrophages reduces tumor progression and metastasis (Qian et al., 2011). I next tested the effect of blocking CCL2-CCR2 signaling on the phenotype of ID8 cells. ID8 tumor-bearing *Zeb1* (+/-) and *Zeb1* (+/+) mice were injected with a CCR2 small molecule antagonist and the CM produced by their respective TAM was use to culture ID8 cells *in vitro*. In line with the experiments above, the CM collected from *Zeb1* (+/+) mice elicited higher *Ccl2* expression in ID8 cells that the CM from *Zeb1* (+/-) mice (Figure 49). Notably, the effect on *Ccl2* expression by the CM from *Zeb1* (+/+) mice was drastically inhibited by the CCR2 antagonist while it had no significant effect on ID8 cells that were cultured with *Zeb1* (+/-) TAMs CM (Figure 53).

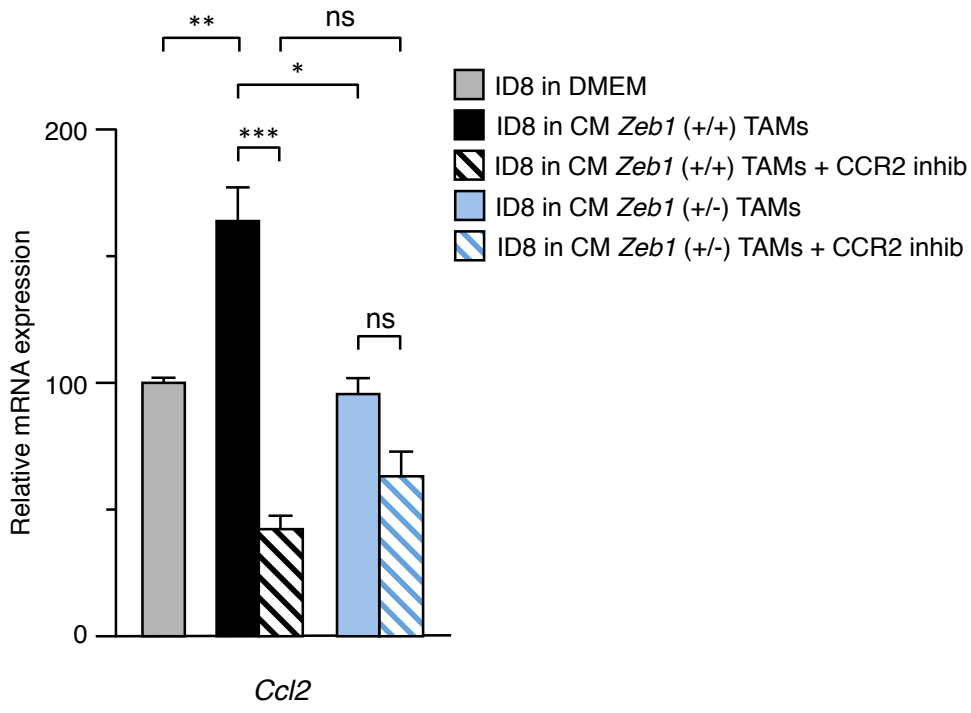

Figure 53. Blocking of CCL2-CCR2 signaling in TAMs inhibited *Ccl2* expression in cancer cells. Wild-type and *Zeb1*-deficient ID8 tumor-bearing mice were injected with a CCR2 antagonist and the CM produced by their respective TAM was added to ID8-luc cells and their expression of Ccl2 assessed by qRT-PCR as described in Methods.

4. More aggressive phenotype by tumor cells elicits a more pro-tumoral phenotype in TAMs

My results above showed the progression of the ID8 cancer model and the phenotype of ID8 cancer cells are determined by the levels of *Zeb1* expression in TAMs. Compared to wild-type TAMs, *Zeb1*-deficient TAMs, which also express lower levels of *Mmp9* and *Ccr2*, trigger a more differentiated and less aggressive phenotype in ID8 cells. Since tumor cells also modulate the phenotype of TAMs, I examined whether a more or less aggressive phenotype of ID8 cells elicits a different TAM response. ID8 carcinoma cells were injected into *Zeb1* (+/+) and *Zeb1* (+/-) mice. After 13 weeks, tumor cells were isolated (ID8RI cells) and reinjected into wild-type mice during 6 weeks (see scheme of the experiment on top of Figure 54).

I isolated TAMs in both experimental conditions and characterized their gene expression profile. It was found that the ID8RI cells obtained from wild-type mice—that consequently express higher levels of *Ccl2* (Figure 48)—produced a stronger macrophage activation toward TAMs than the ID8RI cells isolated from *Zeb1* (+/-) mice (Figure 54). Thus, the expression of *Ccr2, Il1b, Il10, Cd163, Mrc1 and Mmp9* were higher in the TAMs isolated from wild-type mice injected with ID8RI previously grown in a wild-type tumor microenvironment that in the TAMs of also wild-type mice but injected with ID8RI previously grown in a *Zeb1*-deficient background. These results indicate that, independently of the recipient background—all recipient mice were wild-type—the more aggressive and less differentiated ID8RI cells from wild-type have a greater capacity to induce macrophage activation towards TAMs than ID8RI cells that have been previously modulated by *Zeb1*-deficient TAMs.

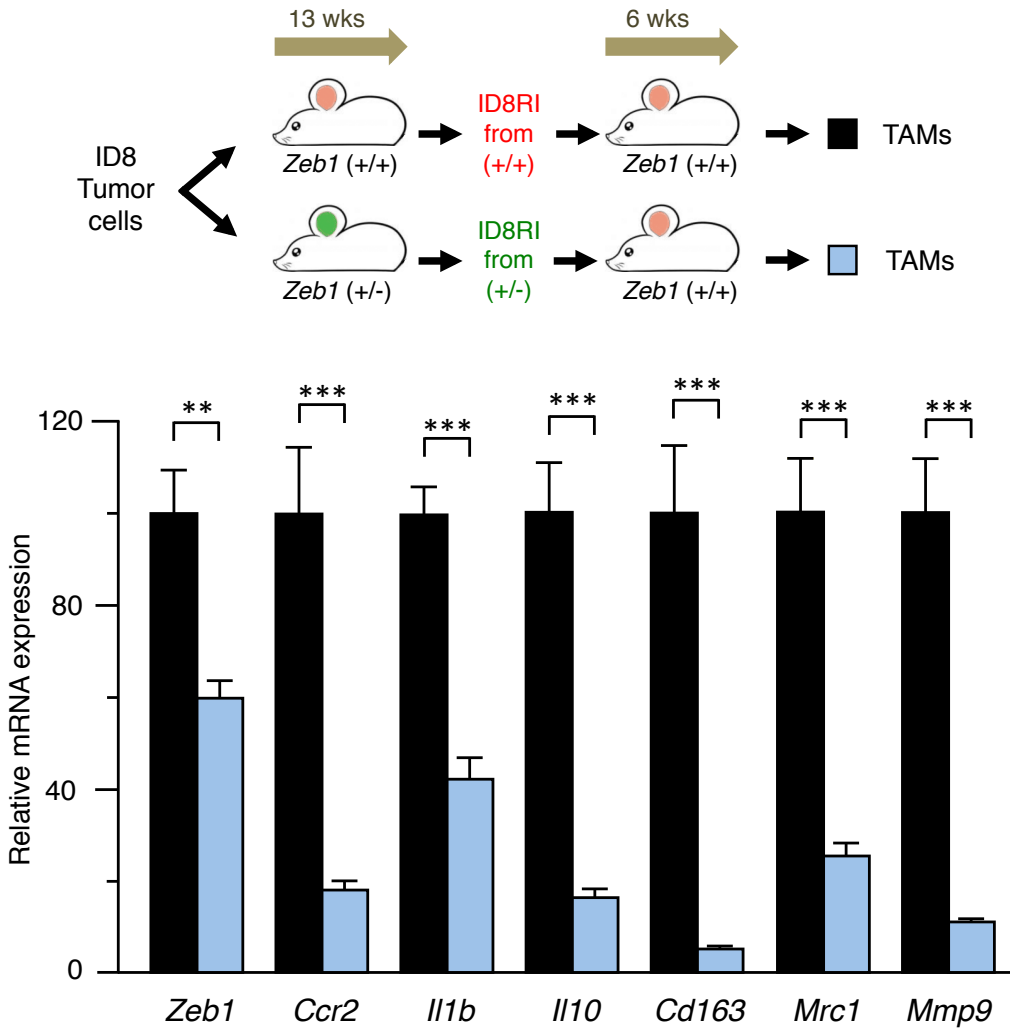

Figure 54. ID8 cells that had been previously inoculated in *Zeb1* (+/+) or *Zeb1* (+/-) mice for 13 weeks (ID8-RI-wt and ID8-RI-het cells, respectively) were reinjected into *Zeb1* (+/+) mice. After 6 weeks, TAMs were isolated and analyzed for their gene expression profile analyzed by qRT-PCR with reference to *Gapdh*.

In line with the higher aggressiveness of ID8RI cells compared to ID8 cells, I found that after 6 weeks ID8RI isolated from wild-type mice cells developed similar levels of tumor deposits and ascites after only 6 weeks than those observed upon 13 weeks with parental ID8 cells. Interestingly, the ID8RI cells isolated from *Zeb1* (+/-) mice resulted in lower ascites and tumor deposits than those rendered by ID8RI obtained from *Zeb1* (+/+) mice (Figures 55). These results indicate that the slower tumor progression of ID8 cells in the context of *Zeb1*-deficient mice is transferable into wild-type mice.

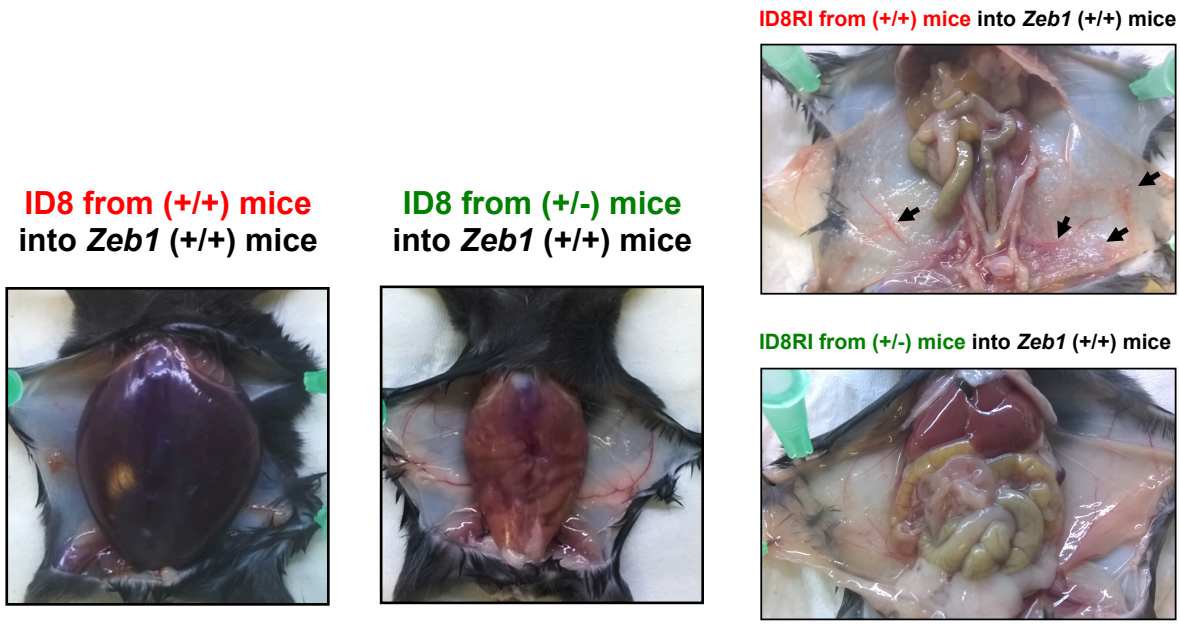

Figures 55. Representative images of *Zeb1* (+/+) mice injected with ID8 RI (+/+) and ID8RI (+/-) showing ascites and tumor deposits in peritoneal cavity.

5. Adoptive transfer of Zeb1-deficient macrophages into mice failed to promote tumor progression

Previous figures have shown for the first time the importance of *Zeb1*-deficient or wild-type microenvironment in tumor progression. Next, I sought to confirm that the reduced and delayed tumor progression of ID8 cells in *Zeb1* (+/-) mice is due to the deficient pro-tumor function of *Zeb1* (+/-) macrophages. It has been reported that adoptive transfer of wild-type macrophages into tumor-bearing mice accelerates tumor progression (Hagemann et al., 2008).

I injected ID8RI cells into wild-type mice that were then divided in three cohorts. Twenty-three days later, one of the cohorts of tumor-bearing mice was injected i.p. with PBS while the other two cohorts were injected i.p. with BMDM derived from either *Zeb1* (+/+) and *Zeb1* (+/-) mice [BMDMs (+/+) and BMDMs (+/-), respectively]. Tumor progression was then followed by luminescence bioimaging up to thirty days from the time of ID8RI cell injection. In line with Hagemann et al. (2008), tumor-bearing mice injected with BMDMs (+/+) displayed an accelerated tumor growth compared to those injected with PBS (Figure 56). Importantly, tumor-bearing mice injected with BMDMs (+/-) displayed a slower tumor progression than those injected with BMDMs (+/+) (Figure 56). These results indicate that expression of *Zeb1* in macrophages (BMDM) and TAMs promotes tumor progression and that *Zeb1*-deficient TAMs are responsible for the reduced tumor progression of the ID8 carcinoma model in *Zeb1* (+/-) mice.

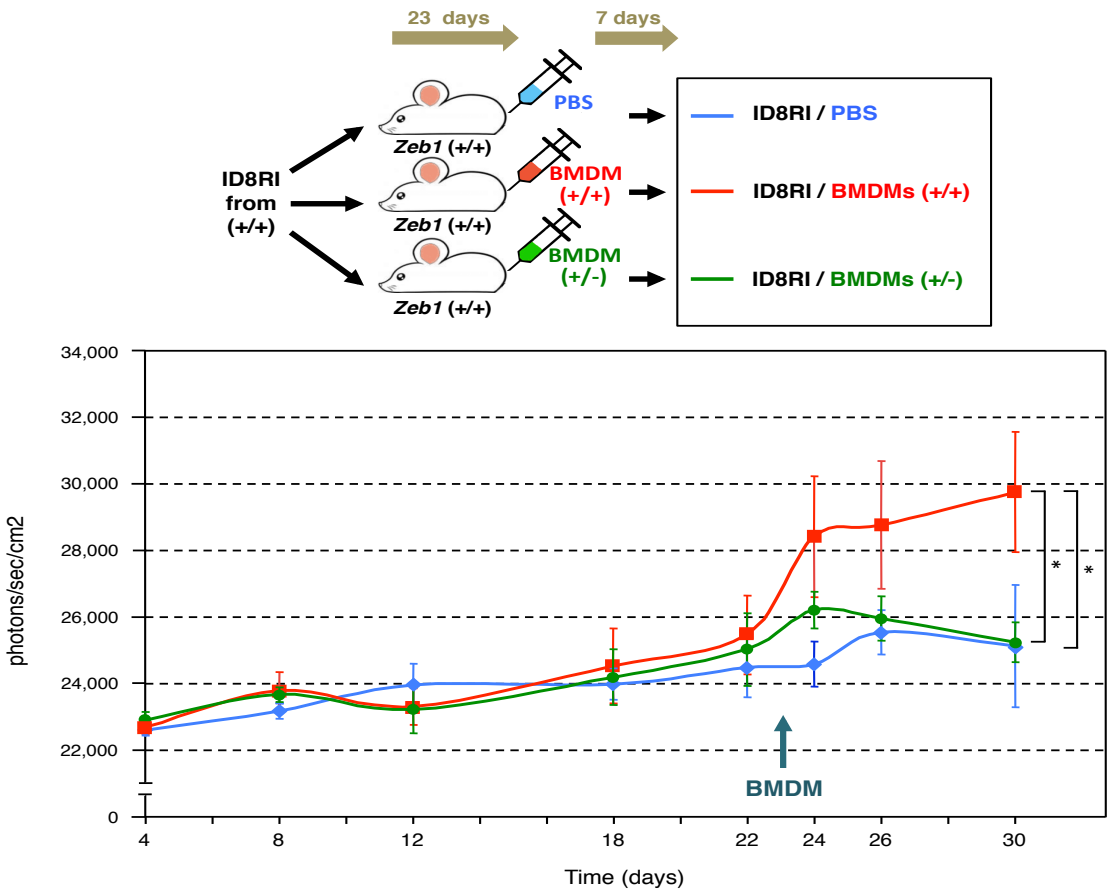

Figure 56. ID8-luc cells isolated from *Zeb1* (+/+) mice 13 weeks upon inoculation (ID8RI-wt) were reinjected in *Zeb1* (+/+) mice that were then divided in three cohorts. At day 23, each cohort was inoculated i.p. with PBS, BMDM from *Zeb1* (+/+) or BMDM from *Zeb1* (+/-) mice. Tumor load progression was followed by bioluminescence and mice were euthanized seven days later.

After all mice were euthanized at day 30, ID8RI cells from the three cohorts were assessed for *Ccl2* expression. ID8RI cells in the cohort that received BMDMs (+/+) expressed higher levels of *Ccl2* than ID8RI cells isolated from mice injected with BMDMs (+/-) (Figure 57). These results further reinforce my results shown above indicating that *Zeb1*-deficient macrophages are unable to induce *Ccl2* in tumor cells.

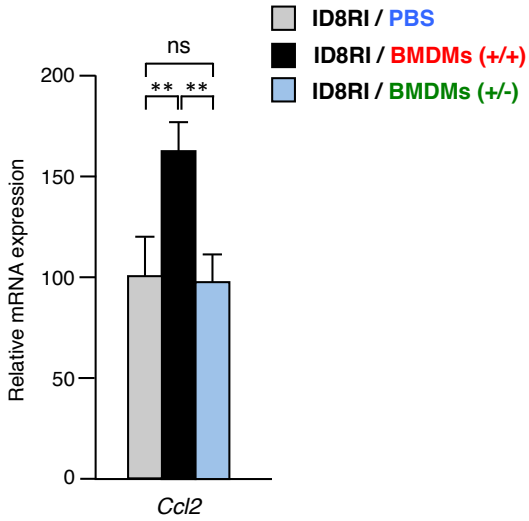

Figure 57. *Zeb1* (+/+) macrophages induce higher expression of *Ccl2* in tumor cells than *Zeb1* (+/-) macrophages. ID8-RI-wt isolated from the experiment in panel were assessed for *Ccl2* expression by qRT-PCR.

6. TAM infiltration in human ovarian carcinomas correlates with higher ZEB1 tumor expression

ZEB1 determines worse prognosis in a wide range of human cancers (Brabletz and Brabletz, 2010). Likewise, high expression of CCL2 in tumors correlates with poorer survival in most human cancers including ovarian carcinoma (Qian et al., 2011; Ostuni et al, 2015). Using survival data for 395 ovarian cancer patients, it was found that patients displaying high expression of both *ZEB1* and *CCL2* (red line in Figure 58) had lower survival rate than those with high levels of *ZEB1* but low *CCL2* or vice versa (green and

yellow lines in Figure 58). Patients with low expression of both *ZEB1* and *CCL2* displayed the best survival probability. In other words, the maximum effect of *ZEB1* as a predictor of reduced survival requires high levels of *CCL2*. This suggests that, at least for some of its tumor-promoting functions, *ZEB1* depends on *CCL2* expression.

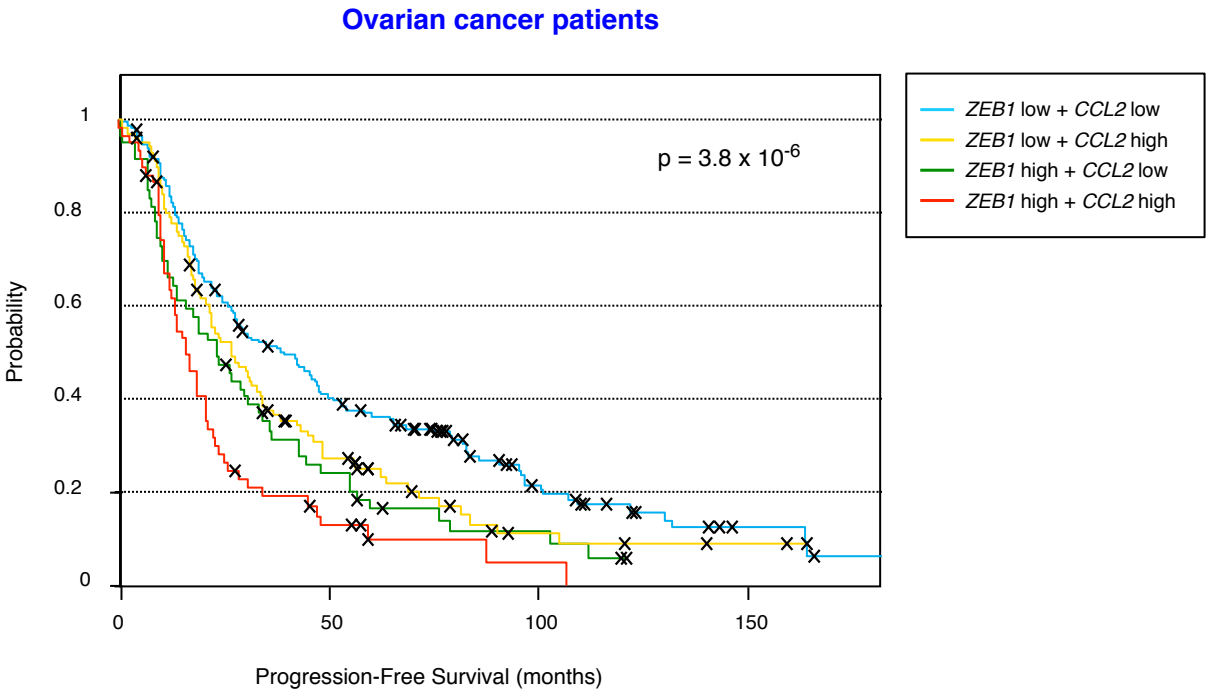

Figure 58. Ovarian cancer patients with the highest expression of *ZEB1* and *CCL2* (red line) have shorter progression-free survival than those with high expression of *ZEB1* but low expression of *CCL2* (green line) or high *CCL2* but low *ZEB1* (yellow line) or that display low levels of both genes (blue line). Their survival probability was plotted in a Kaplan Meier graph according to a best cut off expression as detailed in Supplementary Information.

In most human epithelial tissues, ZEB1 is not expressed in the normal epithelium although it is found in stromal cells. However, ZEB1 greatly increases in most human carcinomas, including epithelial ovarian carcinomas (Jin et al, 2014). To corroborate my results using the ID8 carcinoma mouse model, I investigated ZEB1 expression in TAMs and its association to TAM-associated markers in human epithelial ovarian cancer. To that effect, a series of serous ovarian carcinomas was stained for ZEB1, CCL2, CD163, CCR2 and MMP9 (Figures 59, 60 and 61). It was found that infiltration of the tumor microenvironment by TAMs correlated with higher expression of ZEB1 by tumor cells.

Higher expression of ZEB1 by these TAMs also associated with their higher expression of CCR2 and MMP9. Lastly, expression of ZEB1 in tumor cells associated with that of CCL2. These results further support previous results in this study showing that ZEB1 is expressed in both TAMs and tumor cells and that ZEB1 expression in TAMs induces the expression of TAM-associated markers.

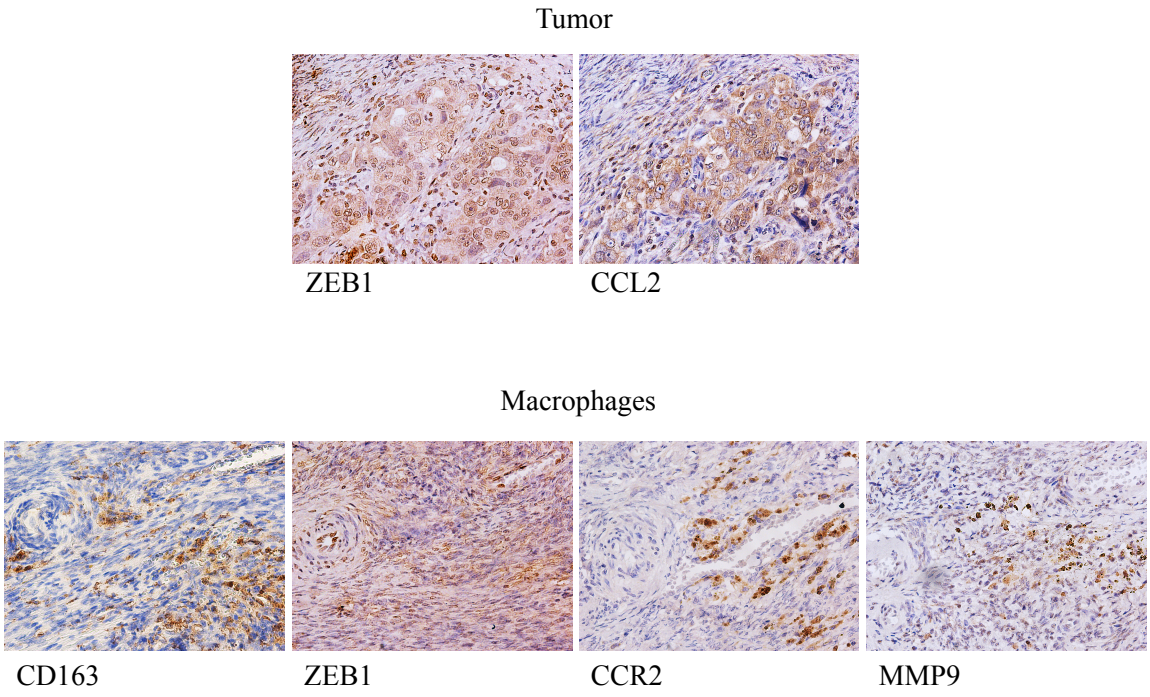

Figure 59. Expression of ZEB1 (HPA027524), CCL2 (2D8), CD163 (10D6), CCR2 (48607), and MMP9 (E11) in human serous ovarian carcinomas. Representative pictures of the tumor and its microenvironment are shown. Magnification 400X.

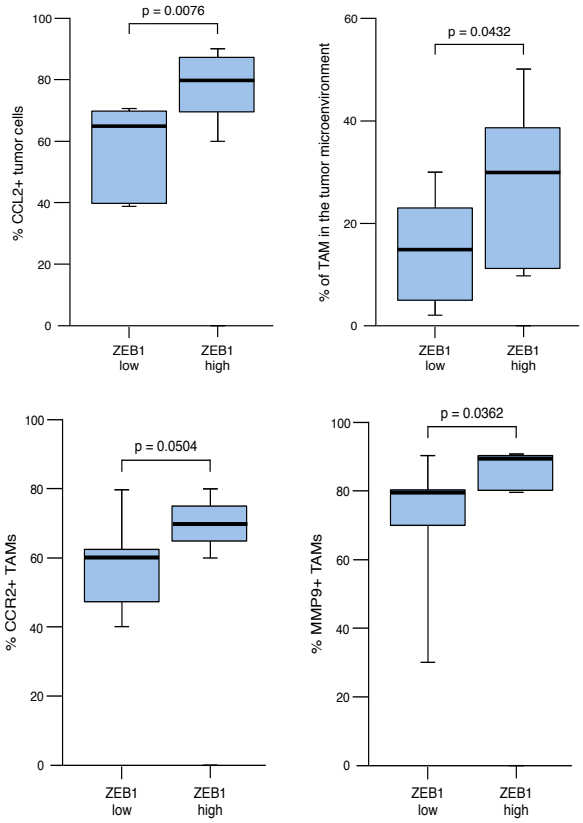

Figure 60. Quantification of data from Figure 55. The percentage of tumor cells and TAMs expressing each protein was determined and cases were then segregated by their expression of ZEB1—in tumor cells or in TAMs—below or above the median into two cohorts (Low ZEB1 and High ZEB1). The means for CCL2 expression in tumor cells (n = 18), the percentage of TAM infiltration—determined by expression of CD163—(n = 18), and the expression of CCR2 (n = 15) and MMP9 (n =15) in TAMs was calculated for the low and high ZEB1 cohorts and the significance of their difference was assessed by a Mann-Whitney U test.

	CCL2 (tumor cell)
ZEB1 (tumor cell)	ρ = 0.57 p = 0.0256

	% TAMs
ZEB1 (tumor cell)	ρ = 0.59 p = 0.0212

	CCR2 (TAMs)	**MMP9 (TAMs)**
ZEB1 (TAMs)	ρ = 0.61 p = 0.0161	ρ = 0.67 p = 0.0067
CCR2 (TAMs)		ρ = 0.75 p = 0.0011

Figure 61. Correlations between relevant protein expression pairs in tumor cells and/or TAMs in serious ovarian carcinomas (n = 15) were assessed by a Spearman's correlation coefficient (r). Their significance is represented by the p value.

In the ID8 mouse model I found that expression of *Zeb1* by TAMs promoted tumor progression. Therefore, I studied whether ZEB1 expression in TAMs affected the prognosis of ovarian carcinoma patients. Importantly, I found that higher expression of ZEB1 in TAMs was associated with poorer survival in these patients (Figure 62).

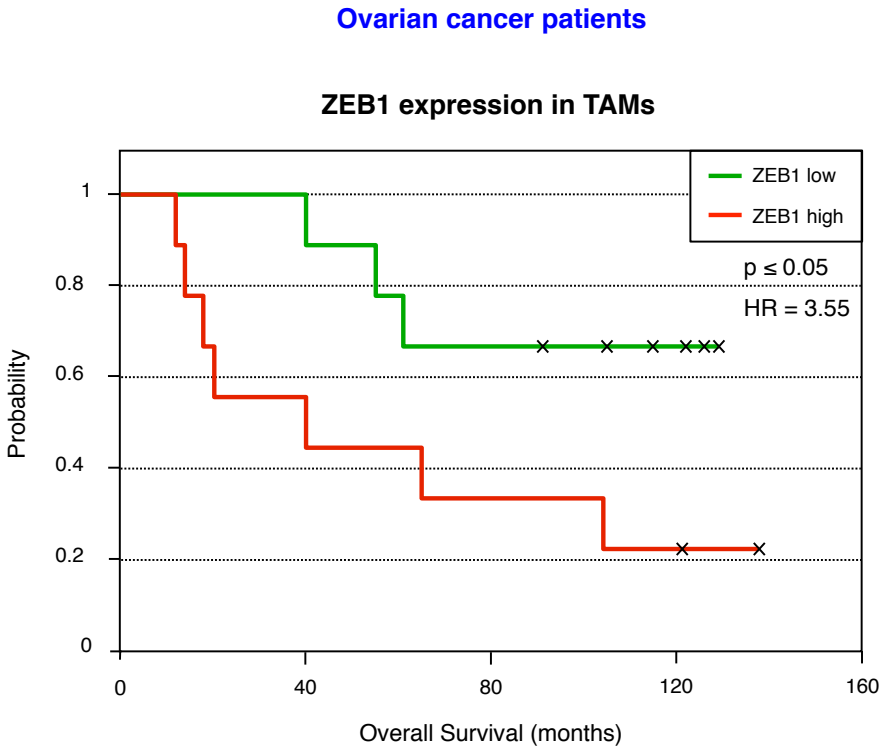

Figure 62 High expression of ZEB1 in TAMs in human serous ovarian carcinomas determined poorer overall survival. Expression of ZEB1 (clone HPA027524) in TAMs (CD163, clone 10D6) was assessed by immunostaining.

DISCUSION

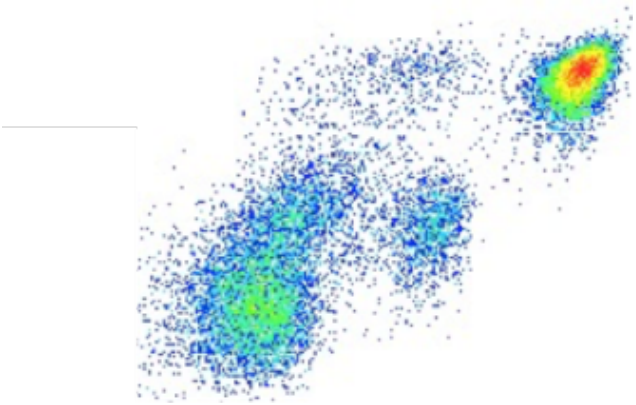

This project has used different technical approaches to determinate the role of *Zeb1* in macrophages both during homeostasis and in the tumor microenvironment. The results shown in this dissertation indicate that ZEB1 regulates the response to inflammatory challenge and tolerance and have also defined a pro-tumoral role of *Zeb1* in the tumor microenvironment beyond its already known expression in tumor cells.

Although ZEB1 has a role in the differentiation of many cellular types, including hematopoietic cells (Vandewalle et al., 2009; Goosens and Haigh, 2012), its expression and function in myeloid differentiation has not been studied. In this study I showed that ZEB1 is expressed in myeloid cells and has an essential role in both their differentiation and activation. Interestingly, during myeloid maturation, monocytes have higher levels of *Zeb1* than macrophages. In turn, SPMs express more *Zeb1* than LPMs that are almost negative for *Zeb1*. In that line, in *Zeb1*-deficient mice the LPM subpopulation and total macrophage count are higher than in normal wild-type mice. Different levels of *Zeb1* expression resulted in distinct status of activation and polarization since *Zeb1* heterozygous macrophages have lower levels of expression of both anti and pro-inflammatory cytokines (Okabe et al., 2014).

Comparison of the RNAseq data from wild-type and *Zeb1*-deficient macrophages confirmed their different polarization/activation pattern as well as provided evidence for the role of ZEB1 in a number of other immune and non-immune functions. Downregulation of *Zeb1* levels in macrophages resulted in the differential expression of over 400 genes, associated to 150 GO pathways. This wealth of information obtained from the RNAseq analysis will also open new areas of research on the role of ZEB1 in macrophages.

Zeb1 regulated and was regulated by *Socs3*, an important gene in macrophage regulation. *Zeb1* was not regulated by or regulate *Socs2*, since *Socs2* (-/-) and *Socs2* (-/-) *Zeb1* (+/-) mice had a similar peritoneal macrophage distribution and gene profile. However, the results with *Socs3* mice showed a potential regulation of *Zeb1* by *Socs3* as $Socs3^{Lyz2cre}$ macrophages expressed less *Zeb1* than *Zeb1* (+/-) animals. Overall, the phenotype of

Socs3^{Lyz2cre}/*Zeb1* (+/-) mice was similar to that of *Zeb1* (+/-) mice but, if anything, even more pronounced. Thus, peritoneal macrophage distribution in these mice showed a large difference between SPM and LPM subpopulations and a similar genetic expression profile. My results indicated that some genes are directly modulated by one of them whereas others, (as the classical *Socs3* targets *Il6*) depended on both genes showing differential expression in the presence or lack of each or in their mutual expression. Despite its structural and functional homology with *Socs3*, there was not regulatory or functional relationship between *Zeb1* and *Socs2*.

Zeb1 also had a role in the phagocytic activity of peritoneal macrophages. Macrophage polarization modulates the capacity of macrophages to in phagocytosis with M1 macrophages being more efficient than M2 macrophages (Martinez and Gordon, 2014). LPMs are responsible for the phagocytosis of apoptotic cells and tissue repair assuming a role in the maintenance of physiological conditions, while SPMs are responsible for controlling infections and inflammatory process. I have showed that LPMs represent a larger share in *Zeb1* (+/-) mice and showed less M2-related gene profile than in wild-type mice and, likewise, *Zeb1*-deficient macrophage presented a higher phagocytic capability than wild-type macrophages. ZEB1 impaired the clearance of malignant cells, but it remains to be studied whether it also enhances macrophage phagocytic capacity of pathogens as well apoptotic cells. For instance, macrophages deficient for *Vim*, a gene activated by *Zeb1,* are more efficient in the phagocytosis of bacteria, which results in lower inflammatory response in acute colitis model (Mor-Vaknin et al., 2013).

Among the genes differentially expressed between both wild-type and *Zeb1*-deficient macrophages was *Ccr2*. Blocking CCL2-CCR2 signaling inhibited the ability of TAMs to upregulate *Ccl2* in cancer cells. In that line, I found that *Zeb1*-deficient macrophages had impaired migration rate upon CCL2 stimulus. The reduced migration of *Zeb1*-defiecient macrophages could be related to the fact that LPM macrophages are tissue-resident macrophages, and they have a role controlling tissue homeostasis whereas SPMs are more similar to dendritic cells with respect to inflammation and antigen presentation and, consequently, they migrate faster than LPMs.

Nevertheless, even in the absence of chemotactic stimuli, *Zeb1* deficient macrophages also displayed lower migratory ability than wild-type macrophages, and the mechanism that modulates this basal motility capacity will be explored in the future. Thus, the RNAseq showed a number of motility-related genes downregulated in *Zeb1*-deficient macrophages, such as those involved in actin polymerization and cellular contractility, and via enhanced ECM degradation and invasion. It is worth noting that ZEB1 regulates motility and prometastatic invasion in tumor cells, through actin cytoskeletal remodeling by downregulating miR-34a expression (Ahn et al., 2012). Taken together these data indicate that as ZEB1 modulates motility and migration in tumor cells, in macrophages would have a similar role regulating their normal migratory capacities.

The role of ZEB1 in the migration of macrophages was also corroborated *in vivo*. *In vivo* migration is influenced by the composition of the local extracellular matrix (ECM) but my *in vivo* model showed that the regulation of *Zeb1* regulating migration is intrinsic to macrophages themselves, independent of the mouse background. Certain MMPs may be involved both positively and negatively in monocyte/macrophage migration. Even double *Mmp2* (-/-) *Mmp9* (-/-) monocytes showed reduced infiltration, suggestive of a reduction in migration (Agrawal et al., 2006). Likewise, knockdown of three *MMP7*, *MMP9* and *MMP18* demonstrated that they are necessary for normal macrophage migration *in vivo* (Tomlinson et al., 2008). It could be therefore postulated that reduced levels of MMP9 in *Zeb1* (+/-) macrophages contribute to their lower migratory capacity.

In macrophages, CSF1 functions as both a growth factor and an important regulator of macrophage motility (Pixley, 2012). An *in vivo* differentiation model in response to CSF1 showed the role of ZEB1 both in monocyte migration as along their differentiation to mature macrophages. In this model, I found that *Zeb1* is blocking LPM subpopulation maturation, this based on the observation of decreased LPM in wild-type mice exposed to CSF1. As discussed earlier, endogenous cytokines modulate myeloid cells attraction, but exogenous bacterial products such as LPS can also mobilize monocytes at the inflammatory focus. In fact, I found that monocyte mobilization to peritoneal cavity

could be mediated by CSF1 or CCL2, and also by tumor cells stimulus, probably for exogenous chemokines that are generated for cancer cells.

Interestingly, *Zeb1*-deficient bone marrow cells displayed improved capacity to differentiate and reconstitute the LPM population compared to wild-type bone marrow cells, in a wild-type animal background where *Zeb1* deficiency in injected myeloid cells is the only variable. Furthermore, these results together with the higher *Zeb1* in monocyte population, suggest that *Zeb1* might have a role in maintaining stemness in hematopoietic progenitor cells and support the hypothesis that *Zeb1* is blocking the maturation of myeloid progenitor cells into a mature macrophage lineage. Also this is supported by the fact that ZEB1 can modulate stemness features in tumor cells (Wellner et al., 2009). These data are also consistent with other studies showing that *Ccr2* is downregulated during myeloid maturation, being therefore a marker of immature monocytes. Similarly *Zeb1* would be acting probably modulating *Ccr2* expression and thus macrophage migration and maturation.

A number of transcription factors participate in the differentiation of progenitor cells into monocytes and then into mature macrophages. Of note, and some of these factors are regulated by ZEB1 (e.g., *Pu.1, c-Myc and c-myb*) (Lawrence and Natoli, 2011; Lavin et al., 2014). My results here set *Zeb1* as a new member of the transcription factors implicated in hematopoietic differentiation. Notably, *Zeb2* regulates plasmocytoid dendritic cell lineage, and in *Zeb2*-deficient mice there is differentiation impairment in myeloid cells (Li et al., 2016, Wu et al., 2016). Hence it is possible to speculate that *Zeb1* has a similar role in myeloid lineage wherein blocking terminal differentiation in macrophages.

In that line, our group is generating *Zeb1* and *Zeb2* floxed mice that will be crossed with *LyzM-Cre* mice in order to obtain the specific deletion of *Zeb1* and *Zeb2* in macrophages. These mice will prove very useful to study to explore whether specific deletion of *Zeb1* in macrophages not only alters the phenotype of TAMs, vis-à-vis TAMs in *Zeb1* (+/-)

mice but also how this influences the progression of the ID8 cancer model. I expect a slower progression of the ID8 model in *Zeb1*$^{f/fLisMCre}$ than wild-type mice. Likewise, my hypothesis is that progression of the ID8 model in the *Zeb2*$^{f/fLisMCre}$ would accelerate it since they would have not the myeloid terminal differentiation and would has more TAM-like immature myeloid cells.

Zeb1 deficiency protected mice from death upon a single dose of LPS (toxic shock), which correlates with the decreased expression of pro or anti-inflammatory genes in their macrophages. Of note, SPM and LPM subpopulations have different responses to LPS *in vivo*. Thus, SPMs produce increased amounts of inflammatory cytokines (i.e. TNFα and RANTES), and LPMs migrate to omentum and decreased in number in peritoneal cavity (Okabe et al., 2014; Rei et al., 2015) and SPM/LPM ratio is altered by *Zeb1* levels. Hence, *Zeb1* (+/-) mice with lesser SPM subset display decreased expression of inflammatory cytokines and improve their survival.

Interestingly, *Zeb1*-deficient macrophages failed to acquire a tolerance state and failed to survive. During tolerance, macrophages undergo a reduction in pro-inflammatory cytokines and adopt a reparative and wound healing polarization profile. In order to understand my *in vivo* results and how *Zeb1* is regulating this process, I examined the gene expression profile in both models for in wild-type and *Zeb1*-deficient mice. *Tnfα* one of the most important pro-inflammatory genes involved in mortality of septic shock was significantly upregulated in wild-type macrophages, but not in *Zeb1*-deficient macrophages. Moreover, the same occurs with the *Il10* gene in tolerance model that was upregulated in wild-type macrophages but not in *Zeb1*-deficient counterparts and the inability of the latter to control inflammation, help explaining the death of *Zeb1* (+/-) mice died in the tolerance model.

LPS in monocytes modulates active histone marks at promoter and enhancers of genes in the lipid metabolism and phagocytic pathways. Furthermore, histone deacetylases (HDACs) are involved in macrophage differentiation, metabolism, and activation (Alvarez-Errico et al., 2014; Lloberas et al., 2016; Novakovic et al., 2016). ZEB1 is a

transcription factor, which in turn can recruit (HDACs), in T cells ZEB1 together with CtBP-2 and HDAC1 repress the IL2 promoter (Wang et al., 2009).

It remains to elucidate whether similar regulation takes place in macrophages through HDAC and whether *Zeb1* can modulate macrophage functions referred above. Indeed, the expression of "non tolerizable" genes as *Il10* depends of the maintenance of H3K4me3 mark of acetylation at different of "tolerizable" genes in front to second inflammatory stimulus (Alvarez-Errico et al., 2014). This information together the fact H3K4me3 regulates transcriptional activation of ZEB1 (Chaffer et al., 2013) indicates that ZEB1 is implicated in the control of inflammation in macrophages.

ZEB1 expression in cancer cells promotes tumor initiation and progression. I show here that, ZEB1 is also induced in TAMs at the TME where it plays a parallel tumor-promoting function than in cancer cells although through a different mechanism. ZEB1 in TAMs activates a *Ccr2-Mmp9-Ccl2* feedback loop between tumor cells and TAMs, and induces a more aggressive phenotype in cancer cells (see model in Figure 63).

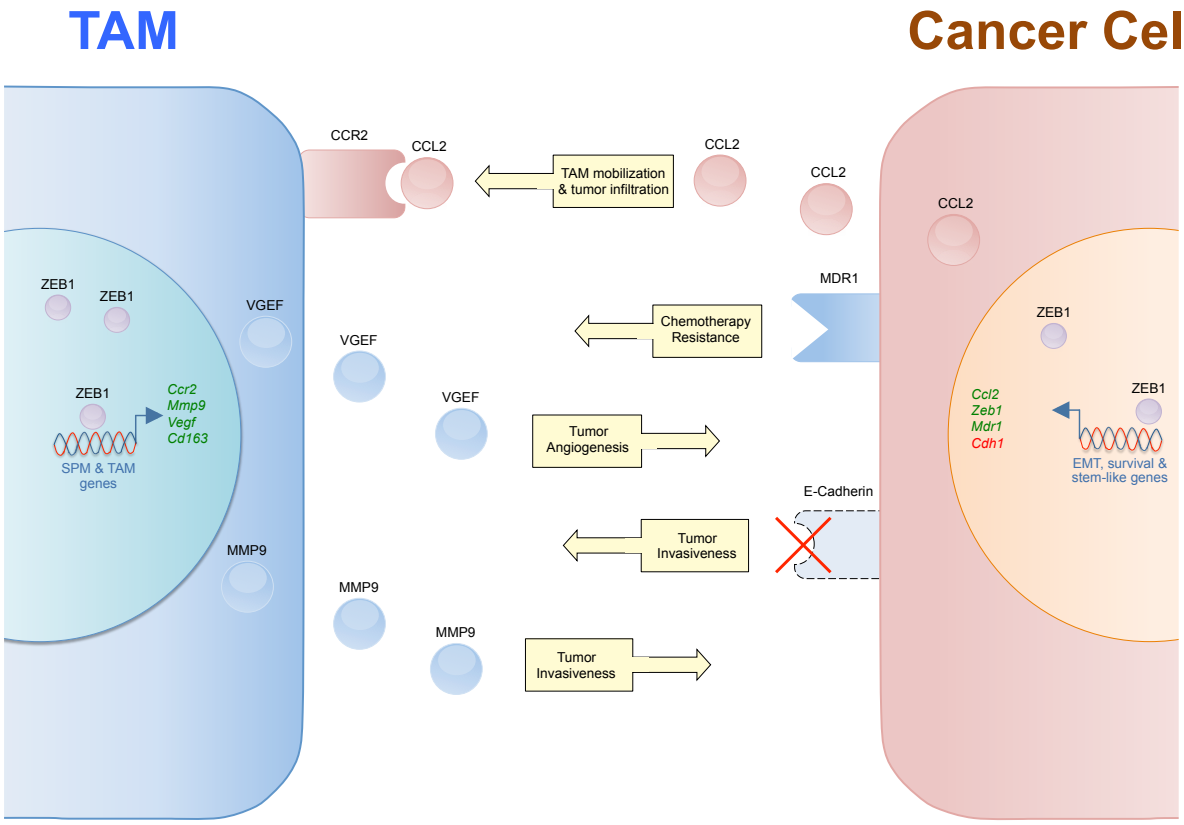

Figure 63. Expression of *Zeb1* in TAMs induces tumor progression by activation of a *Ccr2-Mmp9-Ccl2* loop between TAMs and cancer cells.

Of note, this tumor-promoting loop was inhibited by just a partial downregulation of *Zeb1* in TAMs. Compared to wild-type TAMs, reduced expression of *Mmp9* in *Zeb1* (+/-) TAMs results in lower levels of expression of *Ccl2* in tumor cells. Of note, it was found that a more aggressive phenotype by tumor cells—with higher *Ccl2* and *Zeb1* expression— elicits a more pro-tumoral phenotype in TAMs, including higher levels of *Ccr2* and *Mmp9*. Importantly, injection of wild-type macrophages, but not *Zeb1*-deficient ones, into wild-type tumor-bearing mice accelerated tumor growth and upregulated *Ccl2* expression in tumor cells. In human ovarian carcinomas, TAM infiltration in the microenvironment correlated with ZEB1 expression by cancer cells and higher ZEB1 expression in TAMs associated with higher levels of CCR2 and MMP9. Altogether, my results indicate that, ZEB1 plays an important role in the crosstalk between tumor cells and their microenvironment and that ZEB1 expression in TAMs enhances pro-tumor phenotype in cancer cells and promotes tumor growth.

F4/80^{low} SPM-TAMs express a pro-tumor and pro-angiogenic phenotype and, compared to F4/80^{high} LPM-TAMs, stimulate enhanced tumor growth (Rei et al., 2014). This dissertation found that *Zeb1* is not only restricted to F4/80^{low} SPM normal macrophages and TAMs but that it also expands this subpopulation. Deletion of *Zeb1* downregulated the expression of an SPM-associated gene profile in normal macrophages and TAMs and reduced the F4/80^{low} SPM-TAM population. These effects help explaining the slower progression of tumors in *Zeb1* (+/-) mice and the failure of *Zeb1*-deficient macrophages to accelerate tumor growth compared to PBS when injected in tumor-bearing mice.

Although the expression of ZEB1 among stromal cells of the tumor microenvironment has been noted, the identity of the cell types expressing ZEB1 (e.g., fibroblast, macrophages, other immune cells) had not been until now established (Spaderna et al., 2006; Chaffer et al., 2013; Isella et al., 2015). In that line, this is the first study to characterize the expression and function of ZEB1 in the tumor microenvironment. *Zeb1* expression in macrophages was drastically upregulated when macrophages were exposed to cancer cells. I also showed that the activation of normal macrophages toward a pro-tumoral F4/80^{low} SPM TAMs is compromised in *Zeb1*-deficient mice and that the expression of pro-tumor and pro-angiogenic genes in TAMs was downregulated. Furthermore, I showed that cancer cells also modulate the phenotype of TAMs—ID8RI cells isolated from tumor-bearing wild-type mice trigger a stronger pro-tumoral phenotype in TAMs than ID8RI cells obtained from *Zeb1*-deficient mice.

Importantly, this study shows that, like in tumor cells, *Zeb1* expression in TAMs triggered *in vitro* and *in vivo* a more dedifferentiated and aggressive phenotype in adjacent malignant cells. Thus, *Zeb1* in TAMs upregulates genes associated with a mesenchymal and stem-like phenotype and to resistance to chemotherapy in tumor cells, including expression of *Zeb1* itself. Loss of epithelial markers (e.g., *Cdh1*) and acquisition of an EMT phenotype (e.g., *Vim, Zeb1*) by epithelial cells is required for adenoma-to-carcinoma transition and increased aggressiveness in epithelial tumors (Perl et al., 1998; Liu et al., 2014). In turn, cancer cells induce *Zeb1* in peritoneal macrophages

and TAMs. The role of ZEB1 promoting tumor progression is therefore supported by a positive feedback of its expression between malignant cells and TAMs. Tumor infiltration by TAMs promotes tumor growth, angiogenesis and metastasis (Franklin and Li, 2016) and I found that a partial downregulation of *Zeb1* in TAMs was sufficient to hinder TAM pro-tumor functions and to drastically reduce tumor growth in the ID8 cancer model. Notably, this deficient pro-tumor function of *Zeb1* (+/-) TAMs was transferable into wild-type tumor-bearing mice. Of note, c-myc, a proto-oncogene that promotes cancer cell proliferation, is also expressed by TAMs although its function in TAMs (e.g., tumor promoting or suppressing) has not been studied (Pello et al., 2012; Valledor et al., 2008).

Expression of ZEB1 by malignant cells is a well-established prognostic and predictive biomarker in most cancers (Brabletz and Brabletz, 2010). My results here has shown that downregulation of ZEB1 in TAMs decreases their pro-tumor functions thus setting ZEB1 expression in stromal cells in the microenvironment as a relevant target in cancer therapy. All these data presented here, introduced a new role of ZEB1 in myeloid lineage opening new possibilities to modulate ZEB1 expression in the innate immune system in the context of chronic inflammation, autoimmune disorders and cancer disease. The dual role of ZEB1 promoting tumor progression in cancer cells and TAMs—and through different mechanisms—has important implications for strategies aimed at blocking ZEB1. The simultaneous and mutually reinforcing expression of ZEB1 in TAMs and tumor cells sets ZEB1 as a target in cancer therapy whose expression has to be modulated at multiple levels. Emerging new diagnostic approaches in ovarian cancer patients like liquid biopsies would allow to evaluate ZEB1 levels in peritoneal macrophages in order to determine personalized treatment, prognosis, staging, and response to treatment.

CONCLUSIONS

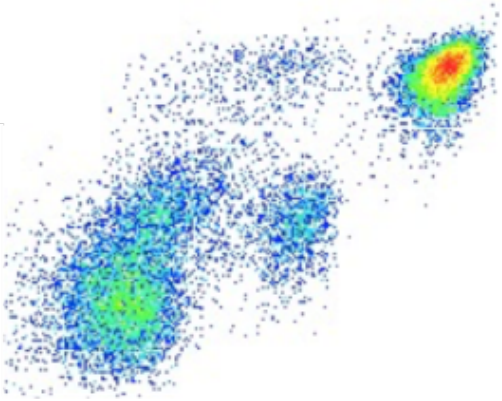

- *Zeb1* inhibits the differentiation of myeloid precursors towards LPMs and activates F4/80^{low}-associated genes.

- *Zeb1* reduces macrophage phagocytic capacity while increasing their migration towards inflammatory foci and the tumor microenvironment.

- *Zeb1* expression in macrophages increases in the context of cancer cells where it reprograms TAMs towards a pro-tumoral phenotype.

- *Zeb1* in TAMs promotes a dedifferentiated and chemotherapy-resistant phenotype in cancer cells and promotes tumor progression *in vivo* by activating a *Ccr2-Mmp9-Ccl2* loop between TAMs and cancer cells.

- In ovarian carcinomas, ZEB1 expression in tumor cells correlates with higher infiltration of TAMs and expression of ZEB1 in both cancer cells and TAMs determines poorer survival.

BIBLIOGRAPHY

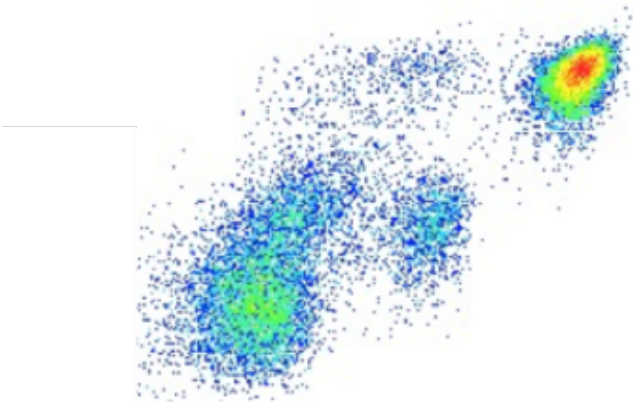

1. Adib-Conquy M, Adrie C, Fitting C, Gattolliat O, Beyaert R, Cavaillon JM.Up-regulation of MyD88s and SIGIRR, molecules inhibiting Toll-like receptor signaling, in monocytes from septic patients. *Crit Care Med.* 2006;34(9):2377-85.

2. Agrawal S, Anderson P, Durbeej M, van RN, Ivars F, Opdenakker G, Sorokin LM. Dystroglycan is selectively cleaved at the parenchymal basement membrane at sites of leukocyte extravasation in experimental autoimmune encephalomyelitis. *J Exp Med.* 2006;203(4):1007–1019.

3. Ahmed AA, Mills AD, Ibrahim AE, Temple J, Blenkiron C, Vias M, Massie CE, Iyer NG, McGeoch A, Crawford R, Nicke B, Downward J, Swanton C, Bell SD, Earl HM, Laskey RA, Caldas C, Brenton JD. The extracellular matrix protein TGFBI induces microtubule stabilization and sensitizes ovarian cancers to paclitaxel. *Cancer Cell.* 2007;12(6):514-27.

4. Ahn YH, Gibbons DL, Chakravarti D, Creighton CJ, Rizvi ZH, Adams HP, Pertsemlidis A, Gregory PA, Wright JA, Goodall GJ, Flores ER, Kurie JM. ZEB1 drives prometastatic actin cytoskeletal remodeling by downregulating miR-34a expression. *J Clin Invest.* 2012;122(9):3170-83.

5. Álvarez-Errico D, Vento-Tormo R, Sieweke M, Ballestar E. Epigenetic control of myeloid cell differentiation, identity and function. *Nat Rev Immunol.* 2015;15(1):7-17.

6. Arango Duque G, Descoteaux A. Macrophage cytokines: involvement in immunity and infectious diseases. *Front Immunol.* 2014;5:491.

7. Arnold CE, Whyte CS, Gordon P, Barker RN, Rees AJ, Wilson HM. A critical role for suppressor of cytokine signalling 3 in promoting M1 macrophage activation and function *in vitro* and *in vivo*. *Immunology.* 2014;141(1):96-110.

8. Arnold L, Henry A, Poron F, Baba-Amer Y, van Rooijen N, Plonquet A, Gherardi RK, Chazaud B. Inflammatory monocytes recruited after skeletal muscle injury switch into antiinflammatory macrophages to support myogenesis. *J Exp Med.* 2007;204(5):1057-69.

9. Arranz A Doxaki C, Vergadi E, Martinez de la Torre Y, Vaporidi K, Lagoudaki ED, Ieronymaki E, Androulidaki A, Venihaki M, Margioris AN, Stathopoulos EN, Tsichlis PN, Tsatsanis C.. Akt1 and Akt2 protein kinases differentially contribute to macrophage polarization. *Proc Natl Acad Sci USA.* 2012;109(24):9517-22.

10. Aurora AB, Porrello ER, Tan W, Mahmoud AI, Hill JA, Bassel-Duby R, Sadek HA, Olson EN. Macrophages are required for neonatal heart regeneration. *J Clin Invest.* 2014;124(3):1382-92.

11. Benoit M, Desnues B, Mege JL. Macrophage polarization in bacterial infections. 2008; *J. Immunol.* 181(6):3733-9.

12. Bergenfelz C., Medrek C., Ekstrom E., Jirstrom K., Janols H., Wullt M., Bredberg A., Leandersson K. Wnt5a induces a tolerogenic phenotype of macrophages in sepsis and breast cancer patients. *J. Immunol.* 2012;188(11):5448–5458.

13. Bertrand JY, Cisson JL, Stachura DL, Traver D. Notch signaling distinguishes 2 waves of definitive hematopoiesis in the zebrafish embryo. *Blood.* 2010; 115(14):2777-83.

14. Biswas SK, Bist P, Dhillon MK, Kajiji T, Del Fresno C, Yamamoto M, Lopez-Collazo E, Akira S, Tergaonkar V. Role for myd88-independent, trif pathway in lipid A/TLR4-induced endotoxin tolerance. *J Immunol.* 2007, 179(6):4083–92.

15. Biswas SK, Lopez-Collazo. E. Endotoxin tolerance: new mechanisms, molecules and clinical significance. *Trends Immunol*. 2009; 30(10):475-487.

16. Bobbs AS, Cole JM, Cowden Dahl KD. Emerging and Evolving Ovarian Cancer Animal Models. *Cancer Growth and Metastasis*. 2015;8(Suppl 1):29-36.

17. Bonome, T, Levine DA, Shih J, Randonovich M, Pise-Masison CA, Bogomolniy F, Ozbun L, Brady J, Barrett JC, Boyd J, Birrer MJ. A gene signature predicting for survival in suboptimally debulked patients with ovarian cancer. *Cancer Res.* 2008;68(13):5478-5486.

18. Brabletz S, Brabletz T. The ZEB/miR-200 feedback loop—a motor of cellular plasticity in development and cancer?. *EMBO Rep*. 2010;11(9):670-7.

19. Brown PO, Palmer C. The preclinical natural history of serous ovarian cancer: defining the target for early detection. *PLoS Med.* 2009;6(7):e1000114.

20. Cai Q, Yan L, Xu Y. Anoikis resistance is a critical feature of highly aggressive ovarian cancer cells. *Oncogene.* 2015;34(25):3315-24.

21. Cain DW, O'Koren EG, Kan MJ, Womble M, Sempowski GD, Hopper K, Gunn MD, Kelsoe G. Identification of a tissue-specific, C/EBPβ-dependent pathway of differentiation for murine peritoneal macrophages. *J. Immunol.* 2013;191(9):4665-75.

22. Cassado Ados A, D'Império Lima MR, Bortoluci KR. Revisiting mouse peritoneal macrophages: heterogeneity, development, and function. *Front Immunol*. 2015;6:225.

23. Cassetta L, Pollard JW. Cancer immunosurveillance: role of patrolling monocytes. *Cell Res*. 2016;26(1):3-4.

24. Chaffer CL, Marjanovic ND, Lee T, Bell G, Kleer CG, Reinhardt F, D'Alessio AC, Young RA, Weinberg RA. Poised chromatin at the ZEB1 promoter enables breast cancer cell plasticity and enhances tumorigenicity. *Cell.* 2013;154(1):61-74.

25. Chen M, Jin Y, Bi Y, Yin J, Wang Y, Pan L. A survival analysis comparing women with ovarian low-grade serous carcinoma to those with high-grade histology. *Onco Targets Ther.* 2014;7:1891-1899.

26. Chau WK, Ip CK, Mak AS, Lai HC, Wong AS. c-Kit mediates chemoresistance and tumor-initiating capacity of ovarian cancer cells through activation of Wnt/β-catenin–ATP-binding cassette G2 signaling. *Oncogene* 2013;32(22):2767-81.

27. Chow A, Brown BD, Merad M. Studying the mononuclear phagocyte system in the molecular age. *Nat Rev Immunol.* 2011; (11):788-98.

28. Colegio OR, Chu NQ, Szabo AL, Chu T, Rhebergen AM, Jairam V, Cyrus N, Brokowski CE, Eisenbarth SC, Phillips GM, Cline GW, Phillips AJ, Medzhitov R. Functional polarization of tumour-associated macrophages by tumour-derived lactic acid. *Nature.* 2014;513(7519):559-63.

29. Colvin EK. Tumor-Associated Macrophages Contribute to Tumor Progression in Ovarian Cancer. *Front Onc*. 2014;4:137.

30. Condeelis J, Pollard JW. Macrophages: obligate partners for tumor cell migration, invasion, and metastasis. *Cell*. 2006;124(2):263-6.

31. Dagouassat M, Suffee N, Hlawaty H, Haddad O, Charni F, Laguillier C, Vassy R, Martin L, Schischmanoff PO, Gattegno L, Oudar O, Sutton A, Charnaux N. Monocyte chemoattractant protein-1 (MCP-1)/CCL2 secreted by hepatic myofibroblasts promotes migration and invasion of human hepatoma cells. *Int J Cancer* . 2010;126(5):1095-108.

32. Davies LC, Taylor PR. Tissue-resident macrophages: then and now. *Immunology*. 2015;144(4):541-8.

33. de Freitas A, Banerjee S, Xie N, Cui H, Davis KI, Friggeri A, Fu M, Abraham E, Liu G. Identification of TLT2 as an engulfment receptor for apoptotic cells. *J Immunol.* 2012;188(12):6381-6388.

34. De Palma M, Lewis CE. Macrophage regulation of tumor responses to anticancer therapies. *Cancer Cell*. 2013 Mar 18;23(3):277-86.

35. Deng H, Maitra U, Morris M, Li L. Molecular Mechanism Responsible for the Priming of Macrophage Activation. *J Biol Chem.* 2013;288(6):3897-3906.

36. Deshmane SL, Kremlev S, Amini S, Sawaya BE. Monocyte chemoattractant protein-1 (MCP-1): an overview. *J Interferon Cytokine Res*. 2009;29(6):313-26.

37. Dobin A, Gingeras TR. Mapping RNA-seq Reads with STAR. *Curr Protoc Bioinformatics.* 2015;51:11.14.1-19.

38. Ebrahem Q, Chaurasia SS, Vasanji A, Qi JH, Klenotic PA, Cutler A, Asosingh K, Erzurum S, Anand-Apte B. Cross-Talk between Vascular Endothelial Growth Factor and Matrix Metalloproteinases in the Induction of Neovascularization *in Vivo*. *Am J Pathol*. 2010;176(1):496-503.

39. Eisele PS, Salatino S, Sobek J, Hottiger MO, Handschin C. The peroxisome proliferator-activated receptor γ coactivator 1α/β (PGC-1) coactivators repress the transcriptional activity of NF-κB in skeletal muscle cells. *J Biol Chem*. 2013;288(4):2246-60.

40. Fang WB, Jokar I, Zou A, Lambert D, Dendukuri P, Cheng N. CCL2/CCR2 chemokine signaling coordinates survival and motility of breast cancer cells through Smad3 protein- and p42/44 mitogen-activated protein kinase (MAPK)-dependent mechanisms. *J Biol Chem*. 2012;287(43):36593-608.

41. Ferriss, JS, Kim Y, Duska L, Birrer M, Levine DA, Moskaluk C, Theodorescu D, Lee JK. Multi-gene expression predictors of single drug responses to adjuvant chemotherapy in ovarian carcinoma: predicting platinum resistance. *PLoS One*. 2012;7(2): e30550.

42. Fleetwood AJ, Lawrence T, Hamilton JA, Cook AD. Granulocyte-macrophage colony-stimulating factor (CSF) and macrophage CSF-dependent macrophage phenotypes display differences in cytokine profiles and transcription factor activities: implications for CSF blockade in inflammation. *J. Immunol*. 2007;78(8):5245-52.

43. Fong MY, Kakar SS. Ovarian cancer mouse models: a summary of current models and their limitations. *J Ovarian Res*. 2009;2(1):12.

44. Franklin RA, Li MO. Ontogeny of Tumor-Associated Macrophages and its implication in cancer regulation. *Trends Cancer*. 2016;2(1):20-34.

45. Freudenberg MA, Galanos C. Induction of tolerance to lipopolysaccharide (LPS)-D-galactosamine lethality by pretreatment with LPS is mediated by macrophages. *Infect Immun.* 1988 ;56(5):1352-7.

46. Ghosn EEB, Cassado AA, Govoni GR, Fukuhara T, Yang Y, Monack DM, Bortoluci KR, Almeida SR, Herzenberg LA, Herzenberg LA. Two physically, functionally, and developmentally distinct peritoneal macrophage subsets. *Proc Acad Natl Sci USA*. 2010;107(6):2568-73.

47. Ginestier C, Hur MH, Charafe-Jauffret E, Monville F, Dutcher J, Brown M, Jacquemier J, Viens P, Kleer CG, Liu S, Schott A, Hayes D, Birnbaum D, Wicha MS, Dontu G. ALDH1 is a marker of normal and malignant human mammary stem cells and a predictor of poor clinical outcome. *Cell Stem Cell* 2007;1(5):555-67.

48. Ginhoux F, Jung S. Monocytes and macrophages: developmental pathways and tissue homeostasis. *Nat Rev Immunol*. 2014;14(6):392-404.

49. Giraudo E, Inoue M, Hanahan D. An amino-bisphosphonate targets MMP-9–expressing macrophages and angiogenesis to impair cervical carcinogenesis. *J. Clin. Invest*. 2004;114:623-33.

50. Gong Y, Hart E, Shchurin A, Hoover-Plow J. Inflammatory macrophage migration requires MMP-9 activation by plasminogen in mice. *J. Clin Invest*. 2008;118(9):3012-24.

51. Gosselin D, Link VM, Romanoski CE, Fonseca GJ, Eichenfield DZ, Spann NJ, Stender JD, Chun HB, Garner H, Geissmann F, Glass CK. Environment drives selection and function of enhancers controlling tissue-specific macrophage identities. *Cell.* 2014;159(6):1327-40.

52. Goossens S, Haigh J. The Role of EMT Modulators in Hematopoiesis and Leukemic Transformation. Hematology : Science and Practice. Ed. Charles H Lawrie. Rijeka, Croatia: InTech, 2012. 101–120.

53. Gottesman MM, Fojo T, Bates SE. Multidrug resistance in cancer: role of ATP–dependent transporters. *Nat Rev Cancer.* 2002;2(1):48-58.

54. Greenaway J, Moorehead R, Shaw P, Petrik J. Epithelial-stromal interaction increases cell proliferation, survival and tumorigenicity in a mouse model of human epithelial ovarian cancer. *Gynecol Oncol.* 2008;108(2):385-94.

55. Hagemann T, Wilson J, Burke F, Kulbe H, Li NF, Plüddemann A, Charles K, Gordon S, Balkwill FR. Ovarian cancer cells polarize macrophages toward a tumor-associated phenotype. *J. Immunol* 2006;176(8):5023-32.

56. Hagemann T, Lawrence T, McNeish I, Charles KA, Kulbe H, Thompson RG, Robinson SC, Balkwill FR. "Re-educating" tumor-associated macrophages by targeting NF-κB. *J. Exp. Med.* 2008;205(6):1261-8.

57. Hagerling C, Casbon A-J, Werb Z. Balancing the innate immune system in tumor development. *Trends in cell biology*. 2015;25(4):214-220.

58. Hanahan D, Weinberg RA. Hallmarks of cancer: the next generation. *Cell.* 2011;144(5):646-74.

59. Hasan N, Ohman AW, Dinulescu DM. The promise and challenge of ovarian cancer models. *Transl Cancer Res*. 2015;4(1):14-28.

60. Hashimoto D, Chow A, Noizat C, Teo P, Beasley MB, Leboeuf M, Becker CD, See P, Price J, Lucas D, Greter M, Mortha A, Boyer SW, Forsberg EC, Tanaka M, van Rooijen N, García-Sastre A, Stanley ER, Ginhoux F, Frenette PS, Merad M. Tissue-resident macrophages self-maintain locally throughout adult life with minimal contribution from circulating monocytes. *Immunity*. 2013;38(4):792-804.

61. Hiratsuka S, Nakamura K, Iwai S, Murakami M, Itoh T, Kijima H, Shipley JM, Senior RM, Shibuya M. MMP9 induction by vascular endothelial growth factor receptor-1 is involved in lung-specific metastasis. *Cancer Cell,* 2002;2(4):289-300.

62. Hoeffel G, Chen J, Lavin Y, Low D, Almeida FF, See P, Beaudin AE, Lum J1, Low I, Forsberg EC, Poidinger M1, Zolezzi F, Larbi A, Ng LG, Chan JK, Greter M, Becher B, Samokhvalov IM, Merad M, Ginhoux F. C-Myb(+) erythro-myeloid progenitor-derived fetal monocytes give rise to adult tissue-resident macrophages. *Immunity*. 2015;42(4):665-78.

63. Huang S Van Arsdall M, Tedjarati S, McCarty M, Wu W, Langley R, Fidler IJ. Contributions of stromal metalloproteinase-9 to angiogenesis and growth of human ovarian carcinoma in mice. *J Natl Cancer Inst.* 2002;94(15):1134-42.

64. Huang X, Venet F, Wang YL, Lepape A, Yuan Z, Chen Y, Swan R, Kherouf H, Monneret G, Chung CS, Ayala A. PD-1 expression by macrophages plays a pathologic role in altering microbial clearance and the innate inflammatory response to sepsis. *Proc Natl Acad Sci U S A*. 2009;106(15):6303-8.

65. Isella C, Terrasi A, Bellomo SE, Petti C, Galatola G, Muratore A, Mellano A, Senetta R, Cassenti A, Sonetto C, Inghirami G, Trusolino L, Fekete Z, De Ridder M, Cassoni P, Storme G, Bertotti A, Medico E. Stromal contribution to the colorectal cancer transcriptome. *Nat Genet.* 2015;47:312-9.

66. Italiani P, Boraschi D. From Monocytes to M1/M2 Macrophages: Phenotypical vs. Functional Differentiation. *Front Immunol*. 2014 ;17;5:514.

67. Jin M, Yang Z, Ye W, Xu H, and Hua X. MicroRNA-150 predicts a favorable prognosis in patients with epithelial ovarian cancer, and inhibits cell invasion and metastasis by suppressing transcriptional repressor ZEB1. *PLoS One*. 2014;9(8):e103965.

68. Jones GE, Prigmore E, Calvez R, Hogan C, Dunn GA, Hirsch E, Wymann MP, Ridley AJ. Requirement for PI 3-kinase gamma in macrophage migration to MCP-1 and CSF-1. *Exp Cell Res.* 2003;290(1):120-31.

69. Keller E, Hall C, Aaronson S. shRNA Materials and Methods of Using Same for Inhibition of DKK-1. 2008; US 20080293053

70. Kim R, Emi M, Tanabe K. Cancer immunoediting from immune surveillance to immune escape. *Immunology.* 2007;121(1):1-14.

71. Kipps E, Tan DS, Kaye SB. Meeting the challenge of ascites in ovarian cancer: new avenues for therapy and research. *Nat Rev Cancer.* 2013;13(4):273-82.

72. Kitamoto S, Egashira K, Ichiki T, Han X, McCurdy S, Sakuda S, Sunagawa K, Boisvert WA. Chitinase inhibition promotes atherosclerosis in hyperlipidemic mice. *Am J Pathol.* 2013;183(1):313-325.

73. Kubo M, Hanada T, Yoshimura A. Suppressors of cytokine signaling and immunity. *Nat Immunol*. 2003;4(12):1169-76.

74. Kwon SJ, Crespo-Barreto J, Zhang W, Wang T, Kim DS, Krensky A, Clayberger C. KLF13 cooperates with c-Maf to regulate IL-4 expression in CD4+ T cells. *J Immunol.* 2014;192(12):5703-5709.

75. Lacey DC, Achuthan A, Fleetwood AJ, Dinh H, Roiniotis J, Scholz GM, Chang MW, Beckman SK, Cook AD, Hamilton JA. Defining GM-CSF–and macrophage-CSF–dependent macrophage responses by in vitro models. *J Immunol*. 2008;188(11):5752-65.

76. Lavin Y, Winter D, Blecher-Gonen R, David E, Keren-Shaul H, Merad M, Jung S, Amit I. Tissue-resident macrophage enhancer landscapes are shaped by the local microenvironment. *Cell*. 2014;159(6):1312-26.

77. Lavin Y, Mortha A, Rahman A, Merad M. Regulation of macrophage development and function in peripheral tissues. *Nat Rev Immunol*. 2015;15(12):731-44.

78. Lawrence T, Natoli G. Transcriptional regulation of macrophage polarization: enabling diversity with identity. *Nat Rev Immunol*. 2011;11:750-61.

79. Le Blanc K, Mougiakakos D. Multipotent mesenchymal stromal cells and the innate immune system. *Nat Rev Immunol*. 2012;12(5):383-96.

80. Lengyel E. Ovarian Cancer Development and Metastasis. *Am J Pathol*. 2010;177(3):1053-1064.

81. Leong KG, Wang BE, Johnson L, Gao WQ. Generation of a prostate from a single adult stem cell. *Nature.* 2008;456(7223):804-808.

82. Levi BP, Yilmaz OH, Duester G, Morrison SJ. Aldehyde dehydrogenase 1a1 is dispensable for stem cell function in the mouse hematopoietic and nervous systems. *Blood*. 2009;113(8):1670-1680.

83. Lewis CE, Pollard JW. Distinct role of macrophages in different tumor microenvironments. *Cancer Res.* 2006;66(2):605-12.

84. Li B, Dewey CN.RSEM: accurate transcript quantification from RNA-Seq data with or without a reference genome. *BMC Bioinformatics*. 2011; 4;12:323.

85. Li F, Faustino J, Woo MS, Derugin N, Vexler ZS. Lack of the scavenger receptor CD36 alters microglial phenotypes after neonatal stroke. *J Neurochem.* 2015;135(3):445-52.

86. Li H, Mar BG, Zhang H, Puram RV, Vazquez, Weir BA, Hahn WC, Ebert B4, Pellman D. The EMT regulator ZEB2 is a novel dependency of human and murine acute myeloid leukemia. *Blood.* 2017;129(4):497-508.

87. Lim SY, Yuzhalin AE, Gordon-Weeks AN, Muschel RJ. Targeting the CCL2-CCR2 signaling axis in cancer metastasis. *Oncotarget*. 2016;7(19):28697-710.

88. Lin ZS, Chu HC, Yen YC, Lewis BC, Chen YW. Krüppel-like factor 4, a tumor suppressor in hepatocellular carcinoma cells reverts epithelial mesenchymal transition by suppressing slug expression. *PLoS One*. 2012;7(8):e43593.

89. Liu J, Matulonis UA. New strategies in ovarian cancer: translating the molecular complexity of ovarian cancer into treatment advances. *Clin Cancer Res*. 2014;20(20):5150-6.

90. Liu Y, Lu X, Huang L, Wang W, Jiang G, Dean KC, Clem B, Telang S, Jenson AB, Cuatrecasas M, Chesney J, Darling DS, Postigo A, Dean DC. Different thresholds of ZEB1 are required for Ras-mediated tumour initiation and metastasis. *Nat Commun.* 2014;5:5660.

91. Lloberas J, Valverde-Estrella L, Tur J, Vico T, Celada A. Mitogen-Activated Protein Kinases and Mitogen Kinase Phosphatase 1: A Critical Interplay in Macrophage Biology. *Front Mol Biosci*. 2016;3:28.

92. Martinez FO, Gordon S. The M1 and M2 paradigm of macrophage activation: time for reassessment. *F1000Prime Rep.* 2014;6:13.

93. Mateescu, B, Batista L, Cardon M, Gruosso T, de Feraudy Y, Mariani O, Nicolas A, Meyniel JP, Cottu P, Sastre-Garau X, Mechta-Grigoriou F..miR-141 and miR-200a act on ovarian tumorigenesis by controlling oxidative stress response. *Nature Med*. 2011;17(12):1627-1635.

94. Medina RJ, O'Neill CL, O'Doherty TM, Knott H, Guduric-Fuchs J, Gardiner TA, Stitt AW. Myeloid angiogenic cells act as alternative M2 macrophages and modulate angiogenesis through interleukin-8. *Mol Med.* 2011;17(9-10):1045-55.

95. Medrano M, Communal L, Brown KR, Iwanicki M, Normand J, Paterson J, Sircoulomb F, Krzyzanowski P, Novak M, Doodnauth SA, Saiz FS, Cullis J, Al-Awar R, Neel BG, McPherson J, Drapkin R, Ailles L, Mes-Massons AM1 Rottapel R. Interrogation of Functional Cell-Surface Markers Identifies CD151 Dependency in High-Grade Serous Ovarian Cancer. *Cell Rep.* 2017;18(10):2343-2358.

96. Mihály, Z, Kormos M, Lánczky A, Dank M, Budczies J, Szász MA, Győrffy B. A meta-analysis of gene expression-based biomarkers predicting outcome after tamoxifen treatment in breast cancer. *Breast Cancer Res Treat.* 2013;140(2): 219-32.

97. Miró-Mur F, Pérez-de-Puig I, Ferrer-Ferrer M, Urra X, Justicia C, Chamorro A, Planas AM. Immature monocytes recruited to the ischemic mouse brain differentiate into macrophages with features of alternative activation. *Brain Behav Immun*. 2016;53:18-33.

98. Mostafavi S, Ray D, Warde-Farley D, Grouios C, Morris Q. GeneMANIA: a real-time multiple association network integration algorithm for predicting gene function. *Genome Biol.* 2008;9 Suppl 1:S4.

99. Mor-Vaknin N, Legendre M, Yu Y, Serezani CH, Garg SK, Jatzek A, Swanson MD, Gonzalez-Hernandez MJ, Teitz-Tennenbaum S, Punturieri A, Engleberg NC, Banerjee R, Peters-Golden M, Kao JY, Markovitz DM. Murine colitis is mediated by vimentin. *Sci Rep*. 2013;3:1045.

100. Murray PJ, Allen JE, Biswas SK, Fisher EA, Gilroy DW, Goerdt S, Gordon S, Hamilton JA, Ivashkiv LB, Lawrence T, Locati M1 Mantovani A, Martinez FO, Mege JL, Mosser DM, Natoli G, Saeij JP, Schultze JL, Shirey KA, Sica A, Suttles J, Udalova I, van Ginderachter JA, Vogel SN, Wynn TA. Macrophage activation and polarization: nomenclature and experimental guidelines. *Immunity.* 2014;41(1):14-20.

101. Nakasone ES, Askautrud HA, Kees T, Park JH, Plaks V, Ewald AJ, Fein M, Rasch MG, Tan YX, Qiu J, Park J, Sinha P, Bissell MJ, Frengen E, Werb Z, Egeblad M. Imaging tumor-stroma interactions during chemotherapy reveals contributions of the microenvironment to resistance. *Cancer Cell.* 2012;21(4):488-503.

102. Nieto MA, Huang R, Jackson RY-J, Thiery JP. EMT:2016. *Cell*. 2016; 166(1):21-45.

103. Novakovic B, Habibi E, Wang SY, Arts RJ, Davar R, Megchelenbrink W, Kim B, Kuznetsova T, Kox M, Zwaag J, Matarese F, van Heeringen SJ, Janssen-Megens EM, Sharifi N, Wang C1, Keramati F, Schoonenberg V, Flicek P, Clarke L, Pickkers P, Heath S, Gut I, Netea MG, Martens JH, Logie C, Stunnenberg HG. β-Glucan Reverses the Epigenetic State of LPS-Induced Immunological Tolerance. *Cell.* 2016;167(5):1354-1368.

104. Noy R, Pollard JW. Tumor-associated macrophages: from mechanisms to therapy. *Immunity.* 2014;41(1):49-61.

105. Okabe Y, Medzhitov R. Tissue-specific signals control reversible program of localization and functional polarization of macrophages. *Cell* 2014; 157(4):832-44.

106. Olmeda D, Jordá M, Peinado H, Fabra A, Cano A. Snail silencing effectively suppresses tumour growth and invasiveness. *Oncogene.* 2007;26:1862-74.

107. Ostuni, R, Kratochvill F. Murray PJ, Natoli G. Macrophages and cancer: from mechanisms to therapeutic implications. *Trends Immunol.* 2015;36(4):229-39.

108. Padda SK, Narayan R, Burt BM, Engleman EG. Tumor Immunology. Reviews in Cell Biology and Molecular Medicine 2015;1:244–299.

109. Parcesepe P, Giordano G, Laudanna C, Febbraro A, Pancione M. Cancer-Associated Immune Resistance and Evasion of Immune Surveillance in Colorectal Cancer. *Gastroenterol Res Pract*. 2016;2016:6261721.

110. Pixley FJ. Macrophage Migration and Its Regulation by CSF-1. *Int J Cell Biol*. 2012;2012:501962.

111. Pello OM, De Pizzol M, Mirolo M, Soucek L, Zammataro L, Amabile A, Doni A, Nebuloni M, Swigart LB, Evan GI, Mantovani A, Locati M. Role of c-MYC in alternative activation of human macrophages and tumor-associated macrophage biology. *Blood.* 2012;119(2): 411-421.

112. Pena OM, Pistolic J, Raj D, Fjell CD, Hancock RE. Endotoxin tolerance represents a distinctive state of alternative polarization (M2) in human mononuclear cells. *J Immunol.* 2011;186(12):7243-54.

113. Pérez-de Puig I, Miró F, Salas-Perdomo A, Bonfill-Teixidor E, Ferrer-Ferrer M, Márquez-Kisinousky L, Planas AM. IL-10 deficiency exacerbates the brain inflammatory response to permanent ischemia without preventing resolution of the lesion. *J Cereb Blood Flow Metab*. 2013;33(12):1955-66.

114. Perl AK, Wilgenbus P, Dahl U, Semb H, Christofori G. A causal role for E-cadherin in the transition from adenoma to carcinoma. *Nature.* 1998; 392(6672):190-3.

115. Postigo A, Dean DC. ZEB represses transcription through interaction with the corepressor CtBP. *Proc Nat Acad Sci USA.* 1999;96(12):6683-8.

116. Postigo A, Depp JL, Taylor JJ, Kroll KL. Regulation of Smad signaling through a differential recruitment of coactivators and corepressors by ZEB proteins. *EMBO J.* 2003;22(10):2453-62.

117. Prinz M, Priller J. Microglia and brain macrophages in the molecular age: from origin to neuropsychiatric disease. *Nat Rev Neurosci*. 2014;15(5):300-12.

118. Pukrop T, Klemm F, Hagemann T, Gradl D, Schulz M, Siemes S, Trumper L, Binder C. Wnt5a signaling is critical for macrophage-induced invasion of breast cancer cell lines. *Proc. Natl. Acad. Sci. USA.* 2006;103(14):5454–5459.

119. Qian BZ, Li J, Zhang H, Kitamura T, Zhang J, Campion LR, Kaiser EA, Snyder LA, Pollard JW. CCL2 recruits inflammatory monocytes to facilitate breast-tumour metastasis. *Nature.* 2011;475(7355):222-5.

120. Qie Y, Yuan H, von Roemeling CA, Chen Y, Liu X, Shih KD, Knight JA, Tun HW, Wharen RE, Jiang W, Kim BY. Surface modification of nanoparticles enables selective evasion of phagocytic clearance by distinct macrophage phenotypes. *Sci Rep.* 2016; 19;6:26269.

121. Quail D, Joyce J. Microenvironmental regulation of tumor progression and metastasis. *Nat Med*. 2013;19(11):1423-1437.

122. Rajaiah R, Perkins DJ, Polumuri SK, Zhao A, Keegan AD, Vogel SN. Dissociation of Endotoxin Tolerance and Differentiation of Alternatively Activated Macrophages. *J Immunol*. 2013;190(9):4763-4772.

123. Rankin EB, Tomaszewski JE, Haase VH. Renal cyst development in mice with conditional inactivation of the von Hippel-Lindau tumor suppressor. Cancer Res. 2006;66:2576-83.

124. Rei M, Gonçalves-Sousa N, Lança T, Thompson RG, Mensurado S, Balkwill FR, Kulbe H, Pennington DJ, Silva-Santos B. Murine CD27(-) Vγ6(+) γδ T cells producing IL-17A promote ovarian cancer growth via mobilization of protumor small peritoneal macrophages. *Proc Natl Acad Sci USA*. 2014;111(34):E3562-70.

125. Reinartz S, Schumann T, Finkernagel F, Wortmann A, Jansen JM, Meissner W, Krause M, Schwörer AM, Wagner U, Müller-Brüsselbach S, Müller R. Mixed-polarization phenotype of ascites-associated macrophages in human ovarian carcinoma: Correlation of CD163 expression, cytokine levels and early relapse. *Int J Cancer* 2014;134(1):32-42.

126. Robinson MD, McCarthy DJ, Smyth GK. edgeR: a Bioconductor package for differential expression analysis of digital gene expression data. *Bioinformatics*. 2010;26(1):139-40.

127. Roby KF, Taylor CC, Sweetwood JP, Cheng Y, Pace JL, Tawfik O, Persons DL, Smith PG, Terranova PF. Development of a syngeneic mouse model for events related to ovarian cancer. *Carcinogenesis.* 2000;(4):585-91.

128. Roger T, Froidevaux C, Le Roy D, Reymond MK, Chanson AL, Mauri D, Burns K, Riederer BM, Akira S, Calandra T. Protection from lethal gram-negative bacterial sepsis by targeting Toll-like receptor 4. *Proc Natl Acad Sci U S A*. 2009;17;106(7):2348-52.

129. Rosas M, Davies LC, Giles PJ, Liao CT, Kharfan B, Stone TC, O'Donnell VB, Fraser DJ, Jones SA, Taylor PR. The transcription factor Gata6 links tissue macrophage phenotype and proliferative renewal. *Science.* 2014;344(6184):645-648.

130. Rosen JM, Jordan CT. The increasing complexity of the cancer stem cell paradigm. *Science.* 2009;324(5935):1670-3.

131. Sánchez-Tilló E, Comalada M, Xaus J, Farrera C, Valledor AF, Caelles C, Lloberas J, Celada A. JNK1 Is required for the induction of Mkp1 expression in macrophages during proliferation and lipopolysaccharide-dependent activation. *J Biol Chem*. 2007;282(17):12566-73.

132. Sánchez-Tilló E, de Barrios O, Siles L, Cuatrecasas M, Castells A, Postigo A. β-catenin/TCF4 complex induces the epithelial-to-mesenchymal transition (EMT)-activator ZEB1 to regulate tumor invasiveness. *Proc Natl Acad Sci USA*. 2011;108:19204-9.

133. Sawada K, Mitra AK, Radjabi AR, Bhaskar V, Kistner EO, Tretiakova M, Jagadeeswaran S, Montag A, Becker A, Kenny HA, Peter ME, Ramakrishnan V, Yamada SD, Lengyel E. Loss of E-cadherin promotes ovarian cancer metastasis via α5-integrin, which is a therapeutic target. *Cancer Res*. 2008;68(7):2329-39.

134. Schulz C, Gomez Perdiguero E, Chorro L, Szabo-Rogers H, Cagnard N, Kierdorf K, Prinz M, Wu B, Jacobsen SE, Pollard JW, Frampton J, Liu KJ, Geissmann F. A lineage of myeloid cells independent of Myb and hematopoietic stem cells. *Science*. 2012;336:86-90.

135. Scott CH, Soen B, Martens L, Skrypek N, Saelens W, Taminau J, Blancke G, Isterdael GV, Huylebroeck D, Haigh J, Saeys Y, Guilliams M, Lambrecht BN, Berx G. The transcription factor Zeb2 regulates development of conventional and plasmacytoid DCs by repressing Id2. *J Ex Med*. 2016, 213 (6) 897-911.

136. Seeley JJ, Ghosh S.Molecular mechanisms of innate memory and tolerance to LPS. *J Leukoc Biol*. 2017;101(1):107-119.

137. Serbina NV, Pamer EG. Monocyte emigration from bone marrow during bacterial infection requires signals mediated by chemokine receptor CCR2. *Nat Immunol*, 2006;7(3):311-7.

138. Sessa R, Yuen D, Wan S, Rosner M, Padmanaban P, Ge S, Smith A, Fletcher R, Baudhuin-Kessel A, Yamaguchi TP, Lang RA, Chen L. Monocyte-derived Wnt5a regulates inflammatory lymphangiogenesis. *Cell Res*. 2016;26(2):262-5.

139. Shalova IN, Lim JY, Chittezhath M, Zinkernagel AS, Beasley F, Hernández-Jiménez E, Toledano V, Cubillos-Zapata C, Rapisarda A, Chen J, Duan K, Yang H, Poidinger M, Melillo G, Nizet V, Arnalich F, López-Collazo E, Biswas SK. Human monocytes undergo functional re-programming during sepsis mediated by hypoxia-inducible factor-1α. *Immunity.* 2015;42(3):484-98.

140. Si Y, Tsou CL, Croft K, Charo IF. CCR2 mediates hematopoietic stem and progenitor cell trafficking to sites of inflammation in mice. *J. Clin Invest.* 2010;120(4):1192-203.

141. Sica A, Mantovani A.J. Macrophage plasticity and polarization: in vivo veritas. *J Clin Invest.* 2012;122(3):787-95.

142. Siles L, Sánchez-Tilló E, Lim JW, Darling DS, Kroll KL, Postigo A. ZEB1 imposes a temporary stage-dependent inhibition of muscle gene expression and differentiation via CtBP-mediated transcriptional repression. *Mol Cell Biol.* 2013;33:1368-82.

143. Silva IA, Bai S, McLean K, Yang K, Griffith K, Thomas D, Ginestier C, Johnston C, Kueck A, Reynolds RK, Wicha MS, Buckanovich RJ. Aldehyde dehydrogenase in combination with CD133 defines angiogenic ovarian cancer stem cells that portend poor patient survival. *Cancer Res.* 2011;71(11):3991-4001.

144. Siolas D, Hannon GJ. Patient-derived tumor xenografts: transforming clinical samples into mouse models. *Cancer Res*. 2013;1;73(17):5315-9.

145. Smith HA, Kang Y. The Metastasis-Promoting Roles of Tumor-Associated Immune Cells. *J Mol Med.* 2013;91(4):411-429.

146. Su S, Liu Q, Chen J, Chen J, Chen F, He C, Huang D, Wu W, Lin L, Huang W, Zhang J, Cui X, Zheng F, Li H, Yao H, Su F, Song E. A positive feedback loop between mesenchymal-like cancer cells and macrophages is essential to breast cancer metastasis. *Cancer Cell* 2014;25(5):605-20.

147. Takagi T, Moribe H, Kondoh H, Higashi Y. dEF1, a zinc finger and homeodomain transcription factor, is required for skeleton patterning in multiple lineages. *Development*. 1998;125(1):21-31.

148. Taube JH, Herschkowitz JI, Komurov K, Zhou AY, Gupta S, Yang J, Hartwell K, Onder TT, Gupta PB, Evans KW, Hollier BG, Ram PT, Lander ES, Rosen JM, Weinberg RA, Mani SA. Core epithelial-to-mesenchymal transition interactome gene-expression signature is associated with claudin-low and metaplastic breast cancer subtypes. *Proc Natl Acad Sci U S A.* 2010;107(35):15449-54.

149. Tomlinson ML, Garcia-Morales C, Abu-Elmagd M, Wheeler GN. Three matrix metalloproteinases are required in vivo for macrophage migration during embryonic development. *Mech Dev*. 2008;125(11-12):1059-70.

150. Tsai JH, Yang J. Epithelial–mesenchymal plasticity in carcinoma metastasis. *Genes Dev*. 2013;27(20):2192-2206.

151. Tsou CL, Peters W, Si Y, Slaymaker S, Aslanian AM, Weisberg SP, Mack M, Charo IF. Critical roles for CCR2 and MCP-3 in monocyte mobilization from bone marrow and recruitment to inflammatory sites. *J Clin Invest*. 2007;117(4):902-9.

152. Turley SJ, Cremasco V, Astarita JL. Immunological hallmarks of stromal cells in the tumour microenvironment. *Nat Rev Immunol*. 2015;15(11):669-82.

153. Underhill DM, Goodridge HS. Information processing during phagocytosis. *Nat Rev Immunol*. 2012;12(7):492-502.

154. van Furth, R, Cohn, Z. A. The origin and kinetics of mononuclear phagocytes. *J. Exp. Med.* 1968;128, 415–435.

155. Valledor AF, Arpa L, Sánchez-Tilló E, Comalada M, Casals C, Xaus J, Caelles C, Lloberas J, Celada A. IFN-{gamma}-mediated inhibition of MAPK phosphatase expression results in prolonged MAPK activity in response to M-CSF and inhibition of proliferation. *Blood.* 2008;112(8):3274-82.

156. Vandewalle C, Van Roy F, Berx G. The role of the ZEB family of transcription factors in development and disease. *Cell Mol Life Sci.* 2009;66(5):773-87.

157. Varol C, Mildner A, Jung S. Macrophages: development and tissue specialization. *Annu Rev Immunol*. 2015;33:643-75.

158. Wang J, Lee S, Teh CE, Bunting K, Ma L, Shannon MF. The transcription repressor, ZEB1, cooperates with CtBP2 and HDAC1 to suppress IL-2 gene activation in T cells. *Int Immunol.* 2009;21(3):227-35.

159. Wang N, Liang H, Zen K. Molecular Mechanisms That Influence the Macrophage M1–M2 Polarization Balance. *Front Immunol*. 2014;5:614.

160. Wei K, Serpooshan V, Hurtado C, Diez-Cuñado M, Zhao M, Maruyama S, Zhu W, Fajardo G, Noseda M, Nakamura K, Tian X, Liu Q, Wang A, Matsuura Y, Bushway P, Cai W, Savchenko A, Mahmoudi M, Schneider MD, van den Hoff MJ, Butte MJ, Yang PC, Walsh K, Zhou B, Bernstein D, Mercola M, Ruiz-Lozano P. Epicardial FSTL1 reconstitution regenerates the adult mammalian heart. *Nature*. 2015;25:479-485.

161. Wellner U, Schubert J, Burk UC, Schmalhofer O, Zhu F, Sonntag A, Waldvogel B, Vannier C, Darling D, zur Hausen A, Brunton VG, Morton J, Sansom O, Schüler J, Stemmler MP, Herzberger C, Hopt U, Keck T, Brabletz S, Brabletz T. The EMT-activator ZEB1 promotes tumorigenicity by repressing stemness-inhibiting microRNAs. *Nat Cell Biol.* 2009;11(12):1487-95.

162. Wen Z, Liu H, Li M, Li B, Gao W, Shao Q, Fan B, Zhao F, Wang Q, Xie Q, Yang Y, Yu J, Qu X. Increased metabolites of 5-lipoxygenase from hypoxic ovarian cancer cells promote tumor-associated macrophage infiltration. *Oncogene.* 2015; 5;34(10):1241-52.

163. Williams CB, Yeh ES, Soloff AC. Tumor-associated macrophages: unwitting accomplices in breast cancer malignancy. *NPJ Breast Cancer*. 2016;2. pii: 15025.

164. Wilson HM. SOCS Proteins in Macrophage Polarization and Function. *Front Immunol*. 2014;5:357.

165. Wolf MJ, Hoos A, Bauer J, Boettcher S, Knust M, Weber A, Simonavicius N, Schneider C, Lang M, Stürzl M, Croner RS, Konrad A, Manz MG, Moch H, Aguzzi A, van Loo G, Pasparakis M, Prinz M, Borsig L, Heikenwalder M. Endothelial CCR2 signaling induced by colon carcinoma cells enables extravasation via the JAK2-Stat5 and p38MAPK pathway. *Cancer Cell*. 2012;22(1):91-105.

166. Wu X, Briseño CG, Grajales-Reyes GE, Haldar M, Iwata A, Kretzer NM, Kc W, Tussiwand R, Higashi Y, Murphy TL, Murphy KM. Transcription factor Zeb2 regulates commitment to plasmacytoid dendritic cell and monocyte fate. *Proc Natl Acad Sci U S A*. 2016;113(51):14775-14780. Wynn TA, Chawla A, Pollard JW. Origins and Hallmarks of Macrophages: Development, Homeostasis, and Disease. *Nature*. 2013;496(7446):445-455.

167. Xue J, Schmidt SV, Sander J, Draffehn A, Krebs W, Quester I, De Nardo D, Gohel TD, Emde M, Schmidleithner L, Ganesan H, Nino-Castro A, Mallmann MR, Labzin L, Theis H, Kraut M, Beyer M, Latz E, Freeman TC, Ulas T, Schultze JL. Transcriptome-based network analysis reveals a spectrum model of human macrophage activation. I*mmunity* 2014;40(2):274-88.

168. Yin M, Li X, Tan S, Zhou HJ, Ji W, Bellone S, Xu X, Zhang H, Santin AD, Lou G, Min W. Tumor-associated macrophages drive spheroid formation during early transcoelomic metastasis of ovarian cancer. *J Clin Invest*. 2016;126(11):4157-4173.

169. Yona S, Kim KW, Wolf Y, Mildner A, Varol D, Breker M, Strauss-Ayali D, Viukov S, Guilliams M, Misharin A, Hume DA, Perlman H, Malissen B, Zelzer E, Jung S. Fate mapping reveals origins and dynamics of monocytes and tissue macrophages under homeostasis. *Immunity.* 2013;38(1):79-91.

170. Zamilpa R, Kanakia R, Cigarroa J, Dai Q, Escobar GP, Martinez H, Jimenez F, Ahuja SS, Lindsey ML. CC chemokine receptor 5 deletion impairs macrophage activation and induces adverse remodeling following myocardial infarction. *Am J Physiol Heart Circ Physiol*. 2011;300(4):H1418-H1426.

171. Zhang F, Wang H, Wang X, et al. TGF-β induces M2-like macrophage polarization via SNAIL-mediated suppression of a pro-inflammatory phenotype. *Oncotarget*. 2016;7(32):52294-52306.

172. Zhang W, Tian J, Hao Q. HMGB1 combining with tumor-associated macrophages enhanced lymphangiogenesis in human epithelial ovarian cancer. Tumour Biol. 2014;35(3):2175-86.

173. Zhang X, Goncalves R, Mosser DM.. The isolation and characterization of murine macrophages. *In: Curr Protoc Immunol*. 2008;Chapter 14.1.

174. Zhang Y, Unnikrishnan A, Deepa SS, Liu Y, Li Y, Ikeno Y, Sosnowska D, Van Remmen H, Richardson A. A new role for oxidative stress in aging: The accelerated aging phenotype in *Sod1*$^{-/-}$ mice is correlated to increased cellular senescence. *Redox Biology*. 2017;11:30-37.

175. Zheng S, Hedl M, Abraham C. Twist1 and Twist2 contribute to cytokine downregulation following chronic NOD2 stimulation of human macrophages through the coordinated regulation of transcriptional repressors and activators. *J Immunol.* 2015;195(1):217-226.